

City Research Online

City St George's, University of London

Citation: Mahmood, M. N. (1975). An integrated chemical-electrochemical method for the recovery of copper from dilute solutions. (Unpublished Doctoral thesis, The City University)

This is the accepted version of the paper.

This version of the publication may differ from the final published version. To cite this item please consult the publisher's version.

Permanent repository link: https://openaccess.city.ac.uk/id/eprint/38127/

Copyright and Reuse: Copyright and Moral Rights remain with the author(s) and/or copyright holders. Copies of full items can be used for personal research or study, educational, or not-for-profit purposes without prior permission or charge, unless otherwise indicated, provided that the authors, title and full bibliographic details are credited, a hyperlink and/or URL is given for the original metadata page and the content is not changed in any way. For full details of reuse please refer to City Research Online policy.

City Research Online: http://openaccess.city.ac.uk/ publications@citystgeorges.ac.uk

AN INTEGRATED CHEMICAL-ELECTROCHEMICAL METHOD FOR THE RECOVERY OF COPPER FROM DILUTE SOLUTIONS

A THESIS SUBMITTED FOR THE DEGREE

OF DOCTOR OF PHILOSOPHY

OF

THE CITY UNIVERSITY

BY

MAHMOOD N. MAHMOOD

TO MY FATHER AND MOTHER

ACKNOWLEDGEMENTS

The Author wishes to thank Dr. A.C.C. Tseung for his continuing supervision, help and encouragement throughout the work; [redacted] and Members of the Materials Research Group for their assistance and many helpful discussions.

Thanks are also due to my wife, M[redacted], for her help and encouragement. Finally the Author expresses his gratitude to his parents, [redacted] for their financial support.

ABSTRACT

Copper can be recovered from dilute solutions both by electrochemical and non-electrochemical methods. The electrochemist, in dealing with the recovery of copper from dilute solutions, is faced with two major problems which decrease the efficiency of recovery:

(a) Hydrogen evolution reaction

(b) Mass transport

These difficulties are currently being overcome by using new cells designed to create increased turbulent flow in the electrochemical reactor.

Results during the course of this work show that copper can be deposited more efficiently in the presence of chloride ions. Furthermore, the results show that carrying out the electrolysis, constant current, at current densities higher than the limiting current results in the formation of a high surface area powdery deposit . The higher surface area will decrease the polarization of the copper electrode and hence add to the improvement of current efficiency.

Partial chemical reduction of the cupric ion to the cuprous state, followed by electrochemical reduction to the copper metal, results in very high current efficiencies. The presence of chloride ions is essential in the integrated chemical - electrochemical process because it stabilizes the cuprous ions formed during the chemical reduction.

Hydrazine and sodium sulphite were two reducing agents used to achieve the partial reduction of the cupric ions to the cuprous ions. Furthermore the efficiency of the process is pH dependent.

CONTENTS

		Page
CHAPTER I		
	Introduction	1
	Recovery of Copper from dilute solutions	3
	Electrochemical Methods	6
	Hydrogen evolution reaction	7
	Mass Transport	8
	References	14
CHAPTER 2		
	Experimental Techniques	
2.1.a	Steady State Potentiostatic Polarisation	16
2.1.b	Experimental	17
2.2.a	Controlled Current	18
2.2.b	Experimental	21
2.3.a	Cyclic Voltammetry	22
2.3.b	Multistep Charge Transfer Reactions	26
2.3.c	Experimental	28
2.4.a	Surface Area Measurements	29
	Electrochemical Principles	29
2.4.b	Some electrochemical techniques used for surface area measurement	31
	(1) Diffusion Measurement	31
	(2) Coulometry	31
	(3) Impedance Bridge	32
	(4) Galvanostatic Method	32
	(5) Charging Curves	33

Page

2.4.c Experimental 35

2.5.a Controlled Potential Electrolysis 35

2.5.b Choice of Optimum Potential 39

2.5.c Experimental 41

Figures 43

References 55

CHAPTER 3

Electrolysis in Chloride Medium

3.1.a Potential pH Diagram 59

3.1.b Results and Discussion 73

3.1.c Effect of Surface Area 80

3.1.d Cyclic Voltammetry 89

a Peak R_1 89

b Peak R_2 90

c Peak R_3 92

Figures 95

References 117

CHAPTER 4

Electrolysis in the Presence of a Reducing Agent.

4.1.a Introduction 120

4.2.a Electrolysis at low pH, using hydrazinium sulphate as the reducing agent 122

4.2.b Electrolysis at pH range 4 - 5 126

Polarisation Curves 127

Page

4.3.a Electrolysis at Higher Temperatures 135

4.3.b Using Sulphite as a Reducing Agent 141

4.4.a Controlled Potential Electrolysis 144

4.4.b Linear Sweep Voltammetry 151

4.5.a Conclusion 152

4.5.b Suggestions for future Work 154

Figures 155

References 186

APPENDIX ONE

a Predominant Ion of Hydrazine in the pH range 2 to 6. 187

b Electrode Potential 188

APPENDIX TWO

Predominant Copper (II) Complexes in Tartrate Solution 191

FIGURE INDEX

CHAPTER 2 — Page

Fig. 2.1 Steady state current potential curve for $CuSO_4$ 42

Fig. 2.2 Cell used for Potentiostatic polarization 43

Fig. 2.2.b Cell used for constant current electrolysis 44

Fig. 2.3 Circuit for potentiostatic polarization 45

Fig. 2.4.a S.C.E. with salt bridge 46

Fig. 2.4.b S.C.E. with salt bridge 47

Fig. 2.5 Circuit diagram for constant current electrolysis 48

Fig. 2.6 Circuit diagram for monitoring the working electrode potential during electrolysis 49

Fig. 2.7 Cyclic voltammetry curves for multistep charge transfer reactions 50

Fig. 2.8 a Triangular wave 51

b Current response

Fig. 2.9 Observed current time response for a copper electrode 52

Fig. 2.10 Cell used for measuring surface area 53

Fig. 2.11 Circuit diagram for measuring surface area 54

CHAPTER 3

Fig. 1 Potential - pH diagram for the system $Cu - H_2O$ at $25^{\circ}C$ 95

Fig. 2	Potential - pH diagram for the system Cu - Cl - H_2O at 25°C, 1.0 m Cl, 0.1 m Cu	96
Fig. 3	Potential - pH diagram for the system Cu - Cl - H_2O at 25°C 1.0 m Cl, 10^{-6} m Cu	96
Fig. 4	Steady state current potential curve for $CuSO_4$ (Stirred Solution)	97
Fig. 5	Steady state current potential curve for $CuSO_4$ (Stirred solution)	98
Fig. 6	Steady state current potential curve for $CuSO_4$ (Stirred Solution)	99
Fig. 7	Potential - time curve during constant current electrolysis	100
Fig. 8	Effect of Chloride ion on copper deposition	101
Fig. 9	The effect of temperature on copper deposition	102
Fig. 10	Change of concentration of copper with time at constant currents of 1mA/Cm^2, 2.14mA/Cm^2, 3mA/Cm^2, 4.28 mA/Cm^2	103
Fig. 11	Variation of efficiency of copper deposition during constant current electrolysis	104
Fig. 12	Variation of surface area during constant current electrolysis	105
Fig. 13	Current potential curve of $CuSO_4$	106
Fig. 14	Current potential curve of $CuSO_4$	107
Fig. 15	Current potential curve of $CuSO_4$	108
Fig. 16	Current potential curve of $CuSO_4$	109
Fig. 17	Current potential curve of $CuSO_4$	110

Fig. 18	Current potential curve of $CuSO_4$	111
Fig. 19	Current potential curve of $CuSO_4$	112
Fig. 20	Current potential curve of $CuSO_4$	113
Fig. 21	Variation of peak current with $CuSO_4$ concentration	114
Fig. 22	Variation of peak potential of peak R_2 with chloride ion concentration	115
Fig. 23	Variation of peak potential of peak R_3 with chloride ion concentration	116

CHAPTER 4

Fig. 4.1	Steady State current potential curve for $CuSO_4$ (Stirred Solution)	155
Fig. 4.2	Effect of varying pH on copper deposition	156
Fig. 4.3	Effect on efficiency of copper deposition caused by varying concentration of hydrazinium sulphate	157
Fig. 4.4	Effect on efficiency of Copper deposition caused by varying the concentration of potassium chloride	158
Fig. 4.5	Effect on efficiency of Copper deposition caused by varying the temperature	159
Fig. 4.6	Steady state current potential curve for $CuSO_4$ (Stirred solution)	160
Fig. 4.7	Steady state current potential curve for $CuSO_4$ (Stirred solution)	161

Fig. 4.8	Effect of varying pH on copper deposition	162
Fig. 4.9	Effect on efficiency of copper deposition caused by varying hydrazinium sulphate concentration	163
Fig. 4.10	Potential time curve during constant current electrolysis	164
Fig. 4.11	Potential time curve during constant current electrolysis	165
Fig. 4.12	Change of concentration of copper with time at constant current electrolysis	166
Fig. 4.13	Variation of efficiency of copper deposition during constant current electrolysis	167
Fig. 4.14	Steady state current potential curve for $CuSO_4$ (Stirred solution)	168
Fig. 4.15	Steady state current potential curve for $CuSO_4$ (Stirred solution) using small platinum electrode	169
Fig. 4.16	Steady state current potential curve for $CuSO_4$ (Stirred solution) using small platinum electrode	170
Fig. 4.17	Current time curve during constant potential electrolysis	171
Fig. 4.17a	Plot of log i against time interpolated from Fig. 4.17	172
Fig. 4.18	Current time curve during controlled potential electrolysis	173
Fig. 4.18a	Plot of log i against time	174
Fig. 4.19	Current time curve during controlled potential electrolysis	175

Fig. 4.19a Plot of log i against time, interpolated from Fig. 4.19 176

Fig. 4.20 Current-time curve during controlled potential electrolysis 177

Fig. 4.20a Plot of log i against time interpolated from Fig. 4.20 178

Fig. 4.21 Current-time curve during controlled potential electrolysis 179

Fig. 4.21a Plot of log i against time, interpolated from Fig. 4.21 180

Fig. 4.22 Current-potential curve of background electrolyte (unstirred solution) 181

Fig. 4.23 Current-potential curve of background electrolyte (unstirred solution) 182

Fig. 4.24 Current-potential curve of $CuSO_4$ (unstirred solution) 183

Fig. 4.25 Current potential curve of $CuSO_4$ (unstirred solution) 184

Fig. 4.26 Current potential curve of $CuSO_4$ (unstirred solution) 185

CHAPTER I

Introduction

Copper, though widely distributed in the earth's crust, is not an abundant element, being present in only about 55 p.p.m. There are areas, however, such as Chile and Zambia; where copper is concentrated in the earth's crust. In 1972, world consumption of new mined copper, ignoring recycled scrap, was between 6 and 7 million tons. (1) The projected growth rate in consumption for the next thirty years is about 5%. Thus consumption in the year 2000 will be between 20 and 30 million tons. (1) At this rate of consumption the pessimistic prediction is that the earth's present known resources of copper will be severely depleted within thirty years. It is, therefore, important to consider the ways in which these resources can be increased. Extracting copper from low-grade ores and recycling copper scrap and waste-products is one such method.

During the last century copper ore could be mined and processed economically only if it contained 10% or more of the metal. With the turn of the century came improvements in the techniques of mineral separation and mining technology. The subsequent discovery of flotation permitted economic recovery of ores containing 1% copper. (2) Bacterial leaching (2), (11) makes use of the ability of certain bacteria to oxidize sulphur. This permits the conversion of insoluble metal sulphide in the main copper ore, chalcopyrite, $Cu\ Fe\ S_2$, to water-soluble sulphates, which can be washed out of the ore.

$$Cu\ Fe\ S_2 + 4O_2 \rightarrow CuSO_4 + Fe\ SO_4$$

The bacteria also oxidize ferrous ions in the solution to ferric ions, which then chemically attack the sulphide mineral and produce soluble copper sulphate. (2)

$$Cu\,Fe\,S_2 + 2Fe_2(SO_4)_3 + 2\,H_2O + 3O_2 \rightarrow Cu\,SO_4 + 5\,Fe\,SO_4 + 2H_2SO_4$$

Copper can thus be economically recovered from ores containing as little as 0.25%. A more detailed account of the wet treatment of low-grade ores can be obtained from reviews by Cooper (6) and Rosenzweig (7).

Civilized society is regrettably becoming consumer orientated and consequently the natural resources of our planet are being devoured at an unprecedented rate. One of the main drawbacks in a consumer society is the amount of domestic and industrial waste it produces. For instance the annual domestic waste in the United Kingdom is 17 million tons, about ten per cent of which is metallic (3). The estimated annual wastage of metals in domestic refuse in the United Kingdom is given in Table I below (3).

Table I Annual domestic metallic refuse in U.K.

Metal	Fe	Ni	Cu	Al.	Zn	Sn
Ton	10^6	400	23,500	40,500	36,000	7,200

Another source of waste is industrial which consists of grinding dust and metallic scrap from industrial and consumer goods which have ended their useful life, such as discarded industrial plants and machinery, electric cables and automobiles.

The metal finishing industry contributes its fair share of metal waste. Metal losses in this industry are caused by accidental floor spillages, leaks in filtration equipment and

wastage in solution purification (4). The greatest losses occur through the dragout of metal-containing solutions into rinse water. The extent of such losses varies. Under the worst conditions, for example in chromium-plating, losses may exceed 85% of the total metal consumption, while at best, losses are rarely less than 10% (4). At an average wastage of 12.5%, the value of nickel lost from a nickel-plating bath in 1968 amounted to approximately £125 per ton of nickel purchases. (5) In the case of copper, if no recovery of copper is carried out/in the metal - finishing industry, the amount of copper wasted is estimated at over 10,000 tons a year in the U.K. alone (13).

From the above paragraphs it is obvious that the recycling of this huge metal wastage and the extraction of metal from low-grade ores, which would entail the recovery of the metal from dilute solutions, should help to increase the world's reserves. This would enable modern industrial societies to indulge more in their sinful waste of the world's wealth, especially at the expense of the underdeveloped countries, which are its major producers.

Recovery of Copper from dilute solutions.

It has already been stated in the preceding paragraphs that the recovery of copper and other heavy metals from dilute and effluent solutions would contribute significantly towards increasing the world's reserves. Coupled with the economic incentive for recovery is the fact that discharged effluents from industries utilizing heavy metals are a source of pollution to mammals and fish, and even very low concentrations are toxic to the bacteria used in the treatment of sewage.

Local authorities have powers to regulate the amount of heavy metals discharged as waste into sewers and rivers. Table II illustrates the limits imposed upon some of these effluents. (33).

Table II Limits in mg/l acceptable to Local Authorities for the discharge of waste effluents containing heavy metals.

Metal	ppm
Arsenic	0.05
Cadmium	0.01
Copper	0.16
Chromium VI	0.05
Lead	0.1
Nickel	1.0
Tin	5.0
Zinc	5.0

Copper can be recovered from dilute solutions by both electrochemical and non-electrochemical methods. Some of the more common non-electrochemical methods are as follows:

(i) Ion exchange (8). Ion exchange resins are used for the recovery of copper from dilute solutions. The advantages (9) of this technique are that 80 - 90% of the water is recirculated and the metal is reclaimed as a salt. In this process, therefore, the saving of water is obviously achieved. The economic disadvantages, however, are numerous (9):-

(a) Precipitated metals or solids in the water can clog the ion exchange resin bed. A filtration installation ahead of the bed is necessary.

(b) Organic compounds such as oils, brighteners, etc., which are commonly used, especially in plating baths, foul the resin bed and it is therefore essential to precede the ion exchange system with a carbon filter.

(c) As can be seen from (a) and (b) above, the costs for installation and equipment are high.

(d) Maintenance costs are heavy since the whole installation has to be back washed frequently in order to keep the bed and filters in good working order.

(ii) Exchange of copper ions by iron ions (10).

In this method the copper can be exchanged for iron by running the dilute solution stream through a packed bed of iron but, as a layer of copper metal is formed on the iron surface, the reaction is impeded and the spent bed, which now consists of iron and copper metals, is removed, and a new iron bed is put in. The copper is then removed mechanically from the iron.

(iii) Precipitation methods. These are usually carried out by adding lime to effect the precipitation of the water rich cupric hydroxide containing approximately 1 - 2% copper (13). In other cases a mixed caustic soda - sodium carbonate solution, at pH 8 - 9, containing hydrazine is added to precipitate cuprous oxide, which contains 50 - 60% copper (13).

Other methods, such as solvent extraction, (3), (12), (32), are becoming more important in the treatment of low-grade ores and leaching bath solutions.

In all the methods mentioned above, the copper recovered is not in a pure state, but is reclaimed as a salt or hydroxide,

and therefore further processing is required to reduce the salt to the metallic state. This constitutes one of the main disadvantages of these methods.

Electrochemical Methods

In the body of a metal all atoms are completely surrounded by others. At a metal surface, however, parts of the atoms are exposed to the surroundings. This fact endows the surface atoms with excess energy, termed surface energy (14). Because of this surface energy, metals tend to attract substances, e.g. hydrogen, impurities available to them within the surrounding medium. The greater the surface energy, the more strongly the metal will attract and bond these substances or be rendered passive (14). On this basis, metals can be divided into three groups, relative to their ease of electrodeposition:- (14, 15)

(a) Those which deposit with a low overvoltage, e.g.:- Ag, Au, Cd, Cu, Zn.

(b) Those which deposit with a high overvoltage, e.g.:- Ni, Co, Cr, Mn, Pt.

(c) Those which cannot be deposited from aqueous solutions as single metal, e.g.:- Mo, W, U, Ti.

Metals of group (a) have a relatively low surface energy, and therefore have little tendency to become passive. Metal ions in the surrounding solution consequently have little competition for the active sites on the metal surface, and this results in ease of electrodeposition.

Metals of group (b) have higher surface energy than group (a) and therefore have a greater tendency to passivity. This will subsequently reduce the number of active sites and hence retard the process of electrodeposition. In addition, since the affinity of these metals to hydrogen is greater than that of group (a), their electrodeposition is always accompanied by greater hydrogen evolution and hence lower current efficiency.

Copper can therefore be recovered electrochemically with relative ease especially in the high concentration region of 1000 ppm. or more. As the concentration lowers the current efficiency is reduced.

The electrochemist, in dealing with the recovery of copper from dilute solutions, is faced with two major problems. (16, 17).

Hydrogen evolution reaction

Hydrogen evolution is the competing reaction to copper deposition. This problem can sometimes be avoided by using an electrode with a high hydrogen overvoltage such as lead, but, as deposition proceeds, the lead cathode behaves less and less as lead and more and more as a copper electrode (17).

One possible way of decreasing the hydrogen evolution reaction is to increase the surface area of the cathode by creating the right conditions for the formation of a powdery deposit. The increase in the surface roughness of the electrode will subsequently reduce the actual current density used, and this reduction will in turn decrease the cathodic polarisation of the electrode and hence reduce the effect of the competing reaction.

This effect can be achieved by using current densities higher than the limiting current density for the system (18) or by using titanium starter electrodes (15).

Mass Transport

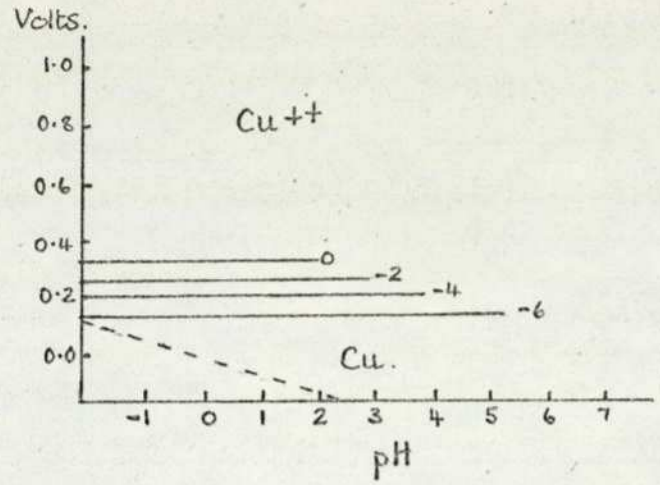


Fig. I. Pourbaix type diagram for Cu/Cu^{2+} system equilibrium (solid lines) and hydrogen evolution potential (dashed line) at 25°C. The horizontal lines describe the Cu/Cu^{2+} potential at the Cu^{2+} concentration shown (g - ion x 10^{x}). Drawn from reference (19).

From Figure (1) it can be seen that the potential separation between hydrogen evolution and copper deposition decreases as the concentration of copper ion in the solution decreases. Because of the decreased potential separation at low copper concentration mass transport of the copper ions becomes more important especially since hydrogen evolution and copper deposition reactions have high exchange current densities.

Mass transport becomes more important at low concentrations because there is an abundance of hydrogen ions in the solution (19) which have much higher diffusion coefficient than the copper ions.

When an electroreduction is occurring at an electrode interface, the equality of the charge transfer flux and transport flux (Fick's First Law)(20) requires that

$$\frac{i}{nF} = - D \left(\frac{dc}{dx}\right)_{x = o} \tag{1.1}$$

In terms of the diffusion layer concept (20) this condition becomes

$$\frac{i}{nF} = - D \left(\frac{dc}{dx}\right)_{x = o} = - D \frac{C_o - C_{x = o}}{\delta} \tag{1.2}$$

where

i = current

D = Diffusion coefficient

δ = Nerst diffusion layer thickness

C = concentration

x = distance from electrode surface

C_o = Bulk concentration

The concentration gradient has a maximum value for

$C_{x = o} = O$,

therefore

$$\lim_{C_{x = o} \longrightarrow o} \left(\frac{dc}{dx}\right)_{x = o} = \lim_{C_{x = o} \longrightarrow o} \left(\frac{C_o - C_{x = o}}{\delta}\right)$$

$$= \frac{C_o}{\delta} \tag{1.3}$$

This maximum concentration gradient corresponds to a maximum or limiting current density, i_L, given by

$$i_L = \frac{- Dn F C_o}{\delta} \tag{1.4}$$

Therefore for a given electrochemical reaction there is a maximum attainable current density. The reaction cannot go faster than i_L because the transport process in the electrolyte bulk is incapable of supplying the electroactive species to the electrode at a faster rate. It can be seen from equation (1.4) that the value of i_L can be increased if the diffusion layer thickness, δ , can be decreased, diffusion coefficient is high, or concentration is high.

These transport problems of the electroactive species to the electrode have created limitations on reaction rates and current efficiencies in industrial operations. Until recently, cell designers have ignored these limitations and, consequently, the maximum current density used has often been small. If an electrochemical plant is run on low current density the return on capital costs will be low.(17) In order to counter this, the designer would have to use bigger cells and bigger electrodes which would entail higher capital costs. (4)

These difficulties are currently being overcome by using new cells designed to create increased turbulent flow in the electrochemical reactor and hence increase the maximum current that can be used to give acceptable current efficiencies. The ability to use higher current densities is a consequence of the reduction of the thickness of the diffusion layer. Table III best illustrates this (4).

TABLE III (4)

Diffusion Layer thickness for various hydrodynamic conditions

	δ (mm)
1. Natural convection with vertical electrodes	0.20
2. Natural convection with horizontal electrodes	0.08
3. Plane electrodes with longitudinal flow. V = 25 cm/s	0.10
4. Rotating cylinder (180 rpm, peripheral vel 94 cm/s)	0.036
5. Periodic disturbances of diffusion layer by net moved along electrode	0.013
6. Gas producing electrode ($1\ cm^3$ gas cm^{-2} $min.^{-1}$)	0.015

Some of the new cell designs developed are:

1. The Fluidized Bed-Electrode

This electrode has been developed at the Universities of Newcastle and Southampton (21, 22, 23, 24, 25, 26). Some of the advantages of the fluidized bed electrode are:

1. Its ability to offer a high electrode area. For example large surface areas ranging from 10 to 1000 cm^2 for each cm^3 of bed can be obtained depending on particle size (25).

2. High rates of mass transfer.

3. Less space is required for its operation.

This system should be useful with slow electrochemical reactions typified by low exchange current densities, because it offers high surface area.

But the disadvantages of this electrode for copper electrodeposition are numerous, some of which are:-

a. Non-uniform potential distribution over the bed particles (25) with the resultant corrosion of copper metal deposited on the beads.

b. The low electronic conductivity of bed electrode could be reflected by high power consumption.

c. The bed has a non-uniform electrochemical activity, and some parts are more active than others.

d. Clogging of bed could occur.

Other cell designs which are promising are:

2. The Rotating-Cylinder electrode (27).

3. Porous, fixed, flow through electrode (10).

4. Restrained bed electrode (34).

5. Periodic disturbance of diffusion layer by controlled abrasion of the cathode (29).

For further information on the new cell designs used in copper recovery, references (4, 16, 17, 19) are recommended.

Finally a brief comparison of chemical and electrochemical methods seems appropriate.

Electrochemical	Chemical
1. Better quality product	1. 60 to 1 per cent of the recovered product is metal.
2. Less labour is needed (30)	

Electrochemical	Chemical
3. Usually cheaper than chemical methods (30)	3. It is cheaper in the case of Nickel where it is precipitated as the carbonate.
4. Cleaner than their counterparts (17)	
5. Both have similar equipment need and cost (30).	

It is also worth remembering that electrochemical methods can be made cheaper by controlling the reaction at the counter-electrode (31) as will be seen later in Chapter Four.

REFERENCES

1. M.J. Cahalan, Chemistry in Brit., 1973, 9, 392.
2. A.W. Fletcher, Trans. Inst. Mining and Metallurgy, Section C, 1970, C247.
3. A.W. Fletcher, Chem. and Industry, 1973, p 414-419.
4. B. Surfleet and V.A. Crowle, Trans. Inst. Metal Finishing, 1972, 50, 227.
5. R. Pinner, Symp. on The Nickel Shortage and Ways of Meeting It, IMF, London, March 1968
6. F.D. Cooper, U.S. Bur. Mines Inform. Circ. 8394 (1968)
7. M.D. Rosenzweig, Chem. Eng., 1967, 74, 88.
8. J.E. Browning (News Editor), Chem. Engr., 78, April 1971, 19, 62.
9. L.E. Lancy, W. Nohse and D. Wystrach, Plating, 1972, p 126-130.
10. D.N. Bennion and J. Newman, J. Appl. Electrochem., 1972, 2, 113.
11. R.C. Gupta and B.R. Sant, J. Sci. Ind. Res., 1970, 29, 372.
12. D.S. Flett, Miner Sci. Eng., 1970, 2, 17.
13. R. Pinner and V. Crowle, Electroplating and Metal Finishing, 1971, March pp 1 - 15.
14. G. Isserlis in Industrial Electrochemical Processes Ed, A.T. Kuhn, Elsevier, Amsterdam - London, New York, 1971, Ch. 9.
15. B. Surfleet, in a lecture given at Salford University 1973.
16. A.T. Kuhn in Electrochemistry of Cleaner Environment, Ed J. O'M. Bockris, Plenum Press, New York - London 1972, Ch. 4.
17. A.T. Kuhn in Modern Aspects of Electrochemistry, ed. J.O'M. Bockris and B.E. Conway, No. 8, Butterworth and Co., 1973, Chapter 5.

18. N. Ibl in Advances in Electrochemistry and Electrochemical Engineering, Ed. C.W. Tobias, Vol 2, Interscience, 1962.

19. A.T. Kuhn, Chemistry and Industry, 1971, pp 473 - 476.

20. Bockris and Reddy, Modern Electrochem. Vol. 2, Macdonald 1970.

21. M. Fleischmann, F. Goodridge, and J.M. Backhurst, U.K. Pat. 23070/66

22. M. Fleischmann et al, J. Electrochem. Soc., 1969, 1600

23. M. Fleischmann et al, J. Electroanal. Chem., 1971, 29, 211.

24. P. Lecraff, Ind. and Eng. Chem., 1969, 61, 9.

25. C.N. Middlestone and A. Douglas, Electrochem. Acta, 1970, 15, 431.

26. D.S. Flett, Chemistry and Industry, 1971, pp 300-302.

27. D.J. Robinson and D.R. Gabe, Trans. Inst. Metal Finish, 1970, 48, 35.

28. A.T. Kuhn and B. Marquis, J. Appl Electrochem, 1972, 2, 275

29. S. Eisner, Plating, 1971, pp 993-996

30. R. Pinner, in a lecture given at Salford University, 1973.

31. A.T. Kuhn, New Scientist, 1967 (5 October), 21

32. D.S. Flett, D.N. Okuhara and D.R. Spink, J. Inorg. Nucl. Chem. 1973, 35, 2471.

33. R.K. Chalmers. Chemistry and Industry, 1973, 554-7

34. A.T. Kuhn and R.W. Houghton, J. Appl. Electrochem., 1974, 4, 69.

CHAPTER II

Experimental Techniques

During the present work it was necessary to employ various electrochemical techniques in order to obtain a better understanding of the project. These techniques will be described in the following sections.

2.1 a. Steady State Potentiostatic Polarisation

It is necessary to study the potential dependence of current in order to determine the limiting current of the system under investigation. This is achieved by measuring the current at various controlled potentials of the working electrode, relative to a reference electrode. In the galvanostatic method of polarisation, the potential of the working electrode is measured at a number of controlled currents. It must, however, be remembered that the system must be allowed to reach a steady state in both methods of polarisation.

In situations where the current is a monotonic function of the potential, both methods give similar results. When the current-potential curve exhibits a maximum or a minimum, for instance, when electrode passivation sets in, the galvanostatic technique can give misleading results (1).

Metals are deposited in a powdery form when the electrolysis is carried out at limiting diffusion currents or higher currents (2). The limiting current is not very well defined because the current distribution over the electrode is not uniform. When the current is increased, the limiting current is reached first at the edges of the electrode.

The formation of a rough deposit starts at the edges of the electrode and gradually spreads over the whole electrode area (3). This results in a limiting current range rather than a well defined limiting current (3).

Automatic recording of polarisation curves using an X - Y recorder and a slow voltage scan rate was employed to measure the limiting current range, since it had been found that when the experiments were carried out manually the results could be subjective and therefore misleading, because of the presence of a limiting current range rather than a well-defined limiting current.

Fig. (2.1) represents such a curve showing the variation in limiting current.

2.1.b Experimental

All chemicals used were analar grade. 2 mls. of 20,200 to ppm of copper sulphate solution were added/200 mls of a solution containing 0.1 M potassium chloride and other salts depending upon the kind of buffer and reducing agent used. The pH of the resulting solution was adjusted to the required pH value, using a pH meter. Before use, the pH meter was calibrated against a pH4 buffer standard. 150 mls. of the solution were placed in the cathode compartment of the cell shown in Fig. 2.2. The anode compartment had 150 mls of 0.1 M potassium sulphate solution. The cell was placed in a water bath set at the required temperature. The solution in the cathode compartment was stirred by a Gallenkamp magnetic stirrer set at number 7 (maximum setting on the stirrer is 10, giving a stirring speed of up to 1,300 stirrings per minute).

The copper electrode was potentiostated as shown in Fig. 2.3 using a Chemical Electronics Potentiostat, type TR40 - 3A, a Solartron Digital Voltmeter (D.V.M.), a Chemical Electronics Linear Sweep generator and a Bryans X - Y recorder, Model 21001. The potential of the working electrode was scanned at a speed of 40 mV per minute. A typical current - potential curve is shown in Fig. 2.1.

The copper electrode used was 99.999% copper, supplied by Kock & Light. The area of the electrode was 7 cm^2. Before each experiment described in this and the following sections the copper electrode was leached in 50% nitric acid solution for 10 seconds, rinsed thoroughly with distilled water, acetone and finally dried with a hair-dryer.

The reference electrode used throughout this work was a Saturated Calomel Electrode (S.C.E.) connected to the cathode compartment through an agar-agar salt bridge as shown in Fig. 2.4a. The reference electrode assembly shown in Fig. 2.4b was used for experiments with solutions containing small concentrations of chloride ions, or solutions free of chloride ions.

2.2.a Controlled Current-Electrolysis

The principle is very simple; copper ions are deposited on to the copper cathode by applying a constant current across the electrolysis cell. This can be easily achieved by using a potentiostat, a voltmeter and a standard resistor. The circuit diagram for the galvanostatic connection is shown in figure 2.5.

According to Faraday's Law, the quantity of Copper deposited during an electrolysis in which Q coulombs have been passed is:

$$W = \frac{MQ}{96484\ n} \qquad (2.1)$$

where

W = Weight of deposited copper metal in g.

n = Number of electrons consumed during the electrochemical reaction.

Q = i x t

i = current in amperes

t = time in seconds

M = Atomic weight of Copper

96484 = The Faraday constant

The efficiency of deposition is given by equation (2.2)

$$\% \text{ efficiency} = \frac{W_o}{W_t} \times 100 \qquad (2.2)$$

where,

W_o = Observed weight of deposited metal during the passage of Q coulombs of electricity

W_t = The theoretical amount of Copper deposited as calculated by equation (2.1).

As the author was using the part per million concentration scale, p.p.m., the calculations of the efficiency of deposition were as follows.

Let,

V = Volume in mls of solution

p_1 = ppm before start of electrolysis

i = current in amperes

t = time in seconds

p_2 = ppm after t seconds of electrolysis

then

$$W_o = (p_1 - p_2) \times V \times 10^{-6} \qquad (2.3)$$

$$W_t = \frac{it \times 63.54}{2 \times 96484}$$

$$\therefore \text{ \% efficiency} = \frac{(p_1 - p_2)V \times 10^{-6} \times 2 \times 96484}{63.54 \times i \times t}$$

$$= \frac{3036.9(p_1 - p_2)\ V \times 10^{-6}}{it}$$

$$= \frac{3.037\ (p_1 - p_2)\ V \times 10^{-3}}{it} \qquad (2.4)$$

The following conditions should be fulfilled to obtain 100% current efficiency (4).

(a) There should be no side reaction.

(b) There should be no leak in the electrical circuit.

The second condition can be disposed of simply by assuming that the equipment used is in good working condition.

Various side reactions can interfere with the main electrochemical reaction depending on the nature and composition of solution used. In the system under investigation the side reaction which reduces the current efficiency is the reduction of water, with the consequent liberation of hydrogen gas, as shown by the equation below.

$$2H^+ + 2e \rightarrow H_2$$

2.2.b Experimental

All solutions were prepared as described in section 2.1.b. 150 mls. of the resulting solution were placed in the cathode compartment of the cell shown in Fig. 2.2 b and the solution stirred as in section 2.1.b. The cell was connected to the circuit shown in Fig. 2.5, and the required current was passed. 5 ml. aliquots of the solution were withdrawn at equal intervals (usually at 15-minute intervals). The aliquots were then diluted to 100 mls. in a 100 ml. volumetric flask, and the resulting solutions were analysed for copper using a Perkins Elmer 290 B Atomic Absorption Spectrophotometer. The wavelength used was 3247Å Before use the spectrophotometer was calibrated against a 10 ppm standard of roughly the same composition as the test solution, and a 0 p.p.m. solution. Each point on the electrolysis curves shown in Chapters 3 and 4, was the average of at least two separate experiments. Since a two compartment cell was used, some of the copper ions diffused to the anode compartment during every experiment. Therefore, after each electrolysis, 5 ml. aliquots from the anode compartment were also withdrawn for copper analysis. The number of ppm of copper found in the anode compartment was added to the results of the cathode compartment in order to correct for the diffusion of copper ions between the two compartments. On average, the anode compartment was found to contain 3 - 6 ppm of copper ions. Therefore all the readings on the electrolysis curve are correct to within 4 ppm.

In a separate set of experiments the cathode potential was monitored against a S.C.E. during the electrolysis.

This was done by using an X - t recorder and the circuit shown in Figure 2.6.

Since the electrolysis experiments were carried out for at least 15 minutes, i.e. 900 seconds, the author used an ordinary stop-clock which was manually operated as the constant current was switched on. Any error due to time lag between switching on the current and the stop clock was assumed to be negligible.

2.3.a Cyclic Voltammetry.

All electrochemical experimentations involve the application of some perturbation to the system, monitoring the resultant response and interpreting the data so obtained.

There are four fundamental parameters of electrochemical experimentation:-

1. Current density.
2. Potential.
3. Time.
4. Concentration.

All techniques, directly or indirectly, are governed by these four parameters. In cyclic voltammetry we are primarily concerned with current, potential and time. (5).

The voltammetric experiment is designed so that the mode of transport of the electroactive species to the electrode surface is well defined. With migration and convection eliminated by using a high concentration of a background, non-interfering electrolyte and preventing vibration and stirring in the solution, the only other transport process is diffusion. The nature of diffusion process depends on the shape of the electrode used (6).

Diffusion to planar electrodes immersed in large amounts of solution is called semi-infinite linear diffusion. Semi-infinite diffusion holds only if the electroactive species diffuses to the electrode surface in one direction only (6). Experimentally, this can be accomplished by using shielded electrodes. With this kind of electrode, linear diffusion holds for electrolysis times of greater than 10^3 seconds. (6). In aqueous solutions unshielded planar electrodes confirm to semi-infinite linear diffusion for electrolysis times of 30 to 40 seconds. (6)

With stationary electrodes, as the potential is increased to the region where the electroactive species is oxidized or reduced, the rate of electron transfer is exponentially related to the applied potential. Electroactive species diffuse towards the electrode surface because a concentration gradient is established. Eventually the rate of electron transfer will be more rapid than the rate of diffusion of electroactive species to the electrode. Then the peak current will be observed (6, 7). Beyond the peak current, the current decays because the concentration gradient decreases as the diffusion layer becomes thicker, i.e. the diffusion layer is increasing in thickness although the species is being reduced, or oxidized as soon as it reaches the electrode.

For linear diffusion where a species in solution is oxidized or reduced, Randles (8) and Sevcik (9) derived the relationship between the peak current and concentration for a reversible electrode process and found it to be

$$i_p = 2.69 \times 10^5 \, n^{\frac{3}{2}} \, A \, D^{\frac{1}{2}} \, V^{\frac{1}{2}} \, C \qquad (2.5)$$

where

i_p = peak current

n = number of electrons consumed in the electrochemical reaction

D = Diffusion coefficient of species.

A = Area of electrodes

V = Potential sweep rate

C = Bulk concentration of species.

It can also be shown that for a reversible reduction process (10)

$$E_p = E_{\frac{1}{2}} - \frac{0.0285}{n} \qquad (2.6)$$

where

E_p = peak potential

$E_{\frac{1}{2}}$ = polarographic half wave potential

and for an oxidation wave

$$E_p = E_{\frac{1}{2}} + \frac{0.0285}{n} \qquad (2.7)$$

Therefore, for a reversible reduction, the peak potential is $\frac{28mV}{n}$ more negative than the half wave potential and for oxidation the peak potential is $\frac{28mV}{n}$ more positive. If the sweep is reversed then the peaks separation for a reversible couple is $\frac{58mV}{n}$.

For irreversible couples the peak separation is more than $\frac{58mV}{n}$ (11) and the rise in current to the peak is less sharp.

Sweep rates can vary from 100 volts per second to less than 10mV/sec. Very slow sweep rates should be avoided in order to prevent convective mixing in the diffusion layer. Convective mixing in the diffusion layer can cause the reduction peak to be more negative than 28/n mV (7).

When a metal is deposited on an inert electrode, the activity of the deposit is much smaller than unity at the beginning of electrolysis and the current will increase at potentials less cathodic than those predicted (12).

Cyclic Voltammetry is useful because it makes the detection of intermediates in electrochemical reactions possible. (13, 14).

Cyclic voltammetry is also practically useful for establishing that a polarographic wave is reversible and that the value of the formal electrode potential obtained by other methods, like polarography and chronopotentiometry can not be questioned (7).

The theory of single scan method has been extended to reversible reactions taking place at cylindrical electrodes (15) and at spherical electrodes (16, 17). Delahay (18) and Nicholson and Shain (10) extended the treatment to cover irreversible electrode processes. Later the treatment was extended to treat electrochemical reactions coupled with chemical reactions (10), chemical reactions coupled between two charge transfer (19, 20), multistep transfer reactions (21, 22), absorption of electroactive species on electrode (23, 24) and non unity electrode reaction orders (25). For further information references (7, 6, 5, 11, 26) should be consulted.

2.3.b Multistep Charge transfer Reactions

A multistep charge transfer reaction (21) can be represented by

$$A + n_1 e \rightarrow B$$

$$B + n_2 e \rightarrow C$$

There are three separate cases to be considered (21).

(1) If A and B react at sufficiently separated potentials with A more easily reducible than B. The i - v curve will then consist of two separate peaks. The first peak corresponds to the reduction of A to B with n_1 electrons. As the potential is scanned towards cathodic values a second peak appears which is made up of 2 parts superimposed (21, 11).

(a) The current for the direct reduction of A to C by $(n_1 + n_2)$ electrons.

(b) Current for the reduction of substance B, which was the product of the first wave, resulting from the diffusion of substance B back to the electrode.

The resultant curve is shown in Fig. (7a).

In order that the separate curves behave as independent reversible waves a minimum potential separation, ΔE^o, of about $^{118}/_{n}$ mV (21) is required.

(2) If ΔE^o is less than $\frac{100 \text{ mV}}{n}$, the individual waves merge, into one broad distorted wave whose peak high and shape are no longer characteristic of a reversible wave as shown in Figure (7.b).

The wave is broadened similar to an irreversible wave, but can be distinguished from an irreversible one, in that the distorted wave does not shift on the potential axis as the scan rate is changed (21).

(3) $\Delta E^o = 0$ and $n_1 = n_2$

The wave shown by Fig. (7.c) is obtained with a peak height intermediate between a one-electron and a two-electron reversible wave and a $E_p - E_{\frac{1}{2}}$ of about 21 mV (21).

(4) B is easier to reduce than A:-

As B becomes easier to reduce than A, the wave height increases and the peak narrows until it reaches the height and shape of a 2e (21) wave. Fig. (7.d)

For systems involving multistep reversible charge transfer reactions with large ΔE separations, the peak positions should not vary as the scan rate is changed, and the value of $\frac{\text{peak current}}{(\text{scan rate})^{\frac{1}{2}}}$ is constant for various scan rate values (21).

For further information, and the application of linear sweep voltammetry to multistep charge transfer reactions references 27, 28, 21 should be consulted.

2.3.c Experimental

All solutions were prepared as described in section 2.1.b. In some experiments potassium chloride concentration was varied. 150 mls. of the solution prepared were placed in the cathode compartment of the cell shown in Fig. 2b.

The solution was purged with oxygen-free nitrogen for roughly ten minutes before the start of each experiment. A planar platinum electrode of 3/2 cm^2 area was used as the cathode and the anode was a 20 cm^2 platinum electrode. Before each experiment the platinum cathode was anodized at a current density of 1 mA/cm^2 in a 50% nitric acid solution for 15 minutes. Finally the platinum cathode was thoroughly rinsed with distilled water.

The circuit and the instruments used were the same as in Section 2.1.b., except that the solution was not stirred. The voltage was scanned from +500 to -500 mV against the S.C.E. The readings of the potential on the X - Y recorder were accurate to within 5 - 10 mV. Before each experiment the X and Y axes on the X - Y recorder were calibrated.

2.4.a. Surface Area Measurements

Many electrochemical and non-electrochemical processes depend on the effective area. Area measurements are needed, for example, in studies of batteries, fuel cells, chemical catalysis and corrosion. There is no reliable method for measurements with porous bodies having areas of 100 cm^2 or less (29).

The classical gas-absorption methods, such as the Brunauer-Emmete-Teller (BET) gas absorption technique (30, 31, 32, 33) in which the area is computed from volume of gas absorbed to form a monolayer on the surface, are time consuming. Moreover there is great uncertainty about relationships between dry areas and wet areas (29).

Electrochemical methods are suitable for areas less than 1000 times the geometric area (29). For very large areas, say more than a thousand times the geometric area, the classical gas absorption methods are recommended (29).

Electrochemical Principle

There are three main electrochemical principles (29, 33) used for the determination of electrode areas.

1. The measurement of the rate of electrolytic production (or consumption), of some chemical, where the rate depends on the electrode area in a known and reproducible manner.

2. Electrochemical deposition (or removal) of an absorbed layer of some chemical species where the fractional surface coverage is known or at least is reproducible. Reliable measurements are possible in this case when atomic dimensions are known. For example, hydrogen or oxygen can be electrolytically deposited on Pt in a reproducible manner and could then be removed quickly by coulometry (34).

However, if the same conditions are used to deposit hydrogen on a clean copper electrode, for example, the same value for coverage as in the Pt case is not likely to result. Therefore, comparison between different substances could not be direct and absolute values of coverage would have to be determined. (29)

3. Measurement of the electrical double layer capacitance:-

A pair of electrodes may be made part of an electrical circuit and the capacitance of the circuit measured by accepted techniques. Proper design of one electrode, (reference electrode) will permit the assignment of the measured capacitance of the other working electrode.

The electrical capacitance of the interface in an electrode-electrolyte system is a measure of the redistribution of charges in response to the potential difference between the two disimilar phases (33). The simplest model for the double layer is that of a parallel-plate capacitor as proposed by Helmholtz, where the charge on the metal is considered to exist entirely on the surface. Although the charge distribution in the solution is more complex and extends some distance into the solution, the layers of ions in solution will approach the contour of the solid electrode (33). Hence the capacitance can be used as a measure of the interfacial area. It should be remembered, however, that charge distribution is dependent on electrode composition, electrolyte compositions and electrolyte concentration.

2.4.b Some electrochemical techniques used for surface area measurement

(1) Diffusion Measurement (Chronoamperometry)

In one dimensional linear diffusion, the current response to an applied constant potential to an unstirred solution is (35).

$$i = \frac{n F A D^{\frac{1}{2}} C}{\pi^{\frac{1}{2}} t^{\frac{1}{2}}} \qquad (2.8)$$

where i = current in amperes

A = Area in cm^2

D = Diffusion coefficient in $cm^2 . sec^{-1}$

C = Concentration in moles per cm^3

t = time in seconds.

Therefore, for a known reaction, measurement of current as a function of time for a fixed potential might be interpreted as an area. It is important, however, to demonstrate that diffusion control existed (rather than kinetic control) and to eliminate all sources of agitation. This technique, however, depends on the electrode geometry and the functional form of diffusion-current relationship differs for different electrode geometries.

(2) Coulometry (29)

The coulometric method depends on the measurement of the quantity of charge required to remove or deposit a known, or reproducible quantity of some substance, for example, the deposition of hydrogen on a platinum surface. The quantity of charge required to remove the deposit can be measured by applying a constant known current and observing the potential - time variation.

The completion of dissolution or deposition is indicated by a rapid variation in potential with time. However, atomic dimensions are required for the calculation in this technique. (36, 34).

(3) Impedance Bridge (37)

One of the most precise devices used for measuring double-layer capacitance is an impedance bridge. The working electrode, polarized with a D.C. source, is placed on one arm of a conventional bridge, and a repetitive perturbation, A.C. signal, is superimposed on this through the bridge circuit. When the bridge is balanced, the capacitance and resistive components of the impedance can then be determined. This technique is not attractive for porous and solid electrodes, because high power losses are sustained when large capacitances such as those anticipated with porous electrodes are involved. (38, 39).

(4) Galvanostatic Method

This technique was investigated by Bowden and Rideal (40) and Wagner (41). In this method, a current step is applied to an electrode in a galvanostatic connection and the resulting potential decay is measured in the non-faradaic region of the step. The electrode capacitance is then evaluated from the equation

$$C = \frac{i}{(\Delta E / \Delta t) A}$$

where C = capacitance of electrode

A = area of electrode

$\Delta E / \Delta t$ = potential - time response

i = current

(5) Charging curves

Experimental currents measured at continuously changing potential (see section 2.3) include a component resulting from the charging or discharging of the double layer at the interface electrode solution.

The differential capacity of the double layer is given by

$$C_d = \frac{-dQ}{dE} \qquad (2.9)$$

where C_d = differential capacity

Q = surface charge density

E = the electrode potential referred to a reference electrode.

For a cathodic sweep $E = E_i - vt$ (2.10)

where E = potential of electrode

E_i = starting potential of sweep

v = scan rate of potential

$$\therefore \frac{dE}{dt} = -v \qquad (2.11)$$

Now,

$$C_d = \frac{-dQ}{dt} \times \frac{dt}{dE} = \frac{1}{v} \frac{dQ}{dt} \qquad (2.12)$$

but,

$$\frac{dQ}{dt} = \text{capacity current per cm}^2 = i_c \qquad (2.13)$$

$$\therefore i_c = AC_d.v. \qquad (2.14)$$

where A = area of electrode.

Therefore, when a triangular wave of small amplitude (about 50 mV) is applied to a working electrode, potentiostated in a non-faradaic region, the electrode will behave as a pure capacitor, i.e. without a faradaic current or ohmic resistance,

the current response will be in the form of a square wave as shown in Fig. 2.8.

The peak to peak amplitude of the resulting square wave represents the current required for charging and discharging the double layer.

If i_{co} = initial peak to peak current of square wave before electrolysis, i.e. at time t = zero

A_o = initial area of electrode before electrolysis

i_{ct} = peak to peak current after electrolysis for t minutes

A_t = final area of electrode after t minutes of electrolysis.

then

$$\frac{i_{ct}}{i_{co}} = \frac{A_t}{A_o} \qquad (2.15)$$

This method is useful for comparison purposes and was, therefore, used in this research for measuring the increase in surface area of the working electrode during the electrolysis. It was found that the reproducibility of this method was within 20%. This was adequate for the purpose of finding the relative increase of the surface area of the electrode during electrolysis.

The bad reproducibility of this method can be ascribed to the following factors.

(a) It is sensitive to impurities in the electrolyte, since it is a potentiostatic method.

(b) The ohmic resistance, which in any real electrode system always exists in series with the capacitor, must be very small.

In fact, the resulting square wave is always distorted because of the two reasons given above as shown in Fig. 2.9.

2.4.c. Experimental

Copper deposition electrolysis was carried out as described in Section 2.2.b. Before and after every electrolysis, the copper electrode was soaked in distilled water and then placed in the cell shown in Fig. 2.10. Compartment A contained 0.5 M potassium sulphate at pH3. The counter electrode was 20cm^2 platinum foil placed in compartment A. Compartment B contained the same solution as compartment A. A commercial S.C.E. was placed in compartment B. Before every measurement compartment A was purged with oxygen-free nitrogen for 15 minutes. A triangular wave of 50mV amplitude was superimposed on the working electrode, potentiostated at -140 mV against the S.C.E. This was achieved by using a Chemical Electronics Wave-form generator, type RB1, and a Chemical Electronics potentiostat described in Section 2.1.a. The response of the copper electrode to the triangular ramp was monitored on a Solartron differential oscilloscope, type CD1400 CX 1442.3 The Circuit diagram for the above experiment is shown in Fig. 2.11.

2.5.a. Controlled Potential Electrolysis

It is the electrode potential that governs the rates and extent of the half electrochemical reactions that take place in a cell. By proper selection of the potential it is possible to isolate and study individual half-reactions to the exclusion of others. Therefore, it is possible to reduce or oxidize one constituent of a mixture while leaving others unaffected. This

selective ability of controlled potential electrolysis makes it a very valuable technique (43).

It is often possible to find conditions under which only a single substance is reduced or oxidized at an electrode whose potential is being controlled and under which only a single product is obtained. Then the total quantity of electricity consumed in the complete reduction or oxidation of No g. moles of starting material is given by Faraday's Law (43).

$$Q_{\infty} = \int_0^{\infty} i\,dt = nFNo \qquad (2.16)$$

where

Q_{∞} = quantity of electricity in coulombs required for completion of reaction

i = current in amperes.

t = time in seconds.

n = number of electrons involved in the half reaction in question.

Integrating the current under such conditions permits the calculation of n if No is known or of No if n is known.

For simple uncomplicated electrochemical reactions, i.e. those that are not coupled to chemical reactions, and only a single electrode reaction can occur with 100% efficiency, the current is governed by the rate of diffusion of reducible (or oxidizable) ions from solution to the electrode surface (44). The following derivation relating current to time and concentration is due to Lingane. (45, 46, 47)

The instantaneous current at any time during the electrolysis is

$$i_t = nF\left(\frac{dN}{dt}\right) \qquad (2.17)$$

where

i_t = instantaneous current

$\frac{dN}{dt}$ = number of g-moles that react at the electrode in unit time

when $\frac{dN}{dt}$ is controlled by the rate of diffusion from the body of the solution, then from Fick's Law

$$\frac{dN}{dt} = D\,A\,\frac{dc}{dx} \qquad (2.18)$$

where

D = diffusion coefficient in $cm^2 \cdot cm^{-1}$

A = Electrode area in cm^2

$\frac{dc}{dx}$ = concentration gradient at the electrode surface.

Combining 2.17and 2.18the instantaneous current is

$$i_t = nFDA\,\frac{dc}{dx} \qquad (2.19)$$

If we follow Nerst (48), and assume that when the solution is well stirred, the concentration of the diffusion layer is virtually a linear function of distance from the electrode then

$$\frac{dc}{dx} = \frac{C_o - C_s}{\delta} \qquad (2.20)$$

where

C_o = Bulk concentration of substance under study

C_s = Concentration of the substance at the electrode surface

δ = Nerst diffusion layer thickness.

Under the usual conditions of a controlled potential reduction with electrode potential about 0.1 volt or more negative than the formal electrode potential, C_s is so much smaller than C_o and

$$\frac{dc}{dx} = \frac{C_o}{\delta} \tag{2.21}$$

$$\therefore \quad i_t = \frac{nFDA}{\delta} C_o \tag{2.22}$$

If V is the volume of solution, then Faraday's Law is

$$C_t \; V = \frac{i_t \; t}{nF} \tag{2.23}$$

where C_t = Instantaneous bulk concentration of electroactive species

$$\therefore \quad \frac{dC_t}{dt} = \frac{i_t}{nF} \; \frac{1}{V} \tag{2.24}$$

Substituting equation (2.21) in (2.24)

$$\frac{dC_t}{dt} = \frac{nFAD \; C_t}{V\delta} \cdot \frac{1}{nF} = \frac{DA}{\delta V} \; C_t \tag{2.25}$$

The solution of equation (2.25) is

$$C_t = C_o \exp \left(- \frac{DA}{V\delta} \right) t$$

$$= C_o \exp (-kt) \tag{2.26}$$

where

$$k = \frac{DA}{V\delta} \tag{2.27}$$

Since

$$i_t \propto C_t$$

$$\therefore \; i_t = i_o \exp(-kt) \tag{2.28}$$

where

i_o = Initial current at start of electrolysis.

Now since

$$\frac{dQ_t}{dt} = i_t \tag{2.29}$$

$$\therefore \quad dQ_t = i_t \, dt$$

$$\therefore \quad \int_0^{\infty} dQ_t = \int_0^{\infty} i_t \, dt$$

$$Q_{\infty} = \int_0^{\infty} i_o \, e^{-kt} \, dt$$

$$= \frac{i_o}{k} = \frac{i_o}{2.303k} \quad \text{(using logarithm to base 10)} \qquad (2.30)$$

When log (current) is plotted against time, i_o is the intercept and k is the slope. Thus the result of a coulometric analysis may be calculated as soon as the electrolysis has run long enough to establish a slope and intercept of the curve. This results in a considerable saving in time effected by obviating the necessity of continuing the electrolysis until completion.

An important factor that affects the reproducibility of the result is the affect of stirring as this will determine the value of the Nerst diffusion layer, since it is difficult to ensure that the magnetic stirrer is placed exactly in the same place and stays there. Therefore, although the value of Q_{∞} is the same for duplicate experiments, the values of i_o and k can be different.

2.5.b. Choice of Optimum Potential

Let the equilibrium potential of the electrode be E_e and the potential at which the working electrode is potentiostated is E_f, then

$$E_e = E^{ol} + \frac{0.059}{n} \log C_e \qquad (2.31)$$

$$E_f = E^{ol} + \frac{0.059}{n} \log C_f \qquad (2.32)$$

where

C_e = Initial concentration of reducible species before start of electrolysis.

C_f = Final concentration of reducible species after completion of experiment.

E^{ol} = Formal electrode potential of system

Therefore,

$$\Delta E = E_f - E_e = \frac{0.059}{n} \log \frac{C_f}{C_e} \quad . \qquad (2.33)$$

Now to carry out the experiment to within 1% of completion, the ratio $\frac{C_f}{C_e}$ must be 10^{-2} or less, therefore

$$\Delta E = \frac{0.059}{n} \times (-2)$$

For a one electron process $\Delta E \simeq$ - 120 mV.

Hence the control potential is set up at about 120 mV more negative than the equilibrium potential for the system under study and the electrolysis is carried out. In fact no advantage is gained by carrying the electrolysis at potentials more negative than the value quoted above.

The best way of finding the optimum potential is to determine the current-electrode potential curve of the particular reaction under exactly the same conditions that will prevail in the actual experiment. Then the potential that occurs at the top of the plateau (or wave) of the corresponding reaction is chosen. Little is gained by employing a control potential greater than that corresponding to the top of the plateau, because as long as the potential is great enough to result in the current being diffusion controlled it becomes indifferent to further increase in potential (47).

2.5.c. Experimental

All solutions were prepared as described in the preceding sections. The cell used was the same as that shown in Fig. 2.a. The potential of the working electrode was potentiostated cathodically at -100 mV against the S.C.E. The resulting current-time response was recorded on an X - t recorder, calibrated before use. The circuit diagram is shown in Fig. 2.

Cu^{2+} = 200 p.p.m.
KCL = 0·005 m.
pH = 2.
Temperature = 25°C.

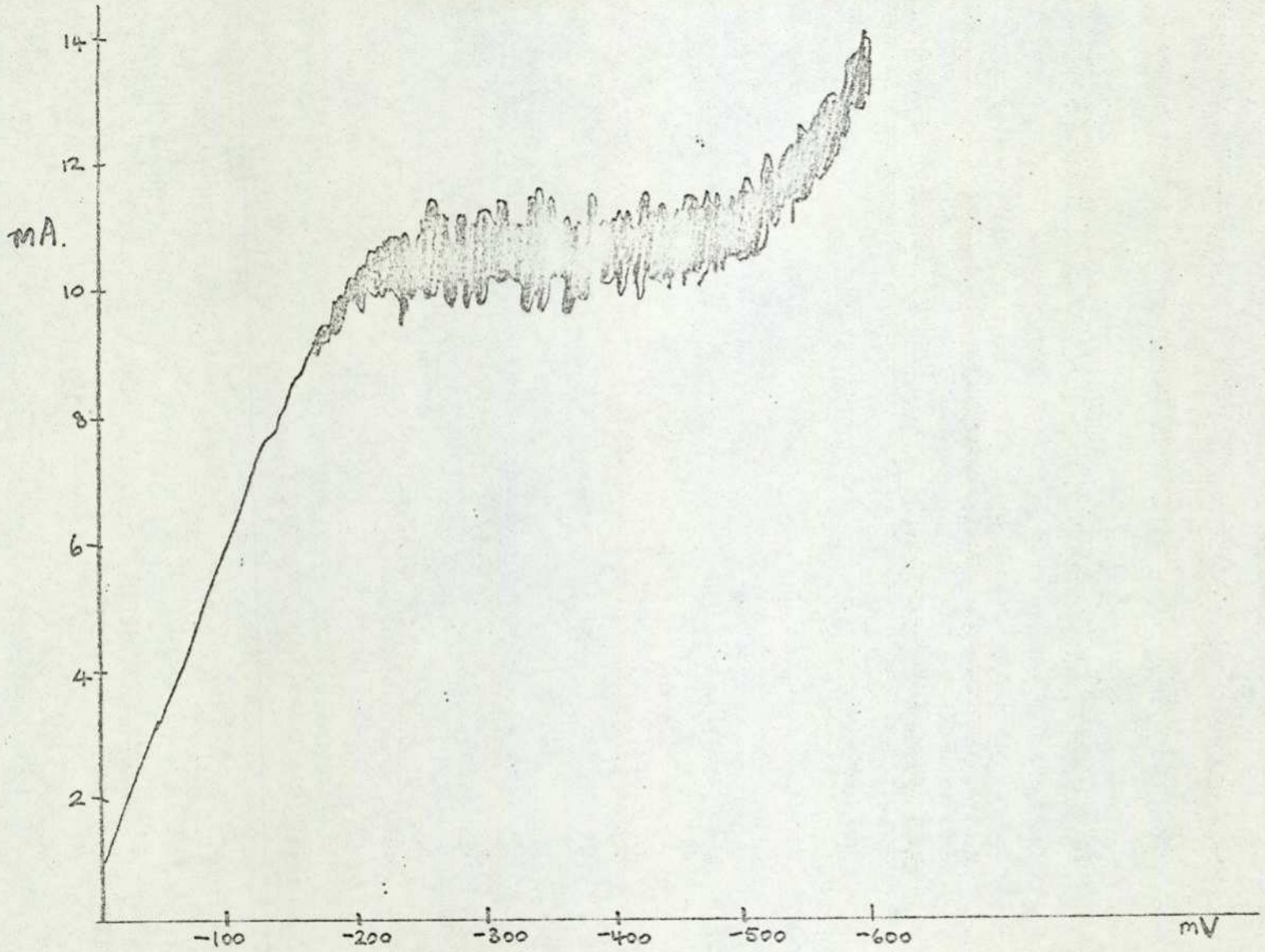


Fig. 2.1.

Steady state Current-potential curve for $CuSO_4$ (stirred solution).

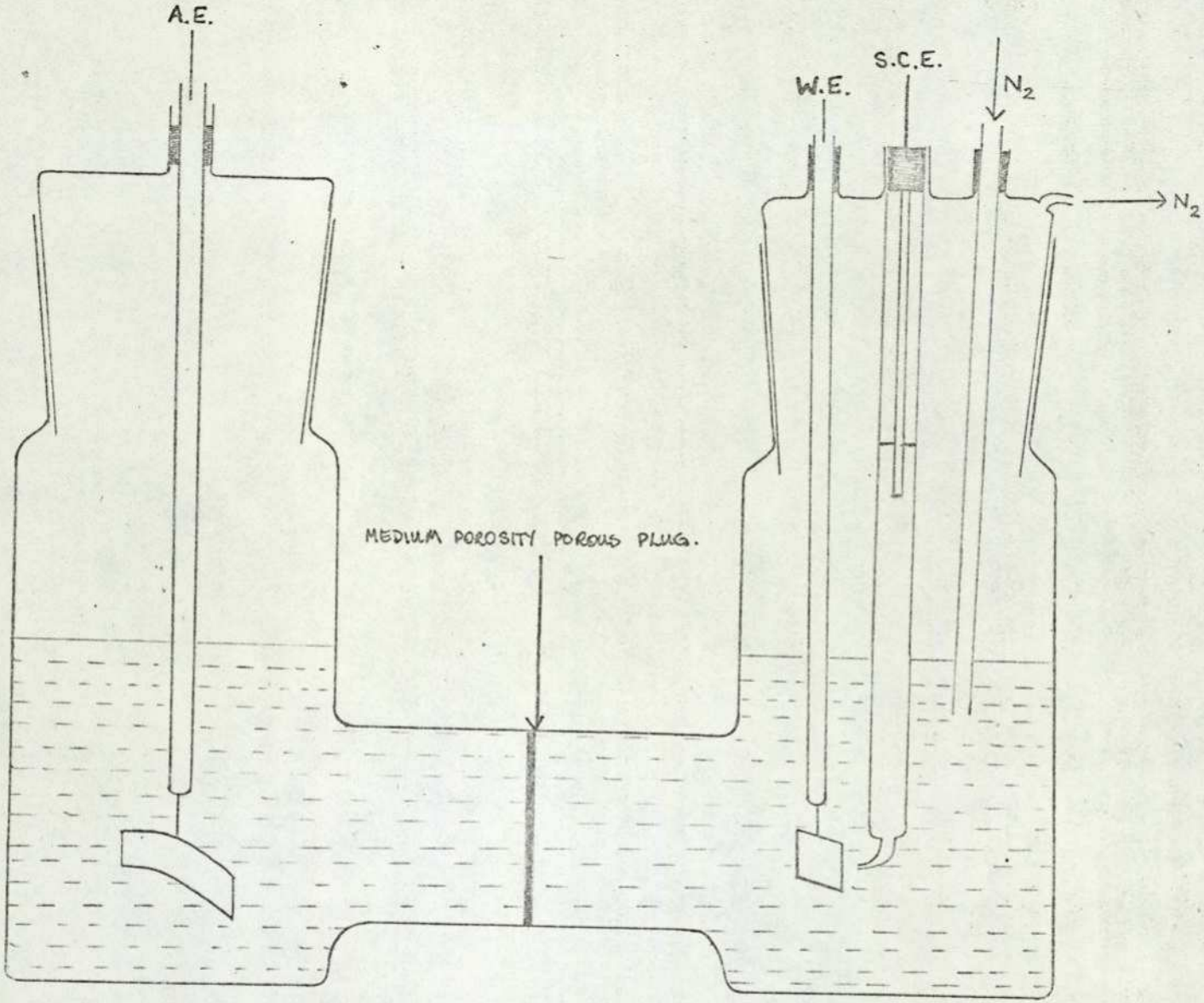


Fig 2.2

CELL USED FOR POTENTIOSTATIC POLARISATION.

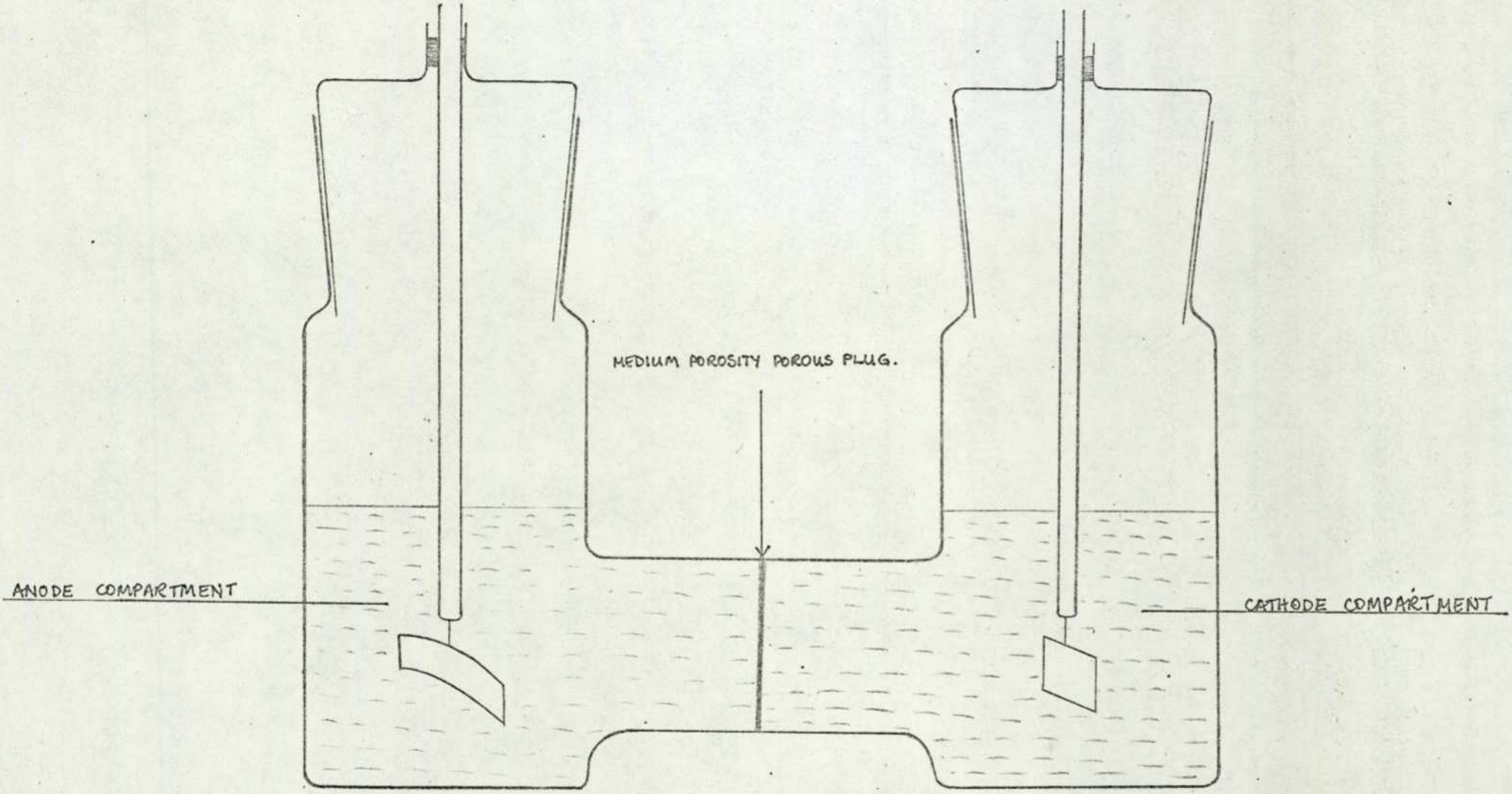


Fig. 2.2b.

CELL USED FOR CONSTANT CURRENT ELECTROLYSIS

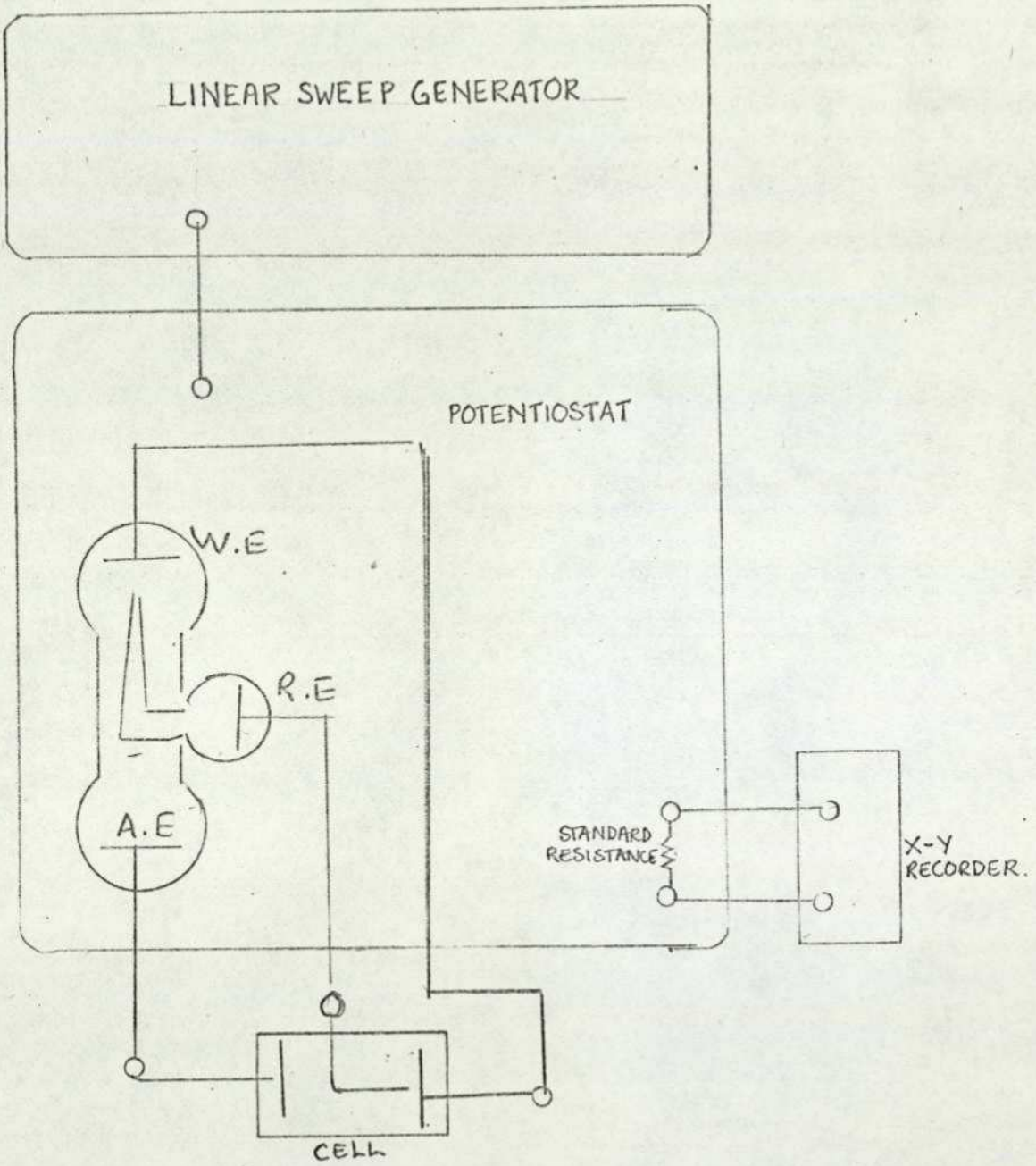


Fig. 2.3.

CIRCUIT FOR POTENTIOSTATIC POLARISATION.

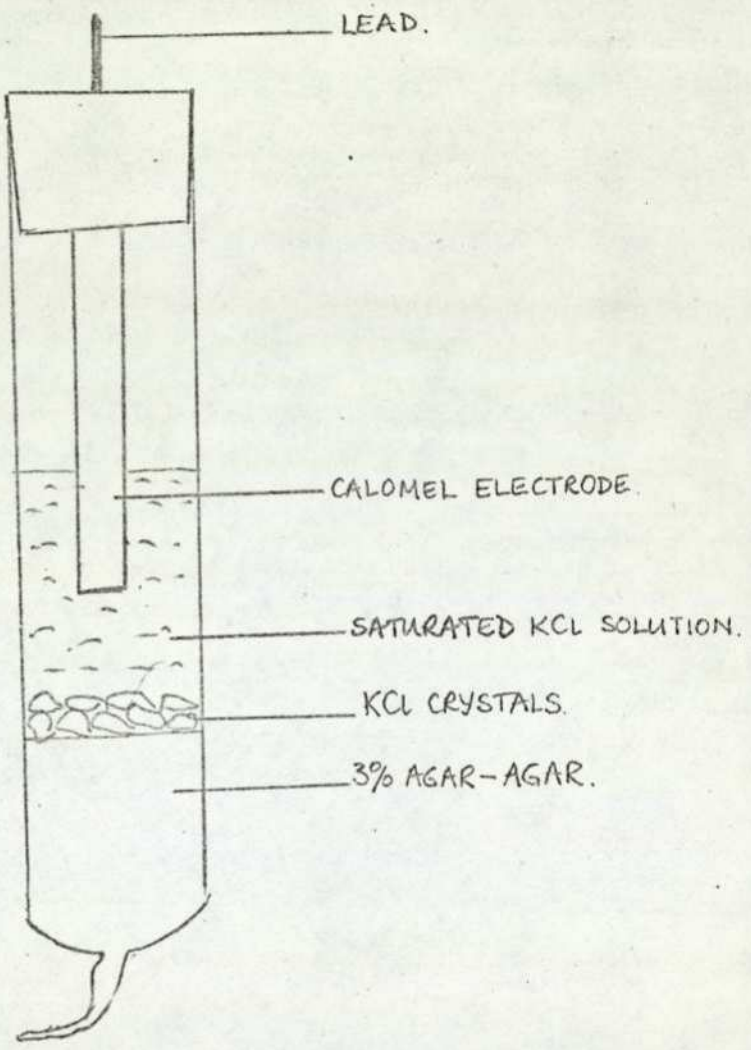


Fig. 2.4a.

S.C.E. WITH SALT BRIDGE

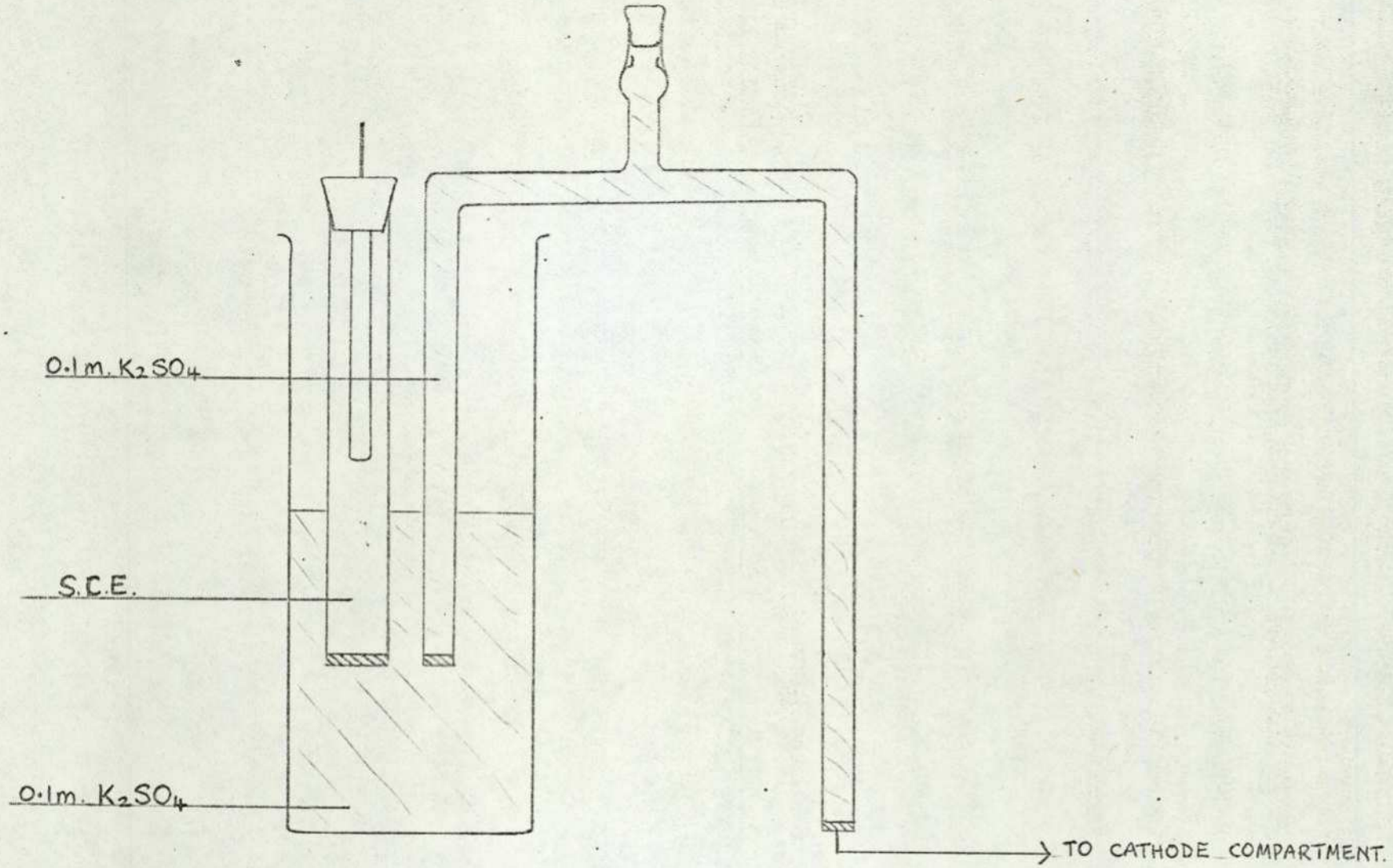


Fig. 2.4b.

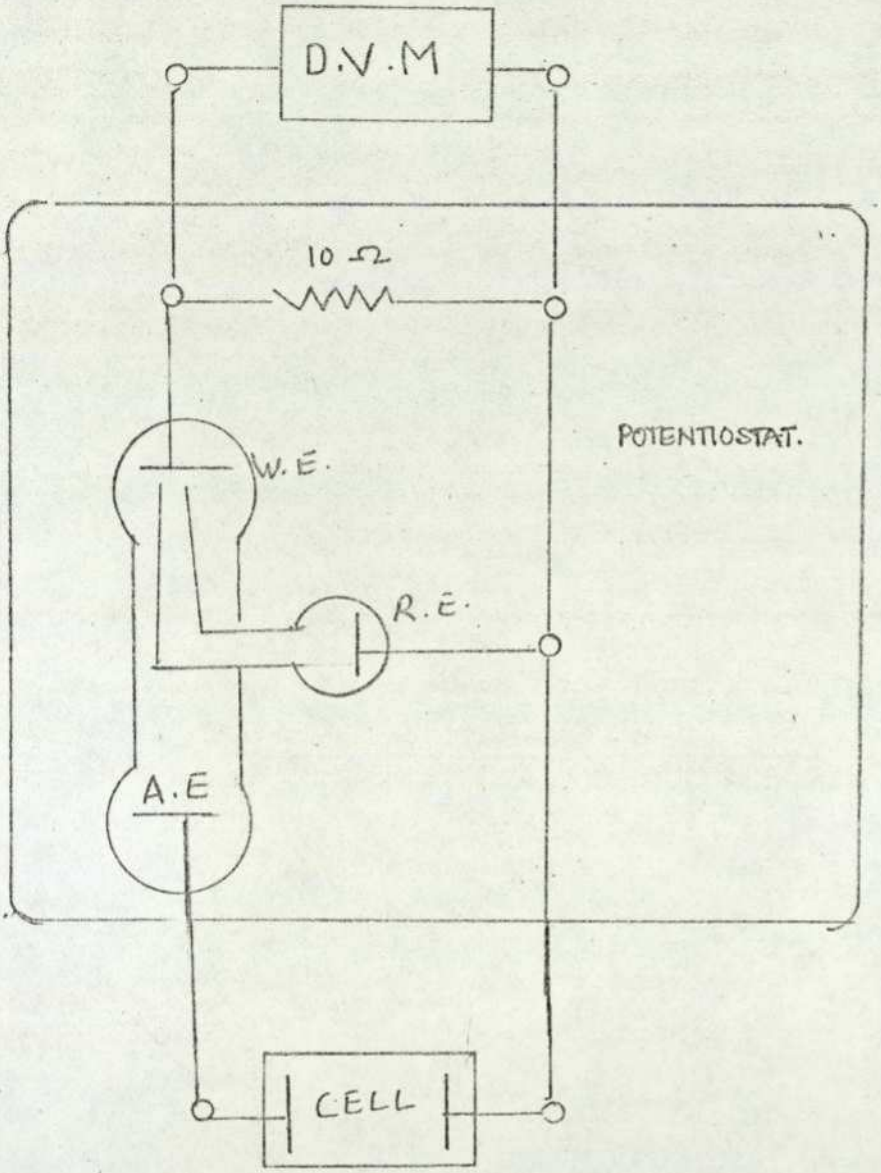


Fig. 2.5.

CIRCUIT DIAGRAM FOR CONSTANT CURRENT ELECTROLYSIS

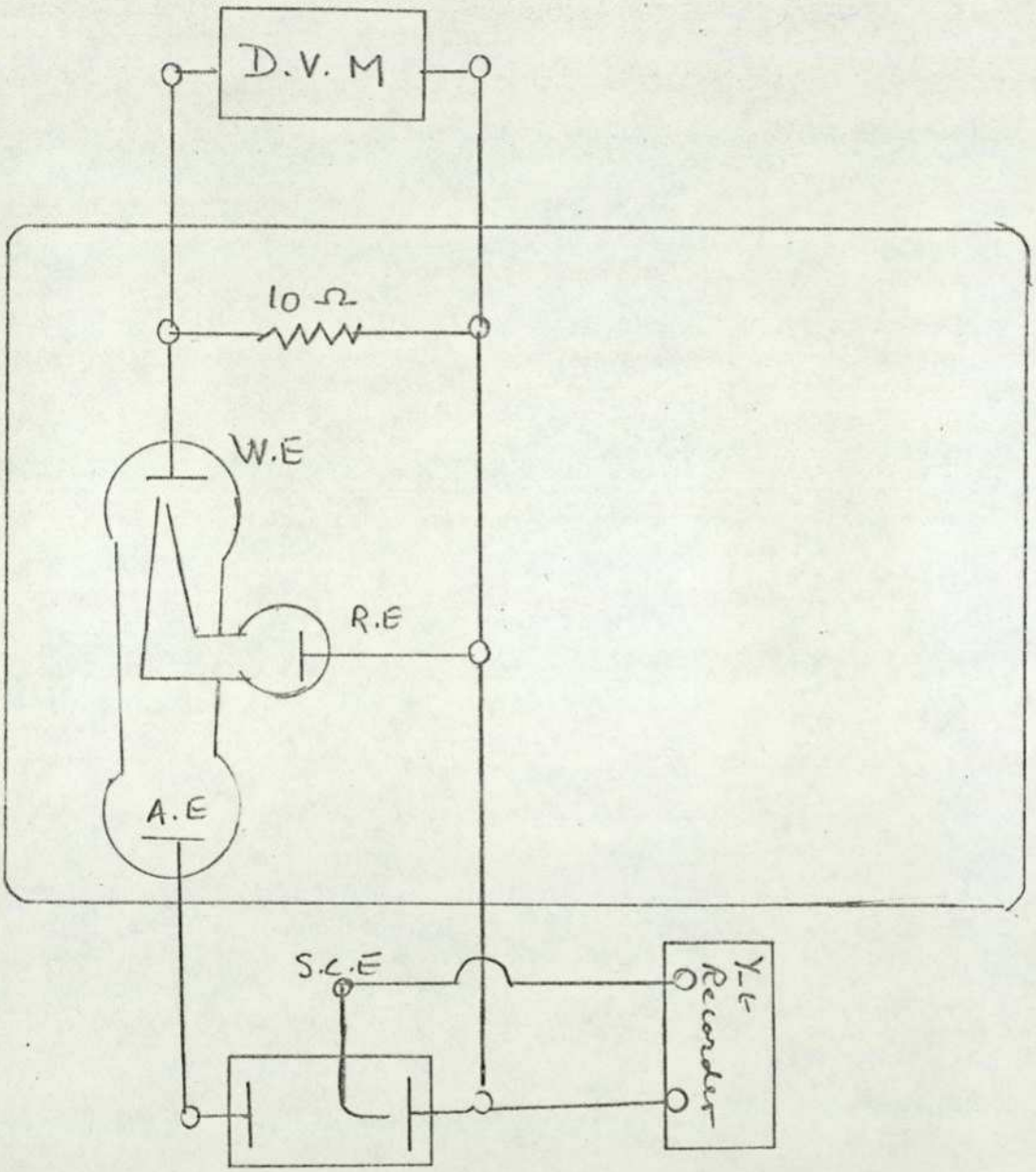


Fig. 2.6.

CIRCUIT DIAGRAM FOR MONITORING THE W.E. POTENTIAL DURING ELECTROLYSIS

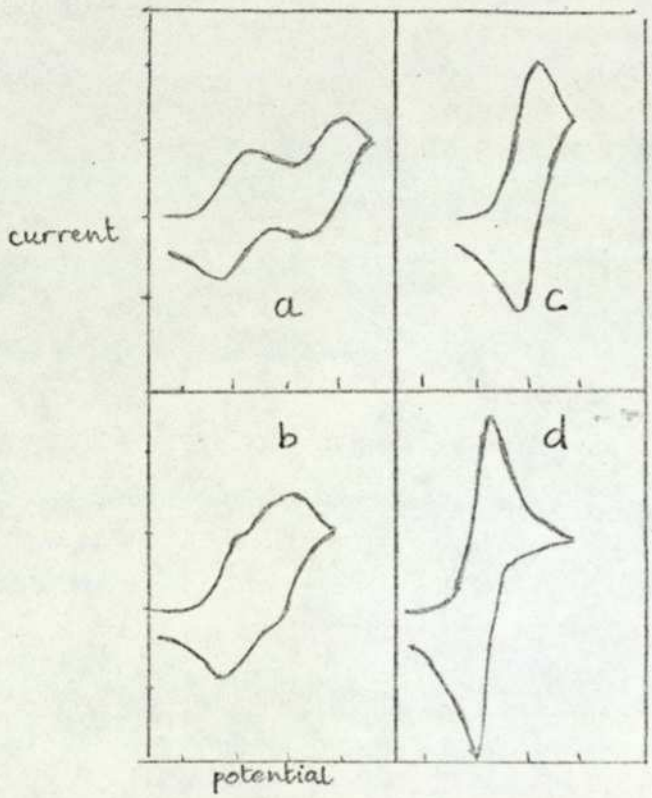


Fig. 2.7. Cyclic Voltammetry curves for multi-step charge transfer reactions, traced from ref. 21.

a. $\Delta E^{\circ} = -180$ mV.

b. $\Delta E^{\circ} = -90$ mV.

c. $\Delta E^{\circ} = 0$ mV.

d. $\Delta E^{\circ} = +180$ mV.

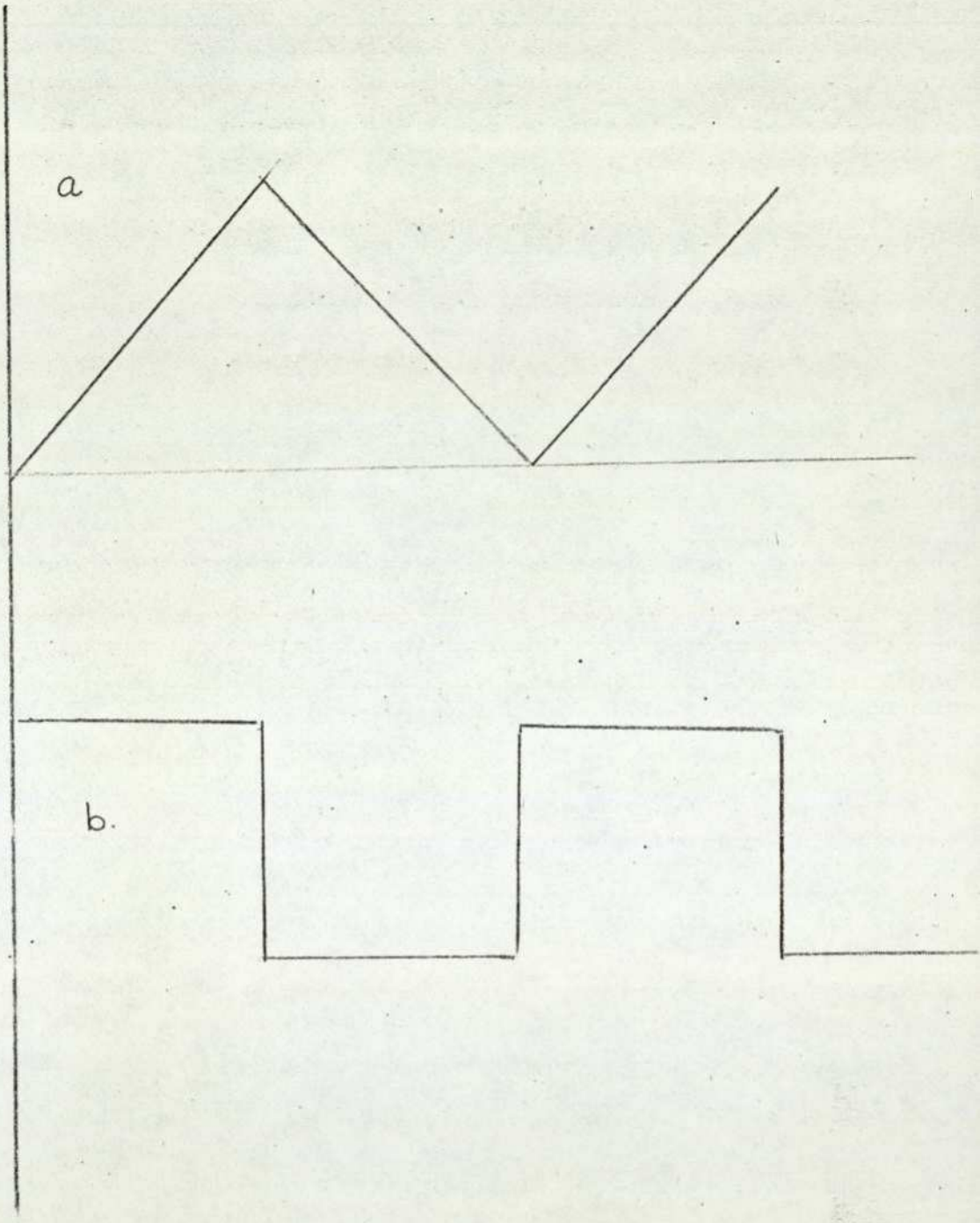


Fig 2.8.

a = TRIANGULAR WAVE , b = CURRENT RESPONSE.

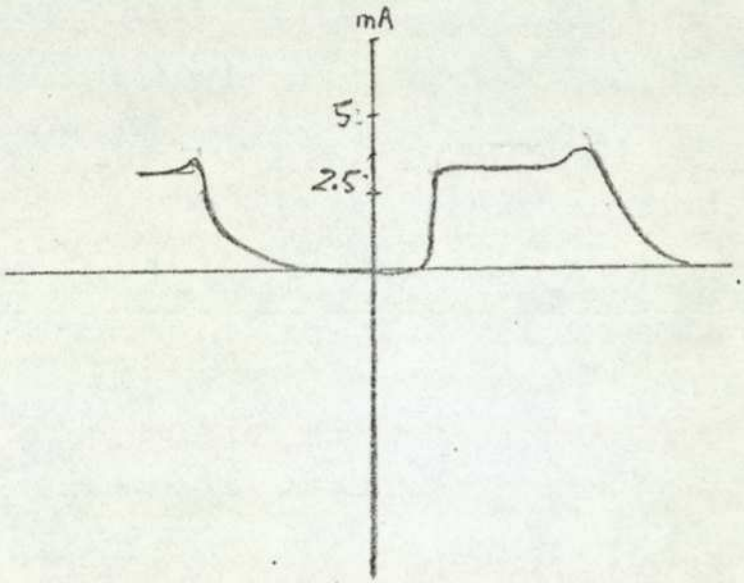


Fig. 2.9.

OBSERVED CURRENT-TIME RESPONSE FOR A COPPER ELECTRODE BEFORE START OF ELECTROLYSIS.

SCAN RATE = 4 V/S, ELECTRODE AREA = 7 cm^2.

PEAK HEIGHT OF TRIANGULAR WAVE = 60 m.V

OSCILLOSCOPE Y SCALE = 500 m.V/cm, RESISTANCE = 200 Ω
X-SCALE = 10 ms/cm

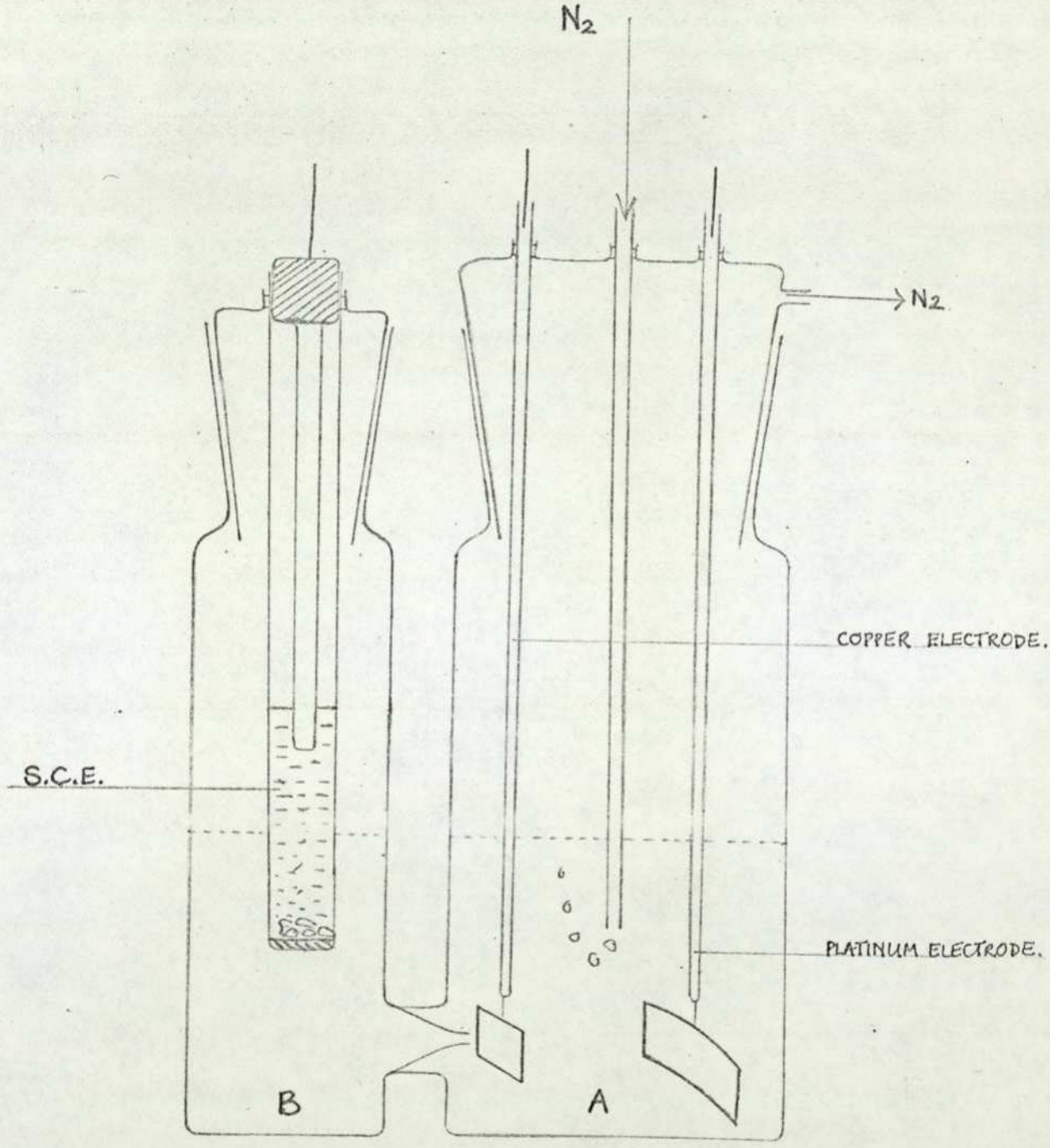


Fig. 2.10.

CELL USED FOR MEASURING SURFACE AREAS.

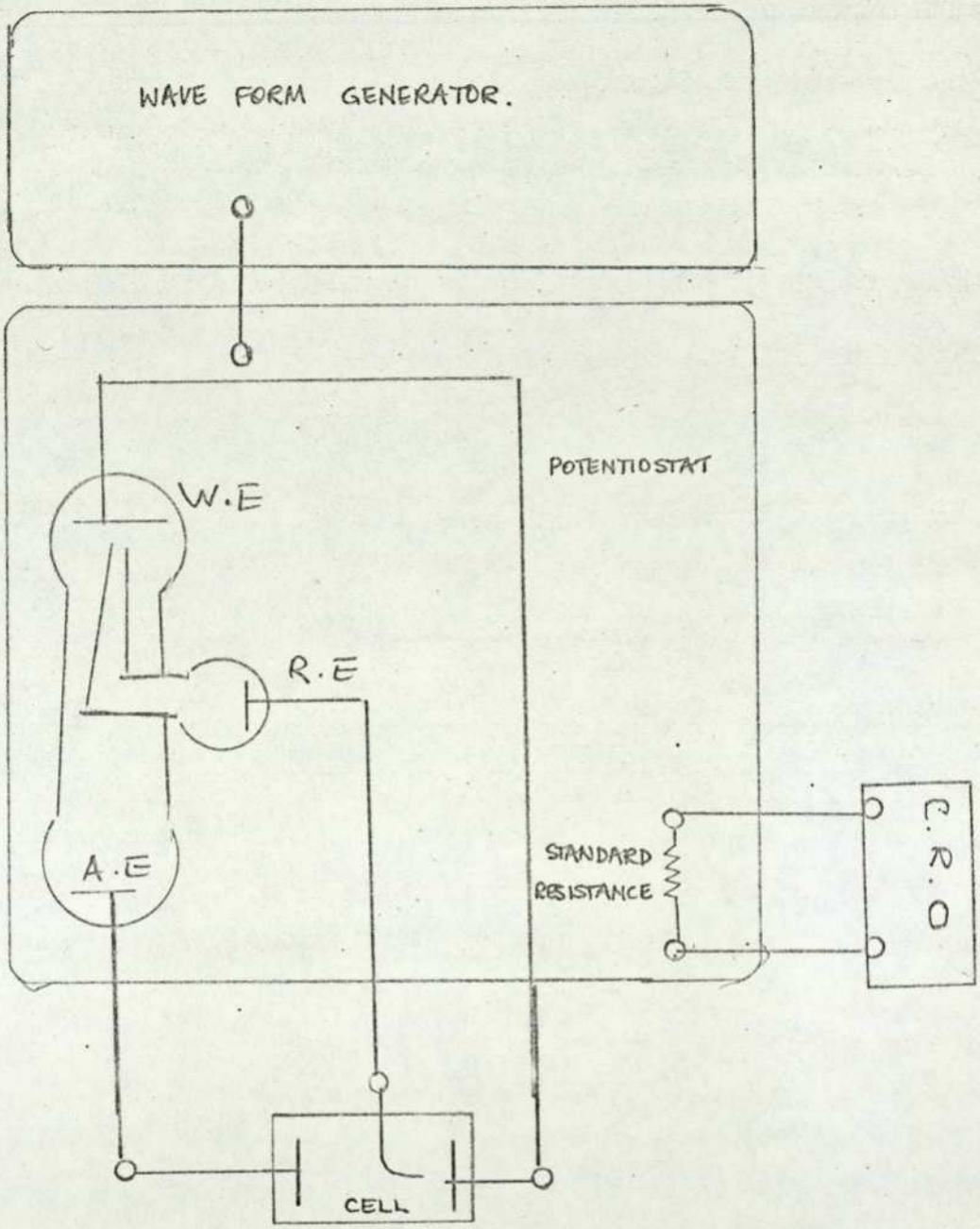


Fig. 2.11

CIRCUIT DIAGRAM FOR MEASURING SURFACE AREAS.

REFERENCES

CHAPTER II

1. E. Yeager and J. Kuta, in Physical Chemistry, an Advanced Treatise, Ed. H. Eyring, D. Henderson and W. Jost, Academic Press, 1970, Vol. 1A, Ch. 4.
2. N. Ibl, in Advances in Electrochemistry and Electrochemical Engineering, Ed. P. Delahay and C.W. Tobias, Interscience, 1962, Vol. 2, pp 49-143
3. N. Ibl and K. Schodegg, J. Electrochem. Soc., 1967, 144, 54.
4. New Instrumental Methods in Electrochemistry, by P. Delahay, Interscience, 1966, Ch. 11.
5. E.R. Brown and R.F. Large in Physical Methods of Chemistry, Ed. A. Weissberger and B.W. Rositer, Wiley - Interscience, 1971, Vol. 1, part IIA, Ch. 6.
6. S. Piekarski and R.N. Adams in Physical Methods of Chemistry, Ed. A. Weissberger and B.W. Rossiter, Wiley - Interscience, 1971, Vol. 1, part IIA, Ch. 7.
7. Electrochemical Techniques for Inorganic Chemist, by J.B. Headridge, Academic Press, Ch. 5, 196
8. J.E.B. Randle, Trans Faraday Soc., 1948, 44, 327.
9. A. Sevcik, Collection Czechoslov. Chem. Comm., 1948, 13, 349.
10. R.S. Nicholson and I. Shain, Anal. Chem., 1964, 36, 706
11. New Instrumental Methods in Electrochemistry, by P. Delahay, Interscience, 1966, Ch. 6.
12. T. Bergins and P. Delahay, J. Amer. Chem. Soc., 1953, 75, 555.

13. Z. Galus and R.N. Adams, J. Phy. Chem., 1963, 67, 862.

14. Z. Galus and R.N. Adams, J. Electroanal. Chem., 1963, 5, 17.

15. M. Nicholson, J. Amer. Chem. Soc., 1954, 76, 2539.

16. R.P. Frankenthal and I. Shain, J. Amer. Chem. Soc., 1956, 78, 2969.

17. W.H. Reinmuth, Anal. Chem., 1960, 32, 1891 and 1793.

18. P. Delahay, J. Amer. Chem. Soc., 1953, 75, 1190.

19. R. Nicholson and I. Shain, Anal. Chem., 1965, 37, 178.

20. R. Nicholson and I. Shain, Anal. Chem., 1965, 37, 190.

21. D.S. Polcyn and I. Shain, Anal. Chem., 1966, 38, 370.

22. D.S. Polcyn and I. Shain, Anal. Chem., 1966, 38, 376.

23. R.H. Wopschall and I. Shain, Anal. Chem., 1967, 39, 1514.

24. R.H. Wopschall and I. Shain, Anal. Chem., 1967, 39, 1527.

25. M.S. Shuman, Anal. Chem. 1969, 41, 142

26. R.N. Adams, Electrochem. at Solid Electrodes, Marcel Dekker, Inc. 1969

27. Y.P. Gokhstein and A.Y. Gokhstein, Advances in Polarography, ed. I.S. Longmuir, Volume II, p 465, Pergamon Press, New York, 1960.

28. D. Polcyn and I. Shain, Anal. Chem., 1966, 38, 376.

29. J.A. McCallum, R. Wittandy and R.F. Redmond, Measurements of True Surface area in Electrodes, Battelle Memorial Institute Technical Report AFAPL-TR-66-31, April 1966, under Contract U.S. Air Force AF33(615), 2225.

30. S. Brunauer, P. Emmett and E. Teller, J. Amer. Chem. Soc., 1938, 60, 309.

31. S. Brunauer, "The Absorption of gases and Vapours", Vol. 1, Princeton University Press, N.J., 1945.

32. P.H. Emmett, "Measurement of the the surface area of Solid Catalysts", Catalysis 1, 31 - 74, Reinhold Publ. Corp., N.Y. 1954.

33. A.J. Salkind in Techniques of Electrochemistry, Ed. E. Yeager and A.J. Salkind, Wiley - Interscience, Chapter IV, 1972.

34. P. Vassie, Thesis, City Univ., 1972.

35. New Instrumental Methods in Electrochemistry, P. Delahay, Ch. 3, Interscience, 1966.

36. New Instrumental Methods in Electrochemistry, by P. Delahay, Interscience Publishers, p.314, 1966.

37. D.C. Grahame, Ann. Rev. Phys. Chem, 1955, 6, 348.

38. J.J. McMullen and N. Hackermann, J. Electrochem. Soc., 1959, 106, 341.

39. R. Payne in Techniques of electrochemistry, Ed. E. Yeager and A.J. Salkind, Wiley - Interscience, Chapter 2, 1972.

40. F.P. Bowden and E.K. Rideal, Proc. Roy. Soc., London, 1928, 120, 80.

41. C. Wagner, J. Electrochem. Soc., 1950, 97, 71,

42. Perie Vassie, A.C.C. Tseung, B. Hobbs, Electrochemical Engineering Symposium, Newcastle, 1971, 1, 123

43. L. Meites in Physical Methods of Chemistry, Ed. A. Weissberger and B.W. Rossiter, Wiley - Interscience, 1971, Chapter 9, part IIA.

44. Coulometry in Analytical Chemistry, G.W.C. Milner and G. Phillips, Pergamon Press, 1967.

45. J.J. Lingane, J. Am. Chem. Soc., 1945, 67, 1916.

46. J.J. Lingane, Analyt. Chem. Acta., 1948, 2, 584.

47. Electroanalytical Chemistry by J.J. Lingane, Interscience, 1953.

48. W.Z. Nerst, Elektrochem. 1900, 7, 267.

CHAPTER 3

ELECTROLYSIS IN CHLORIDE MEDIUM

3.1.a. Potential pH Diagram

In the electromotive series the different redox equilibria are arranged according to increasing standard potential (1). Redox equilibrium means an electrochemical equilibrium.

$$Ox + ne^- \rightleftharpoons Red$$

where Red denotes the reduced form and Ox the oxidized. A reaction to the right is a reduction while a reaction to the left is an oxidation. The standard electrode potential, E^o, for a redox equilibrium is the potential, referred to the standard hydrogen electrode, in which all substances involved in the reaction are in the standard states.

When two redox pairs are brought into contact with each other an overall reaction consisting of a cathodic and an anodic reaction results. The direction of the reaction is such that the pair with the more noble potential, i.e. more positive, is reduced and that with the less noble potential is simultaneously oxidized. The electrode potentials of both the redox pairs thus give an indication of the reaction direction, and the potential differences indicate the extent of the thermodynamic driving force of the reaction. It must be remembered, though, that these electrode potentials are purely thermodynamic data and give no indication or information about the rate or the kinetics of the reaction.

The electrode potentials by themselves are, however, inadequate guides for assessing the direction of the reaction

because they are standard state values. As the Nerst equation shows

$$E = E^{o} + \frac{RT}{nF} \ln \left[\frac{OX}{Red}\right]$$

where $[OX]$ = activity of oxidized species

$[Red]$ = activity of reduced species

A change in activity involves a displacement of the electrode potential. If the solution is very dilute or contains constituents which can form complex compounds with the electroactive species, the displacement can be considerable. This displacement may cause different redox reactions to take place other than that indicated by the standard electrode potential. Another important reason for the inadequacy of the standard electrode potentials and electromotive series is that under certain conditions the metal surface acquires a stable coating of oxide or hydroxide salt, which hinders the ion exchange between electrode and solution and causes a displacement in the equilibrium potential. These passivation processes are pH dependent. Therefore, a potential pH diagram is necessary because in constructing such diagrams all the constituents of the solution are taken into consideration.

The potential pH diagram showing the potential pH dependence for different redox reactions dates back to the 1930s (3). However, it was Pourbaix (2) who developed the potential pH diagram into its present form.

The nature of the potential pH diagram will be illustrated by a diagram for the Cu - H_2O system (4) shown in figure (1). The abscissae represent the pH values and the ordinates represent the electrode potentials. Each line drawn

represents the associated values of pH and potential with equilibrium between the states of the metal and its compounds, as indicated on both sides of the line. The vertical lines correspond to pH- dependent non-redox processes, the horizontal to pH - independent redox processes and the sloped lines to pH - dependent redox processes.

The concentration of the copper ions is represented by numbers -1 to -6 written on the horizontal lines on the left hand side of the diagram. Number -1 represents a concentration of 10^{-1}M and so on. The dotted line b corresponds to reaction

$$O_2 + 4H^+ + 4e \rightleftharpoons 2\,H_2O$$

whose electrode potential (assuming that O_2 pressure = 1) is

$$E = 1.23 - 0.059pH$$

The dotted line a corresponds to the reaction

$$2H^+ + 2e \rightleftharpoons H_2$$

whose electrode potential, assuming that partial pressure of hydrogen is one atmosphere, is

$$E = 0.00 - 0.059\ pH$$

The region between lines (a) and (b) is the stability zone for water at atmospheric pressure. Within this zone lies, in most cases, the redox potential of the aqueous solutions.

At point (B) in Fig. 1. a thermodynamic motivity for the anodic dissolution of copper to copper ions and the cathodic reduction of oxygen to water exists. When conditions correspond to a point within the Cu^{2+} region the, Cu^{2+} state is usually thermodynamically stable, whereas the copper metal is unstable and

tends to dissolve, forming cupric ions. In other words, copper metal corrodes in the Cu^{2+} field. A similar line of reasoning applies to conditions corresponding to a point within the CuO_2^{2-} field.

Within the CuO(s) or Cu_2O(s) field (s denotes solid phase) the metal is passivated. At point (A) in Fig. 1., the reduction of Cu^{2+} to copper metal is thermodynamically favoured. Therefore, the copper metal is immune to corrosion at point (A). The same applies to all points lying within the Cu(s) region.

Mattsson(5) constructed the potential-pH diagram for the system Cu - H_2O - Cl^{1-}. Figs. 2 and 3 show the diagrams for solutions containing 10^{-1}M and 10^{-6}M copper ions in 1 M chloride medium respectively. Some of the basic reactions are discussed below.

The copper system electrode potentials are given by (7)

$$Cu^{2+} + 2e \rightleftharpoons Cu \qquad (3.1)$$

$$E = 0.338 + 0.029 \log [Cu^{2+}] \qquad (3.1a)$$

$$Cu^{2+} + e \rightleftharpoons Cu^{1+} \qquad (3.2)$$

$$E = 0.158 + 0.059 \log \frac{[Cu^{2+}]}{[Cu^{1+}]} \qquad (3.2a)$$

$$Cu^{1+} + e \rightleftharpoons Cu \qquad (3.3)$$

$$E = 0.521 + 0.059 \log [Cu^{+}] \qquad (3.3a)$$

Cupric ions form weak complexes with the chloride ions, therefore, the cupric ion chloride complexes could be neglected for simplicity's sake, and cupric ions could be assumed to exist in the hydrated state in a chloride medium.

The basic reactions between the cuprous and the chloride ions are given by (6).

$$CuCl(s) \rightleftharpoons Cu^{+} + Cl^{-} \qquad (3.4)$$

$$[Cu^{+}]\,[Cl^{-}] = 10^{-6.73} \qquad (3.4a)$$

$$CuCl\,(s) + Cl^{-} \rightleftharpoons CuCl_2^{1-} \qquad (3.5)$$

$$\frac{[CuCl_2^{-}]}{[Cl^{-}]} = 10^{-1.18} \qquad (3.5a)$$

$$Cu^{+} + 2Cl^{-} \rightleftharpoons CuCl_2^{-} \qquad (3.6)$$

$$\frac{[CuCl_2^{-}]}{[Cu^{+}]\,[Cl^{-}]^2} = 10^{5.55} \qquad (3.6a)$$

$$Cu^{+} + 3Cl^{-} \rightleftharpoons CuCl_3^{2-} \qquad (3.7)$$

$$\frac{[CuCl_3^{2-}]}{[Cu^{+}]\,[Cl^{-}]^3} = 10^{5.0} \qquad (3.7a)$$

$$\tfrac{1}{2}\,Cu_2O + \tfrac{1}{2}H_2O \rightleftharpoons Cu^{+} + OH^{-} \qquad (3.8)$$

$$[Cu^{+}]\,[OH^{-}] = 10^{-14.9} \qquad (3.8a)$$

The basic reactions between cupric and chloride ions are (6).

$$Cu^{2+} + Cl^{-} \rightleftharpoons CuCl^{+} \qquad (3.9)$$

$$\frac{[CuCl^{+}]}{[Cu^{2+}]\,[Cl^{-}]} = 1 \qquad (3.9a)$$

$$Cu^{2+} + 2Cl^{-} \rightleftharpoons CuCl_2 \qquad (3.10)$$

$$\frac{[CuCl_2]}{[Cu^{2+}]\,[Cl^{-}]^2} = 10^{0.3} \qquad (3.10a)$$

$$Cu^{2+} + 3Cl^{-} \rightleftharpoons CuCl_3^{-} \qquad (3.11)$$

$$\frac{[Cu\,Cl_3^-]}{[Cu^{2+}]\,[Cl^-]^3} = 10^{-1.15} \qquad (3.11a)$$

$$Cu^{2+} + 4Cl^- \rightleftharpoons Cu\,Cl_4^{2-} \qquad (3.11b)$$

$$\frac{[Cu\,Cl_4^{2-}]}{[Cu^{2+}]\,[Cl^-]^4} = 10^{-3.4} \qquad (3.11c)$$

By combining equations (3.2), (3.2a) (3.4) and (3.4a), equations (3.12) and (3.12a) are derived.

$$Cu^{2+} + Cl^- + e \rightleftharpoons Cu\,Cl\,(s) \qquad (3.12)$$

$$E = 0.555 + 0.059 \log[Cl^-] + 0.059 \log [Cu^{2+}] \qquad (3.12a)$$

By combining equations (3.2), (3.2a), (3.6) and (3.6a), equations (3.13) and (3.13a) are derived.

$$Cu^{2+} + 2Cl^- + e \rightleftharpoons Cu\,Cl_2^- \qquad (3.13)$$

$$E = 0.486 + 0.118 \log[Cl^-] + 0.059 \log \frac{[Cu^{2+}]}{[Cu\,Cl_2^-]} \qquad (3.13a)$$

By combining equations (3.2), (3.2a), (3.7) and (3.7a), equations (3.14) and (3.14a) are derived.

$$Cu^{2+} + 3Cl^- + e \rightleftharpoons Cu\,Cl_3^{2-} \qquad (3.14)$$

$$E = 0.453 + 0.177 \log[Cl^-] + 0.059 \log \frac{[Cu^{2+}]}{[Cu\,Cl_3^{-2}]} \qquad (3.14a)$$

By combining equations (3.3), (3.3a), (3.4) and (3.4a) equations (3.15) and (3.15a) are derived.

$$Cu\,Cl\,(s) + e \rightleftharpoons Cu + Cl^- \qquad (3.15)$$

$$E = 0.124 - 0.059 \log[Cl^-] \qquad (3.15a)$$

By combining equations (3.3), (3.3a), (3.6) and (3.6a), equations (3.16) and (3.16a) are derived.

$$CuCl_2^- + e \rightleftharpoons Cu + 2Cl^- \qquad (3.16)$$

$$E = 0.184 - 0.118 \log [Cl^-] + 0.059 \log [CuCl_2^-] \qquad (3.16a)$$

By combining equations (3.3), (3.3a), (3.7) and (3.7a), equations (3.17) and (3.17a) are derived.

$$CuCl_3^{2-} + e \rightleftharpoons Cu + 3Cl^- \qquad (3.17)$$

$$E = 0.226 - .177 \log [Cl^-] + 0.059 \log [CuCl_3^{2-}] \qquad (3.17a)$$

By combining equations (3.3), (3.3a), (3.8) and (3.8a), equations (3.18) and (3.18a) are derived.

$$\tfrac{1}{2} Cu_2O(s) + \tfrac{1}{2} H_2O + e \rightleftharpoons Cu(s) + OH^- \qquad (3.18)$$

$$E = 0.468 - 0.059\ pH \qquad (3.18a)$$

Finally, by combining equations (3.2), (3.2a), (3.8) and (3.8a), equations (3.19) and (3.19a) are derived.

$$Cu^{2+} + \tfrac{1}{2}H_2O + e \rightleftharpoons \tfrac{1}{2}Cu_2O + H^+ \qquad (3.19)$$

$$E = 0.105 + 0.059pH + 0.059 \log [Cu^{2+}] \qquad (3.19a)$$

These equations are summarised in table 3.1.

TABLE 3.1

EQUATIONS OF THE $Cu/H_2O/Cl$ SYSTEM

	Reaction	E^o
2	$Cu^{2+} + e \rightleftharpoons Cu^{1+}$	0.158
12a	$Cu^{2+} + Cl^- + e \rightleftharpoons CuCl$ (s)	$0.555 + 0.059 \log [Cl^-]$
13a	$Cu^{2+} + 2Cl^- + e \rightleftharpoons CuCl_2^-$	$0.486 + 0.118 \log [Cl^-]$
14a	$Cu^{2+} + 3Cl^- + e \rightleftharpoons CuCl_3^-$	$0.453 + 0.177 \log [Cl^-]$
19a	$Cu^{2+} + \frac{1}{2}H_2O + e \rightleftharpoons \frac{1}{2}Cu_2O + H^+$	$0.105 + 0.059$ pH
3.	$Cu^{1+} + e \rightleftharpoons Cu$ (s)	0.521
15a	$CuCl$ (s) $+ e \rightleftharpoons Cu$(s) $+ Cl^-$	$0.124 - 0.059 \log [Cl^-]$
16a	$CuCl_2^- + e \rightleftharpoons Cu$(s) $+ 2Cl^-$	$0.184 - 0.118 \log [Cl^-]$
17a	$CuCl_3^{2-} + e \rightleftharpoons Cu$(s) $+ 3Cl^-$	$0.226 - .177 \log [Cl^-]$
18a	$\frac{1}{2}Cu_2O + \frac{1}{2}H_2O \rightleftharpoons Cu$(s) $+ OH^-$	$0.468 - 0.059$ pH

N.B. Electrode potentials in this table are referred to the standard hydrogen electrode.

The reactions that are shown in figures (2) and (3) are summarised below in Table 3.2 and numbered as originally numbered by Mattsson (5). For more information reference (5) must be consulted.

Table 3.2

Reactions shown in Figures 2 and 3

Number	Reaction
18	$Cu\,Cl\,(s) + OH^- \rightleftharpoons \frac{1}{2}Cu_2O + Cl^- + \frac{1}{2}H_2O$.
19	$Cu\,Cl_2^- + OH^- \rightleftharpoons \frac{1}{2}\,Cu_2O + 2\,Cl^- + \frac{1}{2}\,H_2O$
20	$Cu\,(OH)_{1.5} \cdot Cl_{0.5}\,(s) \rightleftharpoons Cu^{2+} + \frac{1}{2}Cl^- + 1\frac{1}{2}\,OH^-$
21	$Cu(OH)_{1.5} \cdot Cl_{0.5}\,(s) + \frac{1}{2}OH^- \rightleftharpoons Cu\,O(s) + \frac{1}{2}\,Cl^- + H_2O$
25	$Cu\,Cl\,(s) + e \rightleftharpoons Cu\,(s) + Cl^-$
26	$Cu\,Cl_2^- + e \rightleftharpoons Cu\,(s) + 2\,Cl^-$
27	$\frac{1}{2}Cu_2O(s) + \frac{1}{2}\,H_2O + e \rightleftharpoons Cu(s) + OH^-$
28	$Cu^{2+} + Cl^- + e \rightleftharpoons Cu\,Cl\,(s)$
29	$Cu^{2+} + 2\,Cl^- + e \rightleftharpoons Cu\,Cl_2^-$
30	$Cu(OH)_{1.5}\,Cl_{0.5}\,(s) + \frac{1}{2}\,Cl^- + e \rightleftharpoons Cu\,Cl(s) + 1.5\,OH^-$
31	$Cu(OH)_{1.5}\,Cl_{0.5}(s) + 1\frac{1}{2}Cl^- + e^- \rightleftharpoons Cu\,Cl_2^- + 1\frac{1}{2}OH^-$
32	$Cu(OH)_{1.5}\,Cl_{0.5}(s) + e \rightleftharpoons \frac{1}{2}Cu_2O(s) + \frac{1}{2}Cl^- + \frac{1}{2}OH^- + \frac{1}{2}H_2O$
33	$Cu\,O\,(s) + 2\,Cl^- + H_2O + e \rightleftharpoons CuCl_2^- + 2OH^-$
34	$Cu\,O\,(s) + \frac{1}{2}H_2O + e^- \rightleftharpoons \frac{1}{2}\,Cu_2O(s) + OH^-$
35	$Cu(OH)_3^- + e \rightleftharpoons \frac{1}{2}\,Cu_2O(s) + 2OH^- + \frac{1}{2}H_2O$
36	$Cu(OH)_4^{-2} + e \rightleftharpoons \frac{1}{2}\,Cu_2O(s) + 3OH^- + \frac{1}{2}H_2O$

It can be seen from figures 1, 2 and 3 that the formation of Cu_2O occurs at higher pH values in the presence of chloride ions than it does in their absence. This is an advantage since the higher the pH of the solution, the higher is the potential separation between copper reduction and hydrogen evolution. Therefore, in the presence of chloride ions, one can operate at higher pH values without the fear of depositing Cu_2O. Furthermore, equations 3.2; 3.2a; 3.12; 3.12a; 3.13; 3.13a; and 3.14; 3.14a, show that the reduction of Cu^{2+} ions to Cu^{1+} ions is thermodynamically easier to achieve in the presence of chloride ions. This is an added advantage as the reduction of Cu^{2+} ions to copper metal proceeds through a reduction step which involves the reduction of Cu^{2+} to Cu^{1+} (8, 9, 10)

$$Cu^{2+} \xrightarrow{\text{slow}} Cu^{1+} \rightleftharpoons Cu$$

Bockris and Mattsson (8) found that at high current densities the values of activation overpotential are a linear function of the logarithm of the current density. Therefore, they concluded that a charge transfer process controls the overall rate of copper metal deposition and dissolution. They also found that the linear branches of the anodic and cathodic Tafel plots met at the same point on the log i axis. This indicated to them that the same rate determining step is effective for deposition as well as dissolution reactions of copper metal. Furthermore the same workers found that the slopes of the anodic and the cathodic Tafel plots differed considerably. In other simple metal deposition and dissolution reactions, however, (for example silver from silver perchlorate solution (11, 12) the slopes of the anodic and the

cathodic Tafel plots were found to be the same. These findings excluded the possibility of a simple, one-step reduction, such as

$$Cu^{2+} + 2e \rightleftharpoons Cu$$

being the rate determining step, and suggested that a consecutive reaction is involved, such as

$$Cu^{2+} + e \xrightarrow{slow} Cu^{1+} \quad \text{rate determining step}$$

$$Cu^{1+} + e \rightleftharpoons Cu \quad \text{fast}$$

This seems logical since it would be more difficult to discharge the Cu^{2+} ion to copper metal than the Cu^{1+} ion, due to the fact that the cupric ion is more strongly solvated in water than the cuprous ion. It is, after all, a well known rule that if a metal exists in more than one oxidation state, then the higher oxidation state has a higher degree of solvation in water than its lower counterpart (13, 13a, 14, 15).

The results of Bockris and Mattsson were later confirmed by other workers (9, 10). Since it is out of the scope of this thesis to discuss the mechanism of reduction of Cu^{2+}, the author recommends the thesis published by J.C. Reeve for further information and references on this subject (16).

Using a Rotating Disc Electrode (R.D.E.), Nekrasod and Berezina found (24, 25) that, if the reduction of cupric ions to copper metal is carried out in a solution containing a complexing ligand, like chloride ion, which stabilizes the cuprous state, then the polarization curve for the reduction contains two well-defined waves, corresponding to

$$Cu\ (II) \xrightarrow{e} Cu\ (I) \qquad (3.20)$$

$$Cu\ (I) \xrightarrow{e} Cu\ (0) \qquad (3.21)$$

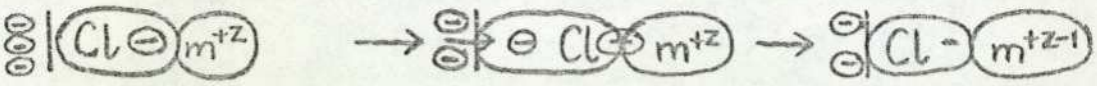
Using a Ring-Disc Electrode and oxidizing the produced cuprous ions at the Ring Electrode, they were able to find the corresponding limiting oxidation current in a solution containing complexing ions (chloride ions). The same workers were also able to detect the oxidation current for cuprous ions in a copper sulphate solution using a Rotating Ring-Disc Electrode. But they found that the value of the ring current, which corresponds to oxidizing the cuprous ions produced was smaller than that of the solution containing chloride ions, and, in fact, they observed only one wave in the cathodic polarization curve of a copper sulphate solution on a Rotating Disc Electrode.

Peters and co-workers (26, 27) studied the chrono-potentiometric behaviour of copper (11) and copper (1) in chloride and bromide media. They also observed two waves corresponding to equations (3.20) and (3.21). They calculated the diffusion coefficient of the cuprous complex $Cu\,Cl_2^-$, and found it to be 1.33 x 10^{-5} $cm^2 . sec^{-1}$, as compared to a value of .78 x 10^{-5} $cm^2 . sec^{-1}$, corresponding to the diffusion coefficient of the cupric ion in the same solution. They concluded that the cuprous state is stable towards disproportionation in halide media, and the equilibrium between the cupric and the cuprous ions is shifted towards the cuprous state in the layers next to the cathode under the influence of a reducing potential (20).

The larger diffusion coefficient of the cuprous complex should assist in the mass transfer and therefore efficiency of deposition, especially if the cuprous ions are present in the bulk of solution before the start of copper deposition.

Heyrovsky (17) offered the following explanation for the favourable effect of chloride ions on the efficiency of copper deposition. The chloride ion is easily polarized and the centre of its electric charge is shifted when subjected to an electric field. The chloride ion seems to promote the transfer of electrons from cathode to the cations. This may be achieved by transmitting the electron through the deformed ion with its negative end attached to the cation and the positive end attached to the cathode. Therefore the chloride ion gives the cation an electron at one end and, at the same time, acquires an electron from the cathode at the other end.

The chloride ion must have some affinity for the cation before it can act as an anion bridge between the cathode and the cation. The mechanism is shown in the diagram below.



The idea of an anion bridge mechanism is not new in chemistry, and manifests itself most clearly in charge - transfer spectra (18, 19), where the first, strong absorption band of a transition metal compound shifts to longer wavelengths as the ligand becomes more easily oxidized (polarized). These bands correspond to transitions in which the metal ion is reduced by the polarized anion. More often, however, the electron displaced during the transition leading to the above mentioned spectra returns to its original position so that there is no net chemical reaction (18).

If a charge transfer band occurs at a sufficiently long wavelength, it means that the energy which must be supplied to achieve a permanent oxidation reduction reaction is very small. Thus a complex of a slightly more oxidizable ion should undergo spontaneous oxidation - reduction reaction. For example, the cupric-halide systems, e.g. Cu^{2+} - Cl , Cu^{2+} - Br and Cu^{2+} - I, have charge transfer bands at quite long wavelengths, as shown by the dark colours of concentrated solutions of cupric chloride or bromide. But upon the addition of an iodide ion to a cupric solution, an oxidation - reduction reaction takes place, resulting in the formation of a cuprous iodide (or cuprous iodide complex, depending on concentration of iodide ion) and the liberation of iodine.

Another example of charge transfer is the mixed valency complexes, such as $K\,Fe^{(III)}\left[Fe^{(II)}(CN)_4\right]$ and $Cs_2\left[Au^{(I)}Cl_2\right]\left[Au^{(III)}Cl_4\right]$ where the ligand transfers electrons from one valency state to the other in the complex, resulting in intense charge transfer bands (19).

It must be stressed that the above examples are by no means conclusive evidence for the anion-bridge mechanism. Heyrovsky offered no direct experimental evidence for the mechanism.

Pomosov and co-workers (20, 21) found that halide ions have a substantial influence on the cathodic deposit, for example, small amounts of chloride ions promote the formation of friable copper deposits. Therefore, to obtain a copper powder with dendritic particle shapes, small concentrations of chloride ions should be deliberately added to the electrolyte.

This was shown (20) by electron microscopic studies and by studying the increase in the transition time (chronopotentiometry) (23). As the chloride ion concentration changes, Pomosov found that the effect of chloride ions on the electrode polarisation during the discharge of the cupric ions results in higher limiting currents. The value of the limiting current reached a maximum at certain chloride ion concentrations. He ascribed the higher values of limiting currents to the anion-bridge mechanism, which lowers the discharge activation energy and therefore promotes the rapid growth of new nucleation sites. These effects will result in increasing the surface area of the electrode which, in turn, has a favourable influence on the efficiency of deposition. In fact, as will be shown later in this chapter, the author's results confirm the fact that chloride ions tend to increase the deposition efficiencies and increase the surface area of the electrode during deposition.

3.1.b Results and Discussion

In all experiments described in this chapter, the concentration of copper (Cu^{2+}) was 200 p.p.m.; pH of the solution was 2; potassium chloride concentration 0.1 molar and temperature of water bath 25°C, unless otherwise stated.

As stated in Chapter Two all results presented in this work are the average of at least two separate experiments. Table 3.2a gives a sample of such results.

TABLE 3.2a

Potassium chloride	=	0.1 molar
pH	=	2
Temperature	=	25°C

Current = 15 mA

Electrode area = 7 cm^2

Volume of Solution = 150 ml.

Time (min)	Copper Concentration (p.p.m.)	Average Result	% Efficiency
0	200		
30	155, 156, 154	155	75.9
60	94, 95	95	88.6
90	45, 47, 49	47	86.6
120	18, 16, 20	18	76.8

Figs. 4, 5 and 6 show the current-potential curves for stirred solutions with and without chloride ions. The figures clearly show that although the limiting current for chloride-free ion solutions is approximately equal to those with chloride ions, it is clear that hydrogen evolution starts at lower electrode potentials in the former case. This was further substantiated by monitoring the potential of the copper cathode during constant-current electrolysis at currents higher than the limiting current, as shown in figs. 7a and 7b. These figures show that the copper cathode is at a more positive potential during the course of electrolysis in the presence of the chloride ions than in their absence. This is reflected by the higher efficiency of deposition of copper from solutions containing chloride ions as shown in table 3.3 and fig. 8.

TABLE 3.3.

pH	=	2
Initial copper concentration	=	200 p.p.m.
Volume of solution	=	150 ml.
Temperature	=	$25^{o}C$
Electrode Area	=	7 cm^2
Constant current	=	15 mA
Time of electrolysis	=	120 min.

KCL concentration	Final concentration of copper after 120 min. electrolysis	% efficiency
0.0 molar	50 p.p.m.	63.3
0.0005 molar	25 p.p.m.	73.8
0.001 molar	18 p.p.m.	76.8
0.003 molar	18 p.p.m.	76.8
0.005 molar	18 p.p.m.	76.8
0.01 molar	16 p.p.m.	77.6
0.02 molar	16 p.p.m.	77.6
0.1 molar	18 p.p.m.	76.8

All the above results show that, as expected, the presence of chloride ions improves the efficiency of deposition. But it was surprising to find that the limiting current for solutions containing chloride ions was slightly lower than for those without chloride ions. A possible explanation for this unexpected discrepancy is that although the diffusion coefficient of the cuprous-ion complex is nearly double that of the cupric ion, it is counteracted by the fact that the deposition of cupric ions requires two electrons,

while that of the cuprous requires one electron, as shown by equations (3.1) and (3.16)

$$Cu^{2+} + 2e \rightleftharpoons Cu \qquad (3.1)$$

$$CuCl_2^- + e \rightleftharpoons Cu + 2Cl^- \qquad (3.16)$$

Assuming that the Nernst diffusion layer is the same for the cupric and the cuprous ions, then the limiting current for Cu^{2+}/Cl^- system is given by equation (3.22)

$$i_l = \frac{n_1 FD_1 C_1 A}{\delta} + \frac{n_2 FD_2 C_2 A}{\delta} \qquad (3.22)$$

where $n_1 = 1$

$n_2 = 2$

D_1 = diffusion coefficient of $CuCl_2^-$

D_2 = diffusion coefficient of Cu^{2+}

C_1 = bulk concentration of $CuCl_2^-$

C_2 = bulk concentration of Cu^{2+}

Since $D_1 \simeq 2D_2$, therefore $n_1FD_1 = n_2FD_2$, therefore equation (3.22) can be reduced to

$$i_l = \frac{n_2 FD_2 A}{\delta} (C_1 + C_2) \qquad (3.23)$$

But, in the absence of reducing agent, $C_2 \gg C_1$, therefore

$$i_l \simeq \frac{n_2 FD_2 A C_2}{\delta} \qquad (3.24)$$

Hence the limiting current should not increase unless there is an appreciable concentration of $CuCl_2^-$ and $D_1 > 2D_2$, as will be shown in Chapter 4.

Table 3.4 shows the results of electrolysis at different pH.

These results indicate that the efficiency of deposition is not affected by pH values up to pH4. At pH values of 4 and above the solution becomes turbid and, finally, a precipitate forms. This is to be expected for the following reason :-

The buffer capacity of an unbuffered solution at pH4 is bad (28), and therefore any slight increase in hydroxyl ion concentration will increase the pH and force the cupric ions to form the insoluble hydroxide. During the electrolysis, because of the side reaction, namely hydrogen ion reduction, the pH of the solution close to the cathode increases.

Table 3.4

Initial copper concentration	=	200 p.p.m.
Current	=	15 mA
Electrode area	=	$7cm^2$
Time of electrolysis	=	120 min.
KCL concentration	=	0.1 molar
Volume of solution	=	150 ml.

pH	Final concentration of copper after 120 min. electrolysis	% efficiency
1	18 p.p.m.	76.8
2	18 p.p.m.	76.8
3	16 p.p.m.	77.6
4	a precipitate was formed	

These results are in agreement with the work of Meyers (29).

Table 3.5 and Fig. 9 show the effect of temperature on the efficiency of deposition. Again, the temperature has little effect on the rate of deposition, in agreement with the paper published by Kuhn (22).

Table 3.5

Initial copper concentration	=	200 p.p.m.
pH	=	2
KCL concentration	=	0.1 molar
Current	=	15 mA
Electrode area	=	7 cm^2
Time of electrolysis	=	60 min.
Volume	=	150 ml

Temperature	Final concentration of copper after 60 min. electrolysis	% efficiency
25°C	95 p.p.m.	88.6
36°C	93 p.p.m.	90.3
45°C	91 p.p.m.	91.9
53°C	90 p.p.m.	92.8

Table 3.6 and Fig. 10 and 11 show the results of electrolysis of solutions containing chloride ions at current densities below and above the limiting current. The cause of the flat maximum in the efficiency curves will be discussed in the next section, but all the results show that the efficiency of deposition is comparable to those systems using sophisticated cell designs.

Table 3.6

K Cl = 0.1 molar

pH = 2

Temp. = 25°C.

Electrode area = 7 cm^2

Volume = 150 ml

	Current mA	Time Minutes	copper conc. p.p.m.	% efficiency
(a)	7 mA			
		0	200	
		60	153	84.98
		90	126	89.2
		120	103	87.7
		180	54	87.99
		240	10	85.9
(b)	15 mA			
		0	200	
		30	155	75.9
		60	95	88.6
		90	47	86.6
		120	18	76.8
(c)	21 mA			
		0	200	
		30	136	77.1
		60	66	80.7
		90	26	69.9
		120	8	57.9
(d)	30 mA			
		0	200	

(d) Continued

Current mA	Time Minutes	Copper conc. p.p.m.	% efficiency
30 mA	15	154	75.9
	30	110	76
	60	45	65.4
	90	10	53.4

3.1.c Effect of Surface Area

Figure 12 and tables 3.7, 3.8, 3.9, 3.10 show the relative increase in surface roughness against time during the electrolysis at different current densities. (i_l = 1.43 mA/cm^2)

Table 3.7

K Cl. = 0.0 molar

i = 2.14 mA/cm^2

$\frac{dv}{dt}$ = 1.53 v/sec

Potential range = -140 to - 190 mV against S.C.E.

Time (Minutes)	i_{ct} (mA)	i_{ct}/i_{co} *
0	0.37	
15	2.6	7.0
30	3.15	8.5
45	3.7	10
60	5.25	14.2
90	6.6	17.8
120	8.21	22.2

* TErms i_{ct} and i_{co} are explained in Chapter two, section 2.4.b.(5)

Table 3.8

K Cl. = 0.005 molar

i = 2.14 mA/cm^2

$\frac{dv}{dt}$ = 1.53 v/sec

Potential Range = -140 to -190 mV against S.C.E.

Time (Minutes)	i_{ct} (mA)	i_{ct}/i_{co}
0	0.4	
15	3.4	8.5
30	5.6	14.4
45	7.	17.5
60	8.6	21.5
90	12.5	31.2
120	17.6	44

Table 3.9

K Cl. = 0.005 molar

i = 1 mA/cm^2 (Less than limiting current)

$\frac{dv}{dt}$ = 1.53V/sec

Potential Range = -140 to - 190 mV against S.C.E.

Time (Minutes)	i_{ct} (mA)	i_{ct}/i_{co}
0	0.34	
60	0.37	1.1
120	0.96	2.8
150	1.88	5.53
180	3.38	9.95
210	7.0	20.5

Table 3.10

K Cl. = 0.005 molar

i = 4.28 mA/cm^2 (Higher than limiting current)

$\frac{dv}{dt}$ = 1.53v/sec

Potential range = -140 to - 190 mV against S.C.E.

Time (Minutes)	i_{ct} (mA)	i_{ct}/i_{co}
0	0.45	
15	7.0	15.5
30	10.9	24.3
45	14	31
60	17.1	38
75	18.5	46.3
90	27.9	62

The copper deposited during the electrolysis at current densities larger than the limiting current density was powdery in form and dark red in colour. Fig. 12 further confirms the fact that the presence of chloride ions should improve the efficiency of copper deposition. The results of tables 3.7 and 3.8 are in agreement with the work of Pomosov and Co-workers (20, 21) in that they show that the presence of chloride ions causes the deposition of a more powdery deposit which results in a higher increase in the surface area of the electrode during deposition.

As the surface area of the electrode increases, the effective current density decreases and subsequently the electrode is polarized at less cathodic potentials as shown in figures, 4, 5 and 6.

Figures 7a and 7b show the decrease in the polarization of the electrode during a large part of the electrolysis. Since at less cathodic potentials the hydrogen evolution reaction is less important, therefore, the efficiency of deposition increases. This explains the maxima observed in figure 11 showing the relationship between current efficiency and time.
for constant Cu^{2+} concentration
Therefore/factors that favour the formation of powdery deposits should increase the efficiency of deposition. According to Ibl (30), the conditions that favour powder formation during electrolysis are summarized in table 3.11.

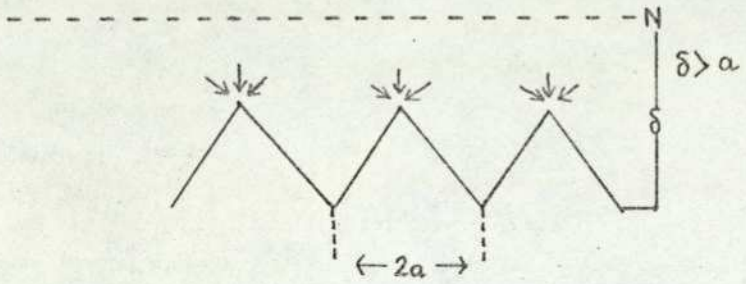
Table 3.11

	Electrolysis Conditions	Change in character of deposit	
1.	Increase of current density	Coherent	Powdery
2.	Decrease of metal concentration	Coherent	Powdery
3.	Increase of Indifferent electrolyte	Coherent	Powdery
4.	Increase of Temperature	Powdery	Coherent
5.	Increase in rate of stirring	Powdery	Coherent

On the whole the structure of a deposit depends strongly on the rate of formation of new nuclei and rate of growth of already existing crystals. Powder formation occurs when the rate of nucleation is large and growth of already existing crystals is small (30). It can be said in general that nucleation becomes faster with increasing current density, that is higher overpotentials, and

decreasing interfacial concentration of metal ions at electrode (30). Therefore all factors that tend to increase the interfacial concentration, like high rate of stirring, and high bulk concentration of metal ion will thus reduce nucleation rate.

The following qualitative explanation for powder formation was put forward by Ibl (31).



Consider a metal surface which has some initial roughness, with small crests and recesses. If the characteristic length, a, is smaller than δ, the crests are privileged from the viewpoint of mass transport because the crest is more accessible for mass transfer than the recess. The current density distribution depends not only on the mass transport, but also on transport of charge through solution and electric double layer, i.e. on conductivity and over voltage. When the current density is dominated mainly by conductivity and electrode geometry, then the current distribution is called primary. Under these conditions, the local current density is larger at the crest than in the recess, because the crest is privileged from the viewpoint of transport of charge through the solution, and lines of electric flux converge towards the crest.

Overvoltage, however, tends to make the current distribution more uniform (secondary current distribution).

The decisive parameter is the polarization parameter, P, (which has the dimensions of length) defined as (32)

$$P = K \frac{d\eta}{di} \tag{3.25}$$

where

K = specific conductivity

$\frac{d\eta}{di}$ = slope of current voltage curve.

If P is larger than a, the characteristic length of the profile, the current distribution is uniform over the profile (32, 33). This is interpreted qualitatively as follows. Along the interface between crest and recess there is in the solution an ohmic potential drop ΔE_R, which must be compensated for by the difference $\Delta\eta$, between the overvoltage at the crest and in the recess.

Therefore, $\Delta E_R + \Delta\eta = 0$ (3.26)

Now, if $\frac{d\eta}{di}$ is large, a negligible increase in current at crest will be enough to create an increase in overvoltage which is sufficient to compensate ΔE_R. The total overvoltage $\Delta\eta$ can be split into activation overvoltage $\Delta\eta_a$ and concentration $\Delta\eta_c$.

Therefore, $\Delta E_R + \Delta\eta_a + \Delta\eta_c = 0$ (3.27)

$\Delta\eta_a$ and $\Delta\eta_c$ have different signs. The concentration of the metallic cation at the interface electrode - solution is larger at the crest than in the recess. The concentration overvoltage is larger at the recess than at the crest, therefore, $\Delta\eta_c$ has the same sign as ΔE_R but opposite to $\Delta\eta_a$. Hence $\Delta\eta_c$ cannot

contribute towards making the current distribution more uniform than would correspond to primary current distribution. On the contrary, it counteracts the equalizing action of $\Delta\eta_a$ and tends to make the current distribution non-uniform.

If $\Delta\eta_c$ is large, the current distribution will be non-uniform even if $\frac{d\eta}{di}$ is large.

An extreme case is that of limiting currents, where the value of $\Delta\eta_c$ tends to be exceedingly large. Under these conditions, the influence of concentration overvoltage is overwhelming, and the current distribution is controlled by mass transport. Since the crests of a microprofile are privileged from the viewpoint of diffusion under mass transport control, the local current densities are higher on crests than on recesses. Hence, geometric irregularities of the surface will then tend to grow.

Below the limiting current, $\Delta\eta_c$ changes only slowly, and the influence of $\Delta\eta_a$ is more prominent. Therefore, if P is large, the crests are not privileged, and the local current densities tend to be the same on the crests and in the recesses.

The activation overpotential for the deposition of metals from molten salts is very small because of the high temperatures involved, and, indeed, it is well known that it is very difficult to obtain even deposits in molten salt electrolysis, even below the limiting currents.

Further work by Ibl and co-workers (34) confirmed that the surface area of the copper electrode increased during electrolysis at currents higher than the limiting current.

The results in table 3.9, and curve C in fig. 12 confirm the above argument and show that electrolysis at currents lower than the limiting current result in a negligible increase in the surface area of the electrode for a long period during the course of the electrolysis.

Table 3.12 is compiled from the results of table 3.6, and Figs. 10 and 11. The table compares the efficiency of deposition resulting from passing the same quantity of charge at different current densities.

Table 3.12

Initial concentration of copper ions = 200 p.p.m.

Limiting diffusion current of system = 10 mA

Current (mA)	Time (minutes)	Coulombs	Final p.p.m.	% efficiency
7	90	37.8	126	89.2
	180	75.6	54	87.99
15	42	37.8	128	87.00
	84	75.6	58	86.00
21	30	37.8	136	77.00
	60	75.6	66	80.7

It is obvious from table 3.12 that electrolysis at high current densities is to be preferred, since it results in a higher rate of deposition with favourable current efficiencies, because of the large increase in surface area of the electrode, but it must

be emphasized that there is an optimum and electrolysis at too high currents might not be economical, especially as the concentration of the metal ions in the solution is depleted as shown in the results of electrolysis at 30 mA in table 3.6.

One disadvantage in the formation of a powdery deposit is that the metal so formed is more active than the coherently deposited metal, and therefore tends to redissolve in to the solution at a faster rate. This was shown by doing the electrolysis at 2.14 mA/cm^2 for various periods and then allowing the electrode to stand in the resulting solution for 30 minutes. The solution was then analysed for copper and the results are shown in table 3.13.

Table 3.13

Rate of deposited copper dissolution.

Time of electrolysis (minutes)	Increase in copper ion concentration after 30 min.
0	3 p.p.m.
30	18 p.p.m.
60	19 p.p.m.
90	20 p.p.m.

It is, therefore, preferable to operate at higher current densities, i.e. at higher rates of deposition, so as to reduce the time of electrolysis and thus minimize the effect of redissolution of the deposited metal.

3.1.d Cyclic Voltammetry

Figures 13 to 19 show the current - potential curves for unstirred solutions of copper sulphate containing 200 p.p.m. copper at pH 1 and varying potassium chloride concentrations. The scan-rate in each experiment was 50 mV/sec. The potential was scanned from +500 mV to - 500 mV against the saturated calomel electrode. Only the reduction peaks will be discussed here since this project was concerned with the reduction of copper ions to copper metal.

Each figure consists of three reduction peaks, denoted by R_1, R_2 and R_3. This is in agreement with the work of Bruckenstein (35) who used chloride-free sulphuric acid solution as a background electrolyte. Bruckenstein assigned the first two reduction peaks to mono-layer formation of copper atoms, and the third peak to the direct reduction of cupric ions to the metal, as given by equation 3 - 1.

$$Cu^{2+} + 2e \rightleftharpoons Cu \qquad 3.1$$

Breiter (36) also ascribed the peaks to the formation of different layers of copper.

The author offers the following interpretation of the peaks.

a Peak R_1

Peak R_1 occurs at about +350mV. against the S.C.E. When the platinum electrode is potentiostated at -300 mV for 5 - 10 minutes, a copper deposit can be observed. If the potential of the resulting electrode is then scanned from +500mV to -500mV, peak R_1 disappears, while peaks R_2 and R_3 may still be observed, as shown in Fig. 20. If, however, an oxidized platinum electrode is used, i.e. an electrode treated anodically, before use, as described in Section then, on increasing the concentration of copper sulphate and on

scanning the electrode potential from +500mV to -500mV, there is no change in the height of peak R_1, as shown in Fig. 21. This seems to indicate that the peak is due to precathodic deposition of copper metal at potentials more anodic than expected. This undervoltage phenomenon results energetically from the contribution of heat of absorption of the metal atoms on the platinum metal surface to the energy of activation of the discharge - reaction (36).

b Peak R_2

Peak R_2 may be the result of any one of the following chemical reactions. (All potentials are referred to the S.C.E., whose electrode potential is 0.244V at 25°C) (37)

$$Cu^{2+} + 2e \rightleftharpoons Cu \qquad E^{o} = 0.094 \qquad 3.1$$

$$Cu^{2+} + e \rightleftharpoons Cu^{1+} \qquad E^{o} = -0.086 \qquad 3.2$$

$$Cu^{2+} + Cl^{-} + e \rightleftharpoons CuCl\,(s) \qquad E^{o} = 0.311 + 0.059 \log[Cl^{-}] \qquad 3.12$$

$$Cu^{2+} + 2Cl^{-} + e \rightleftharpoons CuCl_2^{-} \qquad E = 0.242 + 0.118 \log[Cl^{-}] \qquad 3.13$$

It was found that the position of peak R_2 changed as the chloride ion concentration was varied, as shown in figs. 13 to 19 and table 3.14.

Table 3.14

Copper concentration	= 200 p.p.m.
pH	= 1.0
Scan rate	= 50 mV/sec
Electrode Area	= 3.2 cm^2
Temperature	= 25°C

KCl concentration (molar)	log [KCl]	Peak position mV
0.04	-1.398	+10
0.1	-1	+55
0.4	-0.398	+110
0.5	-0.301	+120
0.8	-0.097	+155
1.0	0	+175

A plot of the peak potential against the logarithm of chloride ion concentration gives a slope of +114 and an intercept of 165mV, as shown in Fig. 22. These results show that the peak potential for peak R_2 is given by equation 3.28

$$E^{O} = 0.165 + 0.114 \log \left[Cl^{-}\right] \qquad 3.28$$

As the slope of the plot is 0.114V, therefore, peak R_2 may be assigned to equation 3.13.

These results are in agreement with the work of Peters (26) and Vydra (38), who found the following results for peak R_2, shown in table 3.15.

Table 3.15

E^{O} values of Peak R_2

	E^{O}	Technique	Electrode used	Medium	Reference
1.	0.1	Chronopotentiometry	Au	1m.KCl ,pH2	26
2.	0.15	Cyclic Voltammetry	Glassy carbon electrode	1m.KCl ,pH4	38

Fig. 21 and table 3.16 show the result in change of peak current as the concentration of copper sulphate was changed.

Table 3.16

KCl = 1.0m

pH = 1.0

Scan rate = 50mV/sec

Temperature = 25°C

Peak current = i_p ($A \times 10^{-3}$)	$CuSO_4$ concentration (mde/ml. $\times 10^{-6}$) = c	i_p/c
0.75	3.15	240
1.2	4.72	250
1.6	6.23	260
2.0	7.75	260
2.35	9.26	250
2.8	10.75	260
		average = 253 ± 8.15

The results in table 3.16 further prove that peak R_2 must be assigned to an electrochemical reduction reaction rather than to monolayer formation of copper, because of the change of the peak height with the change of concentration.

c Peak R_3

Peak R_3 may be the result of any one of the following electrochemical reactions.

$$Cu^{2+} + 2e \rightleftharpoons Cu \qquad E^o = 0.094V \qquad 3.1$$

$$Cu^{1+} + e \rightleftharpoons Cu \qquad E^o = 0.277V \qquad 3.3$$

$$CuCl_2^- + e \rightleftharpoons Cu + 2Cl^-$$

$$E^o = -0.06 - 0.118 \log [Cl^-] \qquad 3.15$$

Again it was found that R_3 peak position changed as the chloride ion concentration was varied, as shown in Figs. 13 to 19, and table 3.17.

Table 3.17

Copper Sulphate concentration = 200 p.p.m.

pH = 1.0

Scan rate = 50 mV/sec

Electrode Area = 3.2 cm^2

Temperature = 25°C

KCl concentration (molar)	log KCl	Peak position (mV)
0.04	-1.398	-125
0.1	-1	-160
0.4	-0.398	-225
0.5	-0.301	-235
0.8	-0.097	-270
1.0	0	-280

A plot of peak potential against the logarithm of chloride ion concentration gives a straight line with a slope of -118 mV and an intercept of -280mV. Therefore, the equation for peak R_3 is given by 3.29

$$E^{o} = -.280 - .118 \log \left[Cl^{-}\right] \qquad 3.29$$

Since the slope of the straight line is -118mV, therefore peak R_3 may be assigned to equation 3.16.

Furthermore, the experiments were carried out at pH 1, 2 and 3 (KCl = 0.1 molar; scan rate = 50 mV; $CuSO_4$ = +3.15 molar; temperature = 25°C) and there was no change in peak positions of

peaks R_1, R_2 and R_3. These results exclude the possibilities of reactions 3.18 and 3.19 from occurring.

$$\tfrac{1}{2}Cu_2O(s) + \tfrac{1}{2}H_2O \rightleftharpoons Cu(s) + OH^{1-} \qquad 3.18$$

$$E^o = 0.242 - 0.059\ pH$$

$$Cu^{2+} + \tfrac{1}{2}H_2O + e \rightleftharpoons \tfrac{1}{2}\ Cu_2O + H^{1+} \qquad 3.19$$

$$E^o = -0.139 + 0.059\ pH$$

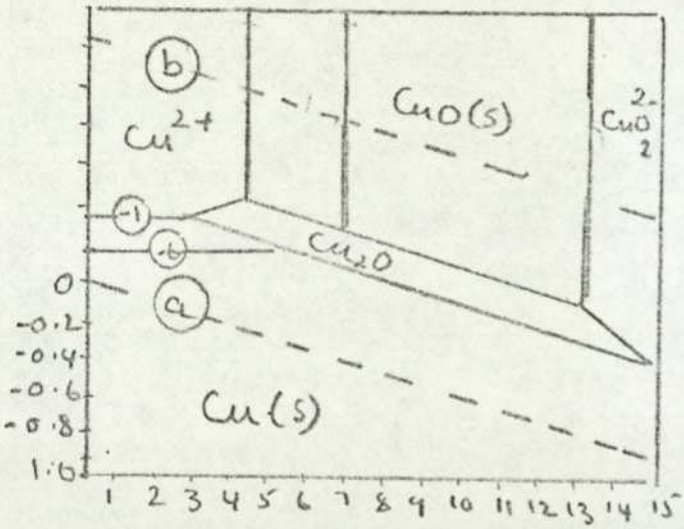


Fig. 1

Potential - pH diagram for the system $Cu - H_2O$, at 25°C.

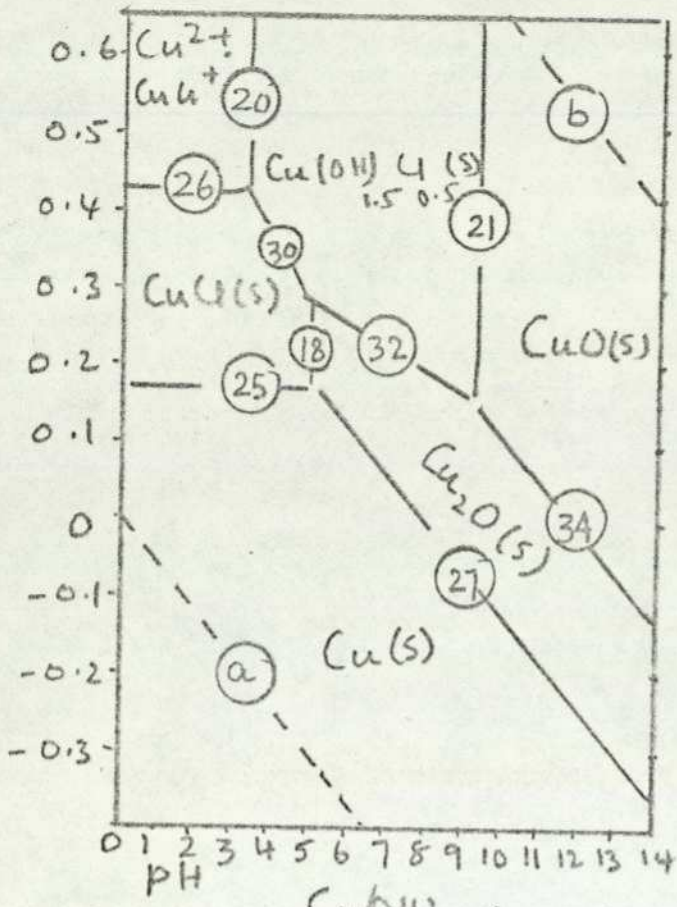


Fig.2

Potential - pH diagram for the system Cu - Cl - H_2O at 25°C. 1·0m. Cl., 0·1m. Cu.

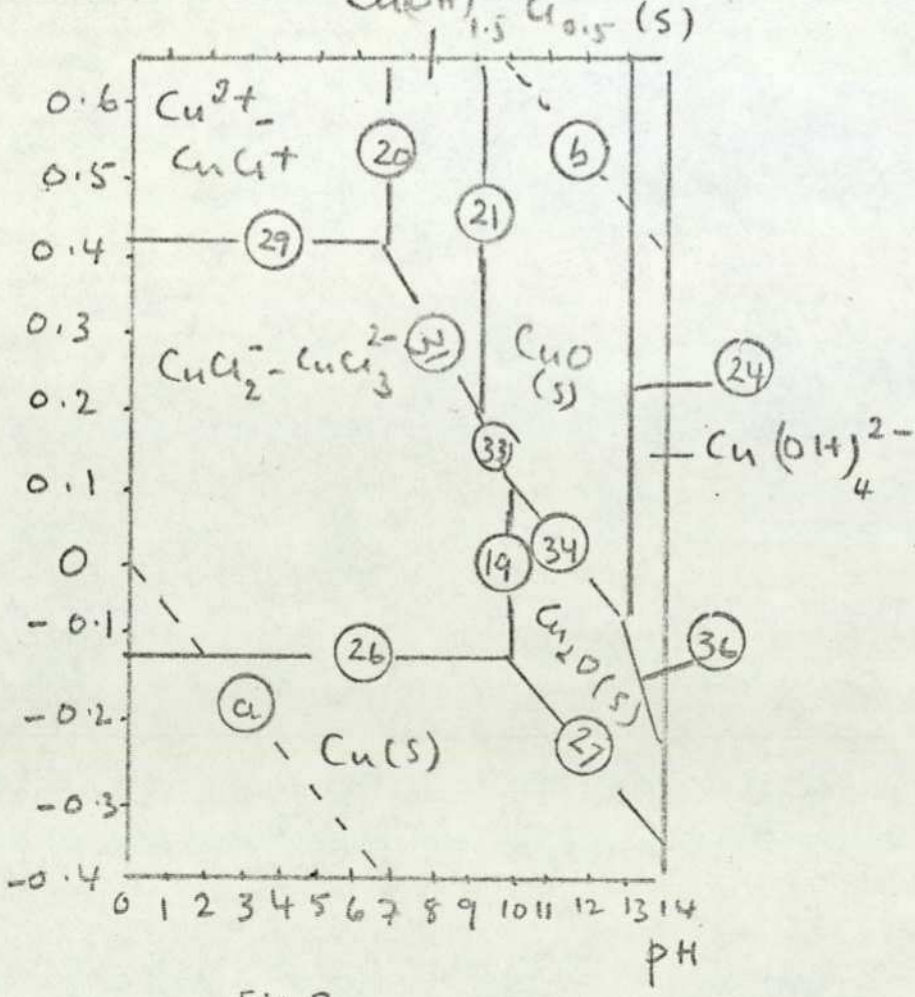


Fig.3

Potential - pH diagram for the system Cu - Cl - H_2O at 25°C. 1·0m. Cl., 10^{-6}m. Cu.

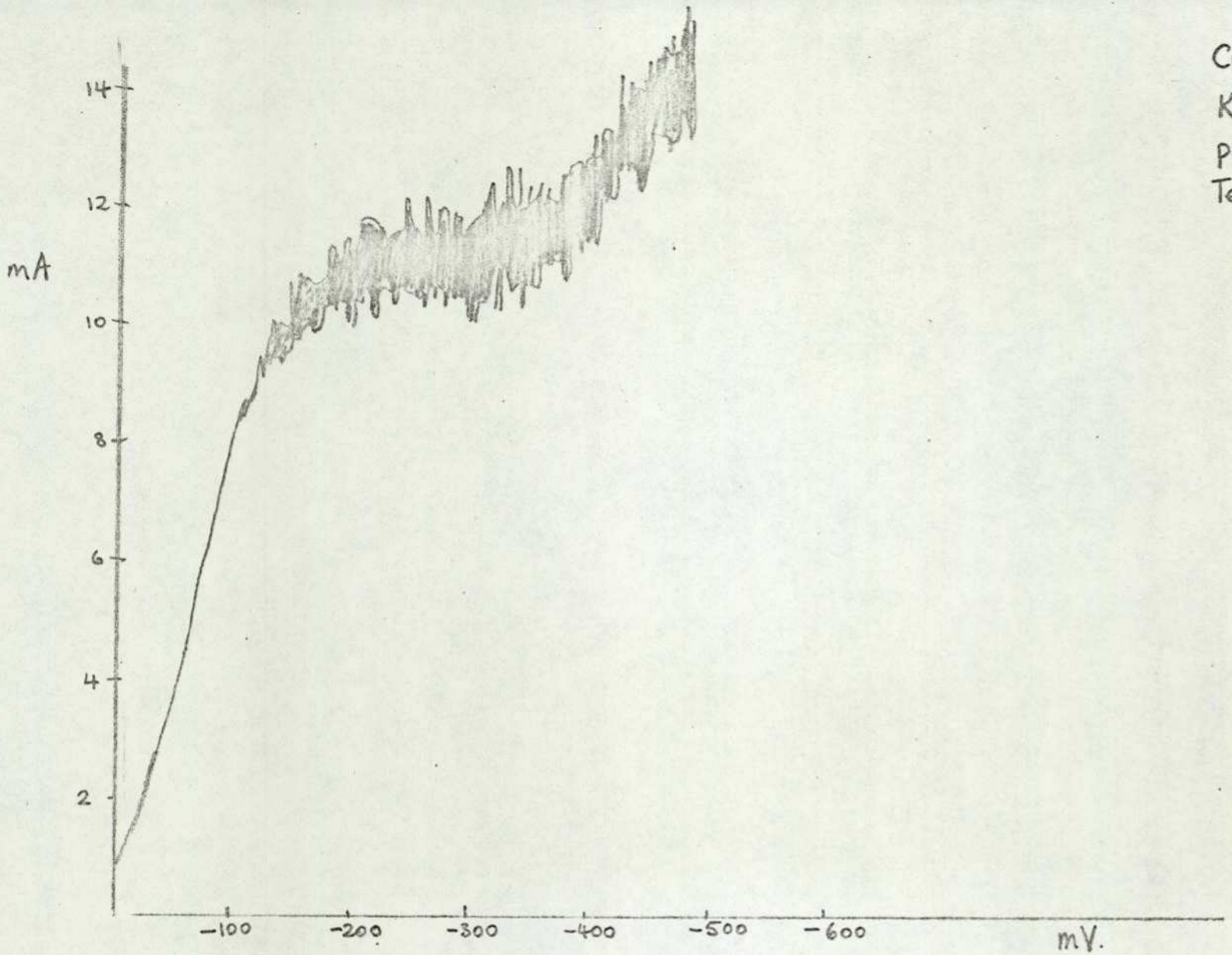


Fig. 4.

Steady state Current-potential curve for $CuSO_4$ (stirred solution)

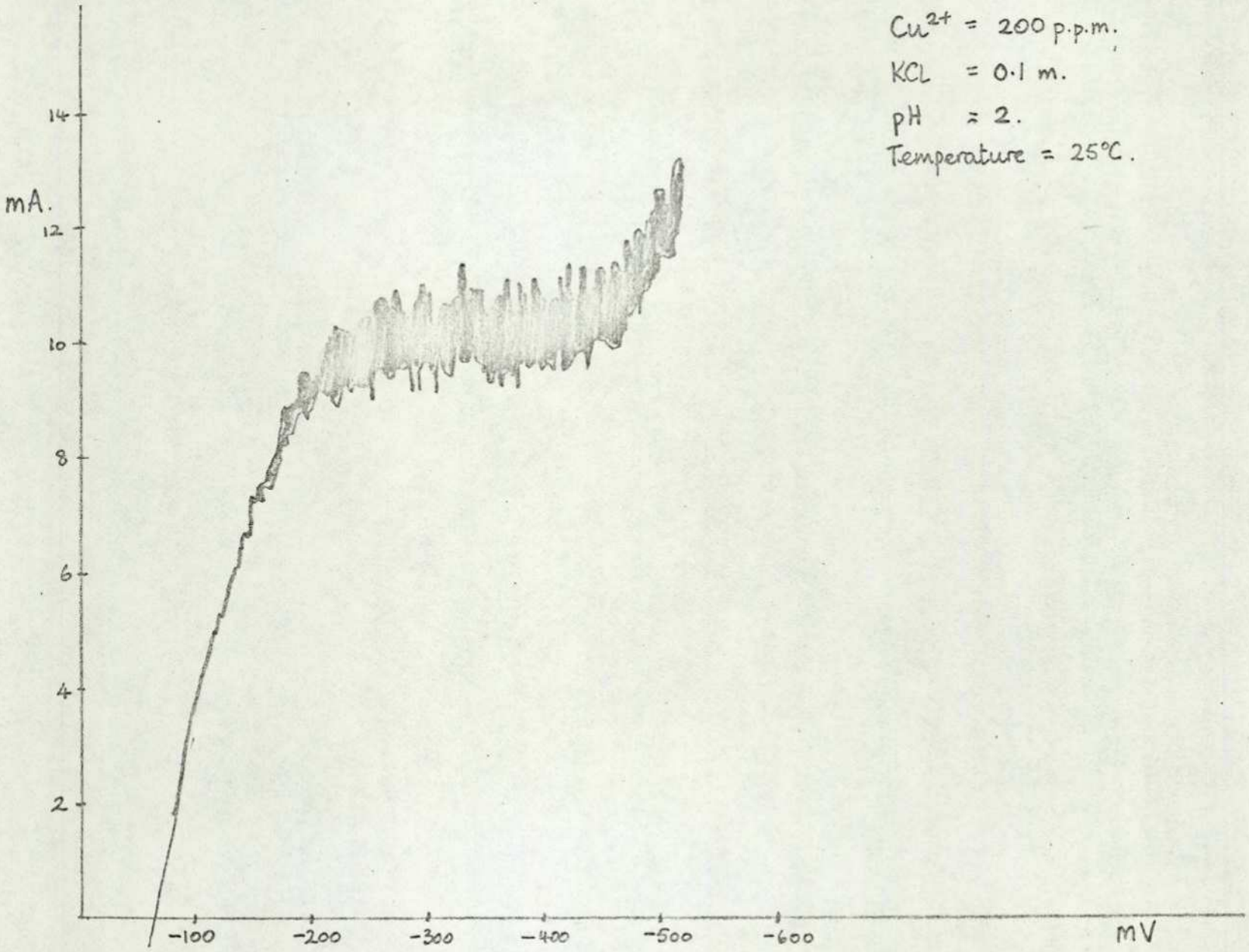


Fig. 5

Steady state Current-potential curve for $CuSO_4$ (stirred solution)

Cu^{2+} = 200 p.p.m.
KCl = 0·005 m.
pH = 2.
Temperature = 25°C.

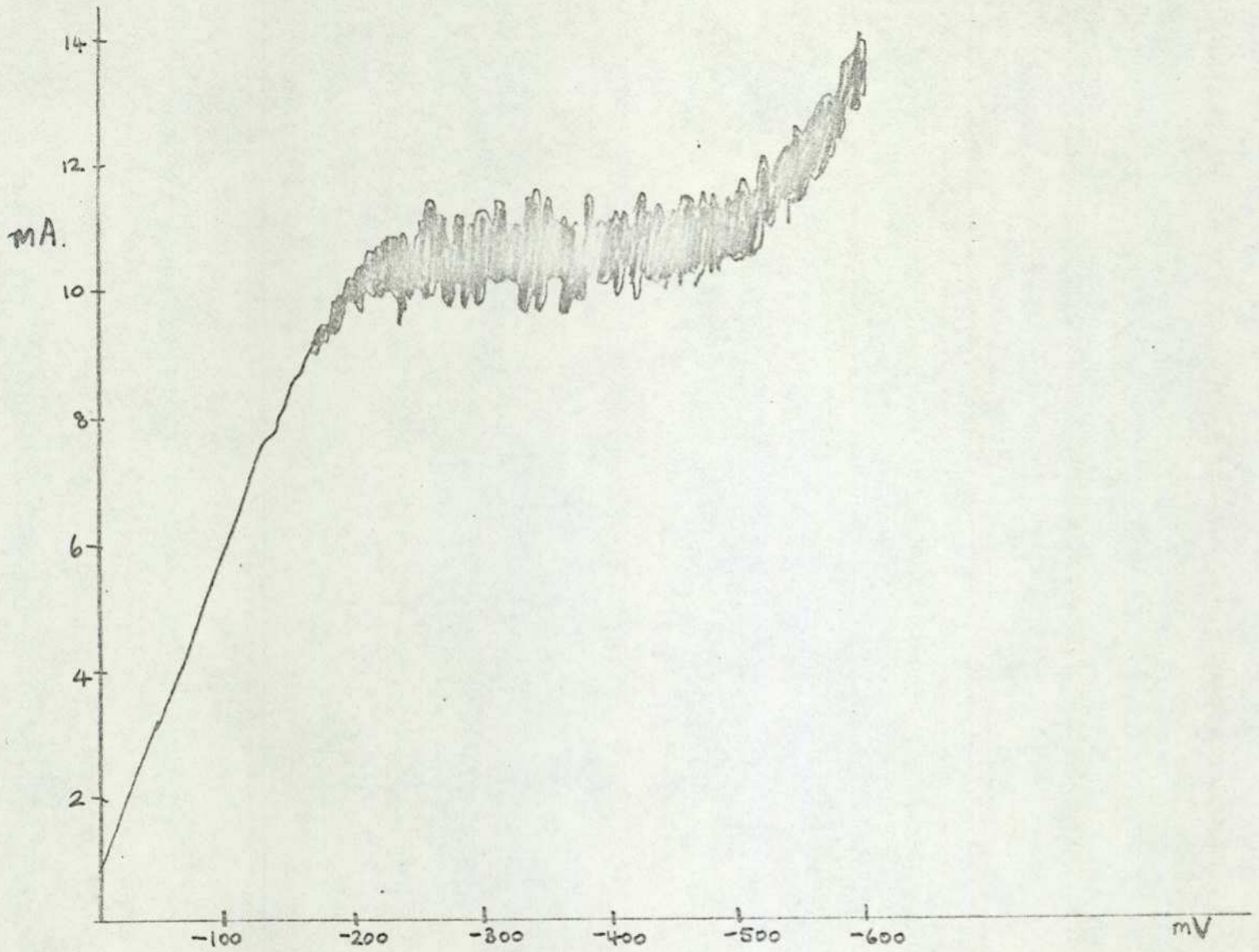
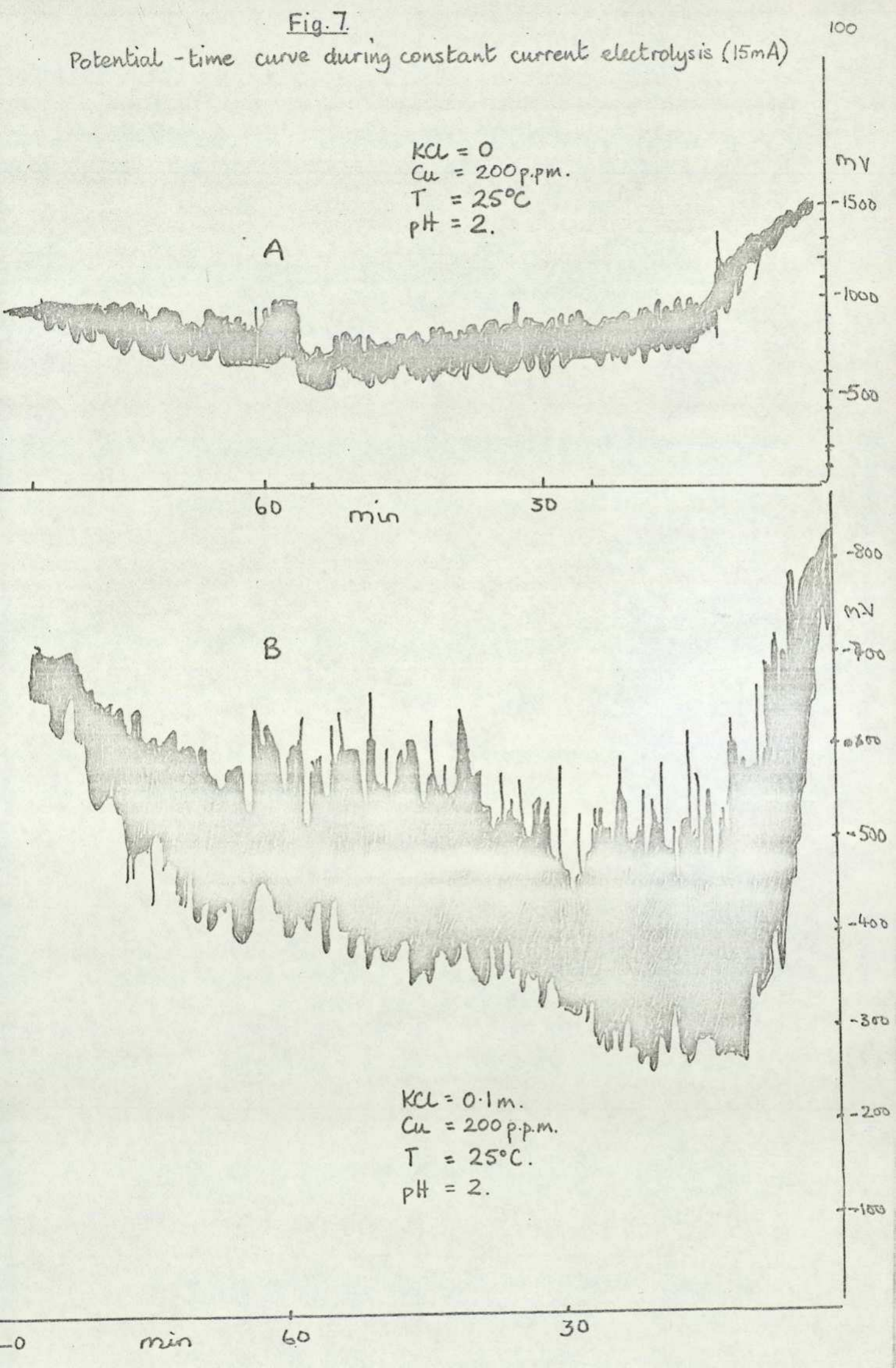


Fig.6.
Steady state Current-potential curve for $CuSO_4$ (stirred solution).

Fig. 7.

Potential - time curve during constant current electrolysis (15mA)



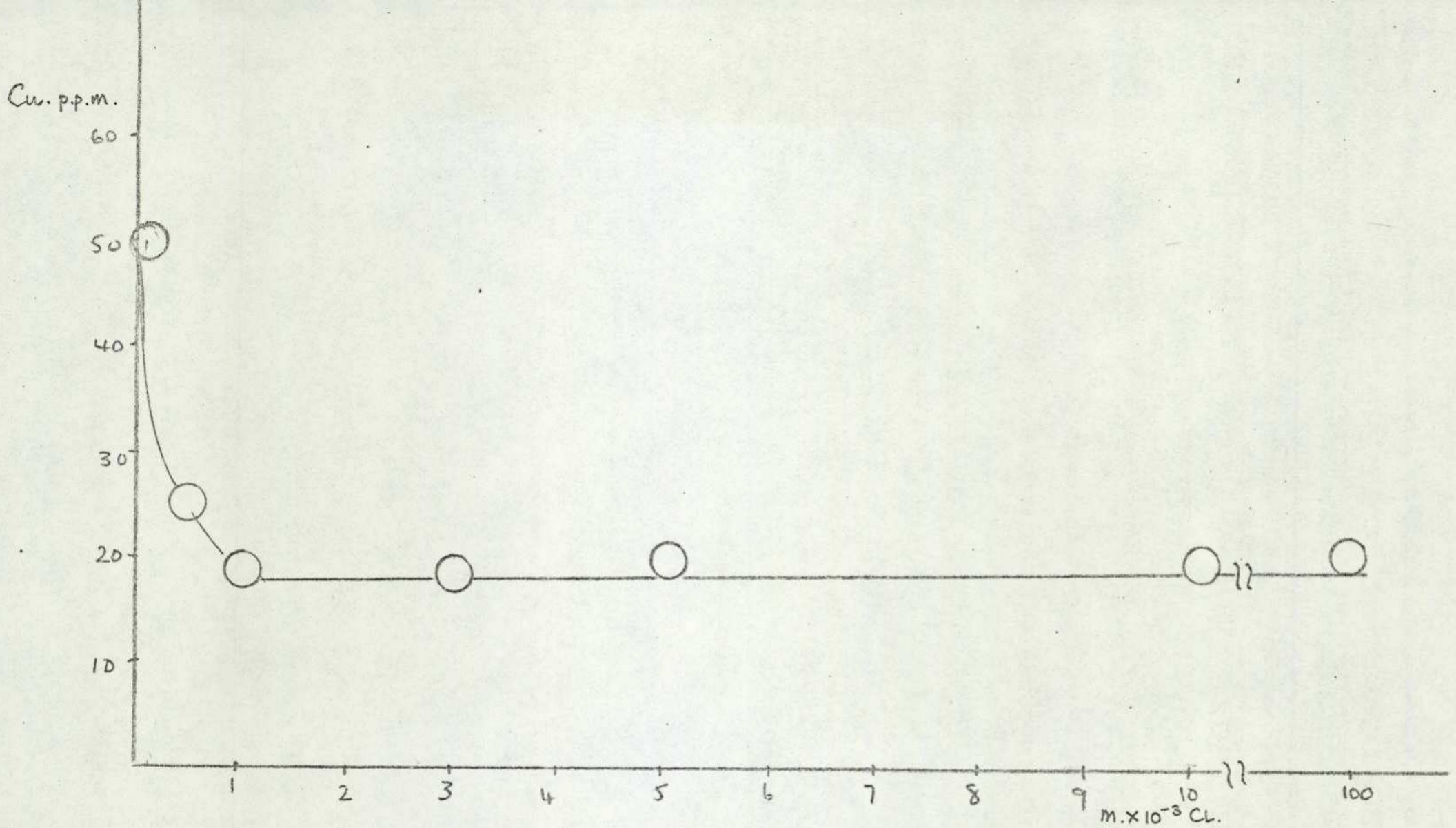


Fig. 8

The effect of Chloride ions on Copper deposition.

Initial copper concentration = 200p.p.m.
KCl. = 0·1 m.
Time of electrolysis = 120min.
Current density = 2·14 mA/cm²
pH = 2.

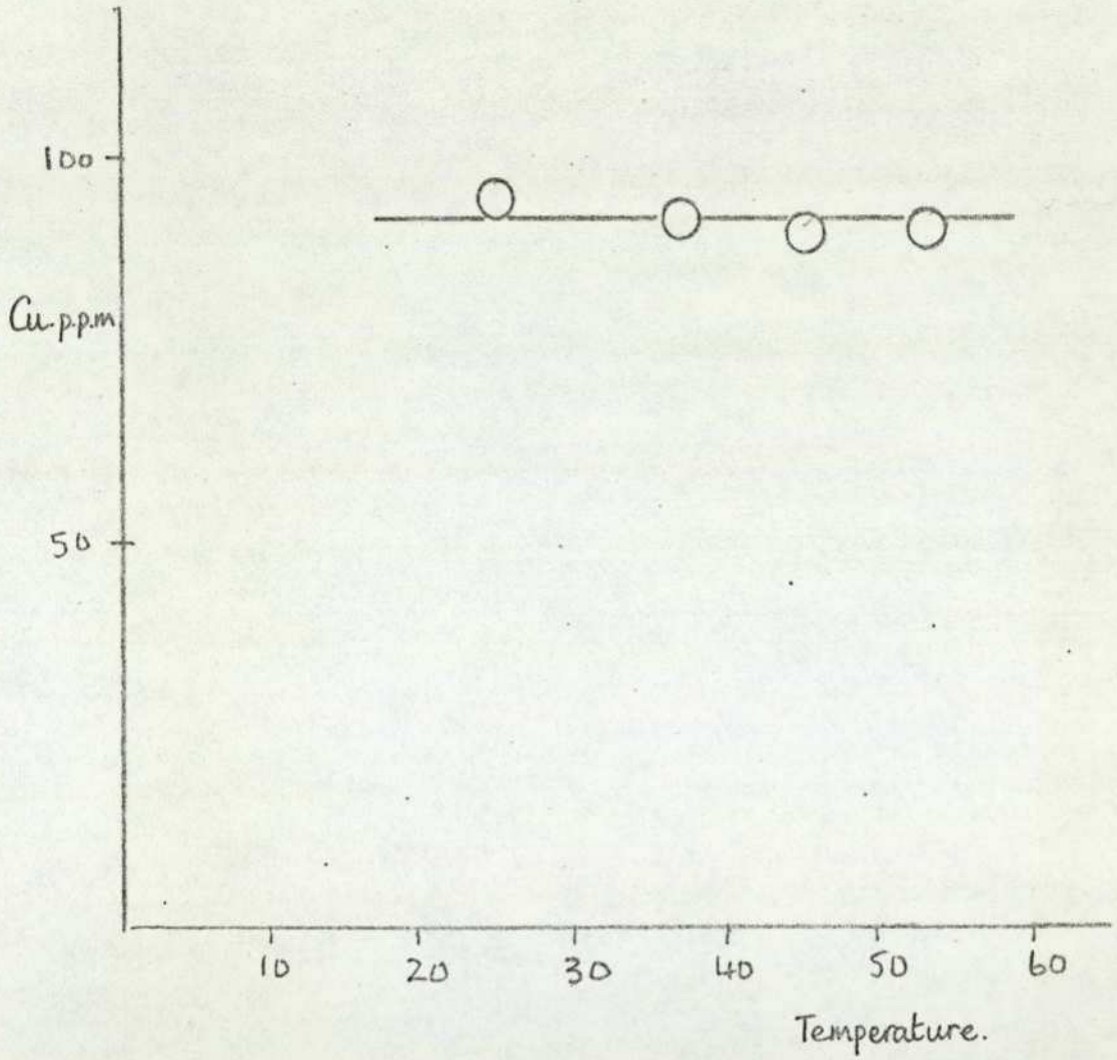


Fig. 9.

The effect of temperature on copper deposition.

Initial copper concentration = 200 p.p.m.
KCl = 0·1 m.
Time of electrolysis = 60 min.
Current density = 2·14 mA/cm^2
pH = 2.

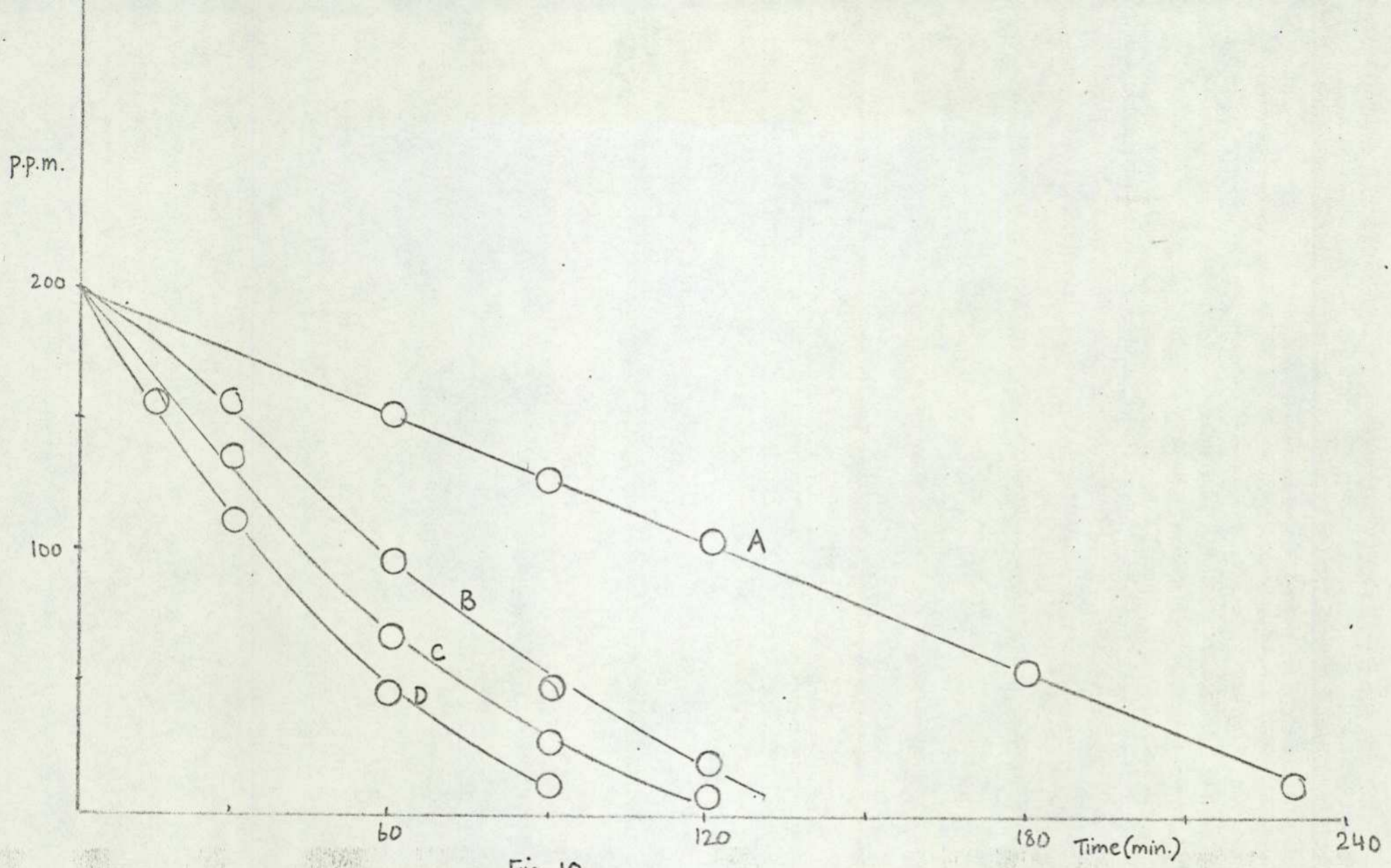


Fig. 10

Change of concentration of copper with time at constant currents of:-

A = 1mA/cm²; B = 2·14 mA/cm²; C = 3mA/cm²; D = 4·28 mA/cm²

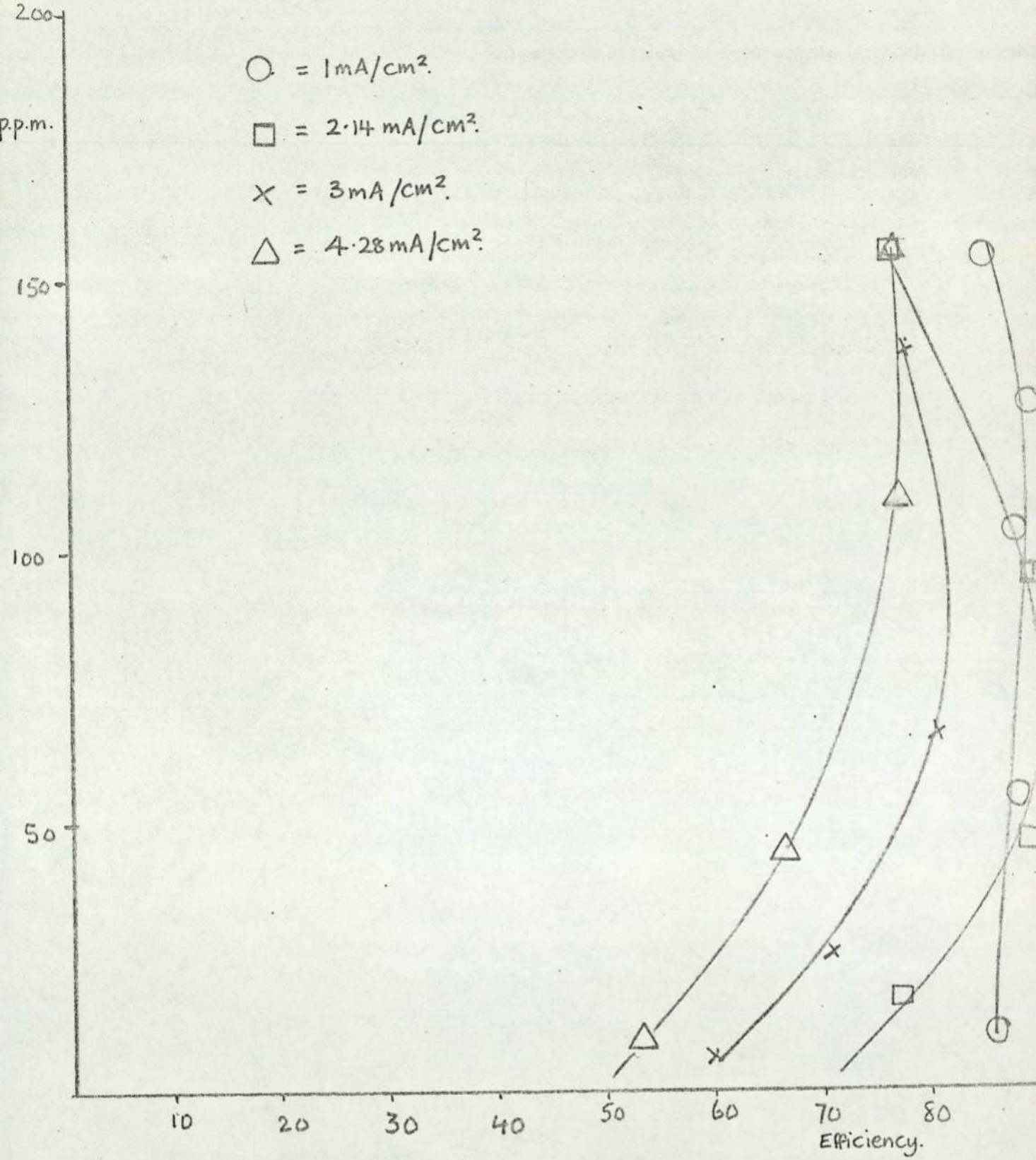


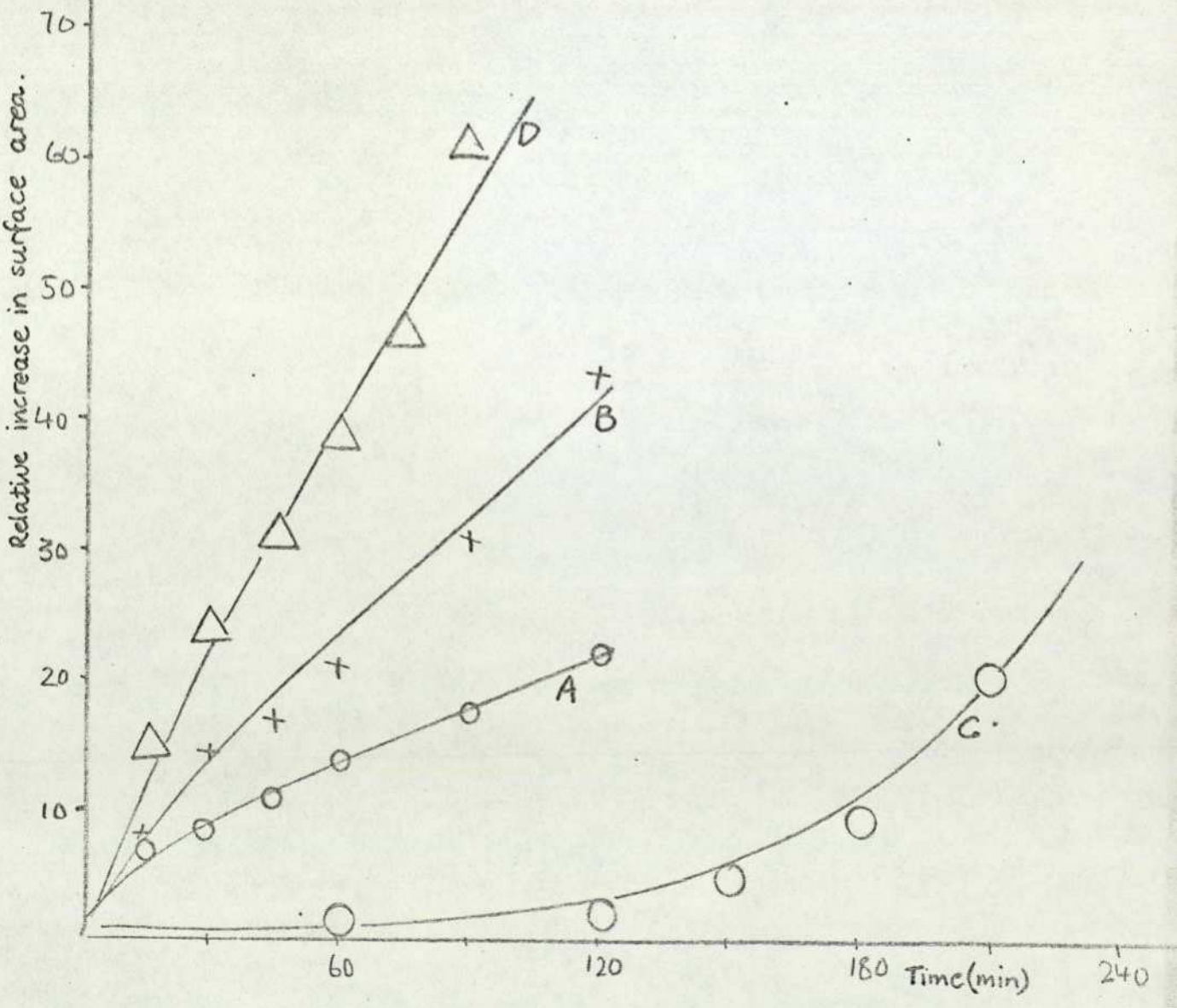
Fig. 11.

Variation of efficiency of copper deposition during constant current electrolysis.

Fig. 12.

Variation of surface area during constant current electrolysis.

A = 2·14mA/cm²; KCL = ·005m.
B = 2·14 mA/cm²; KCL = 0
C = 1 mA/cm²; KCL = ·005m.
D = 4·28mA/cm²; KCL = ·005m.



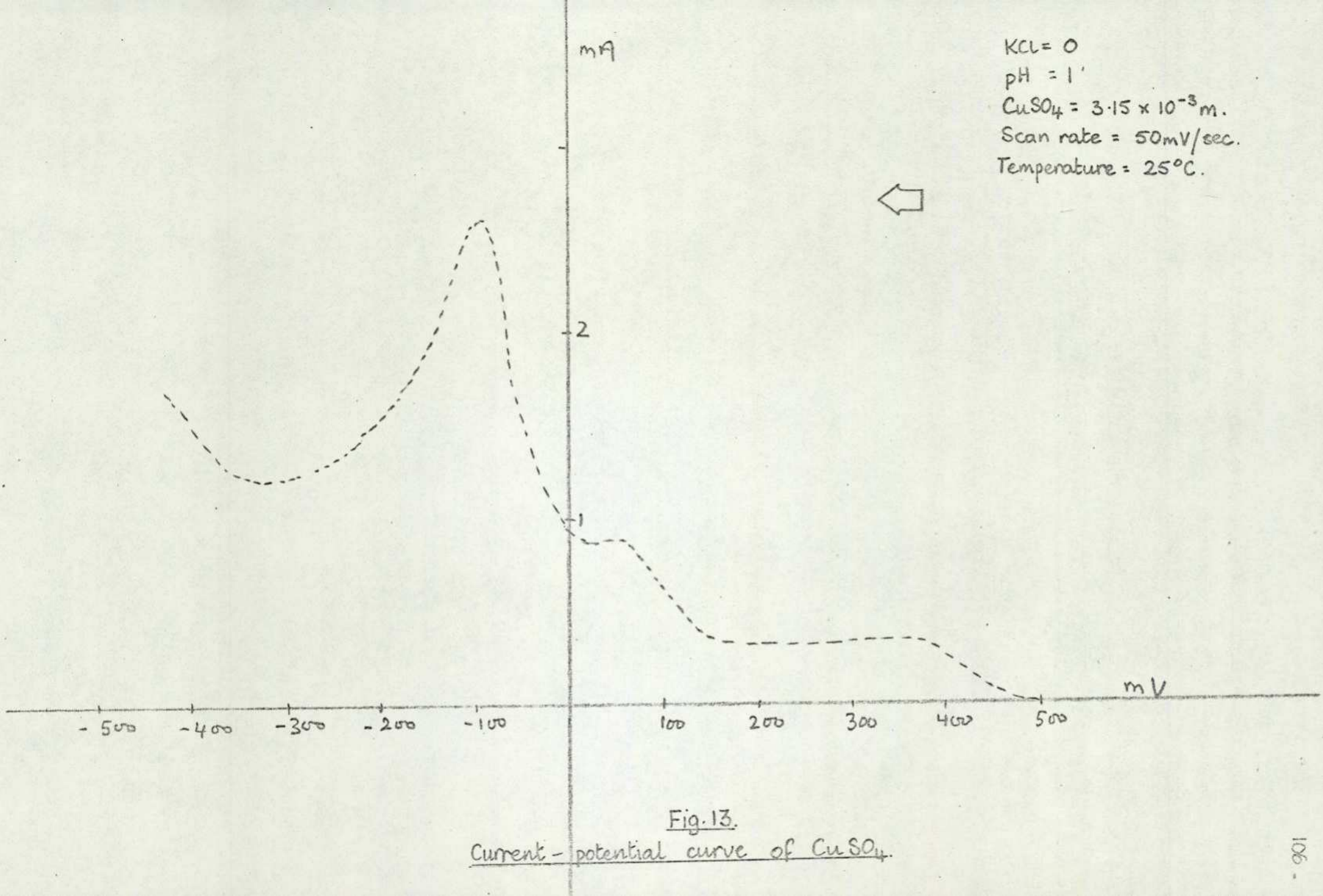
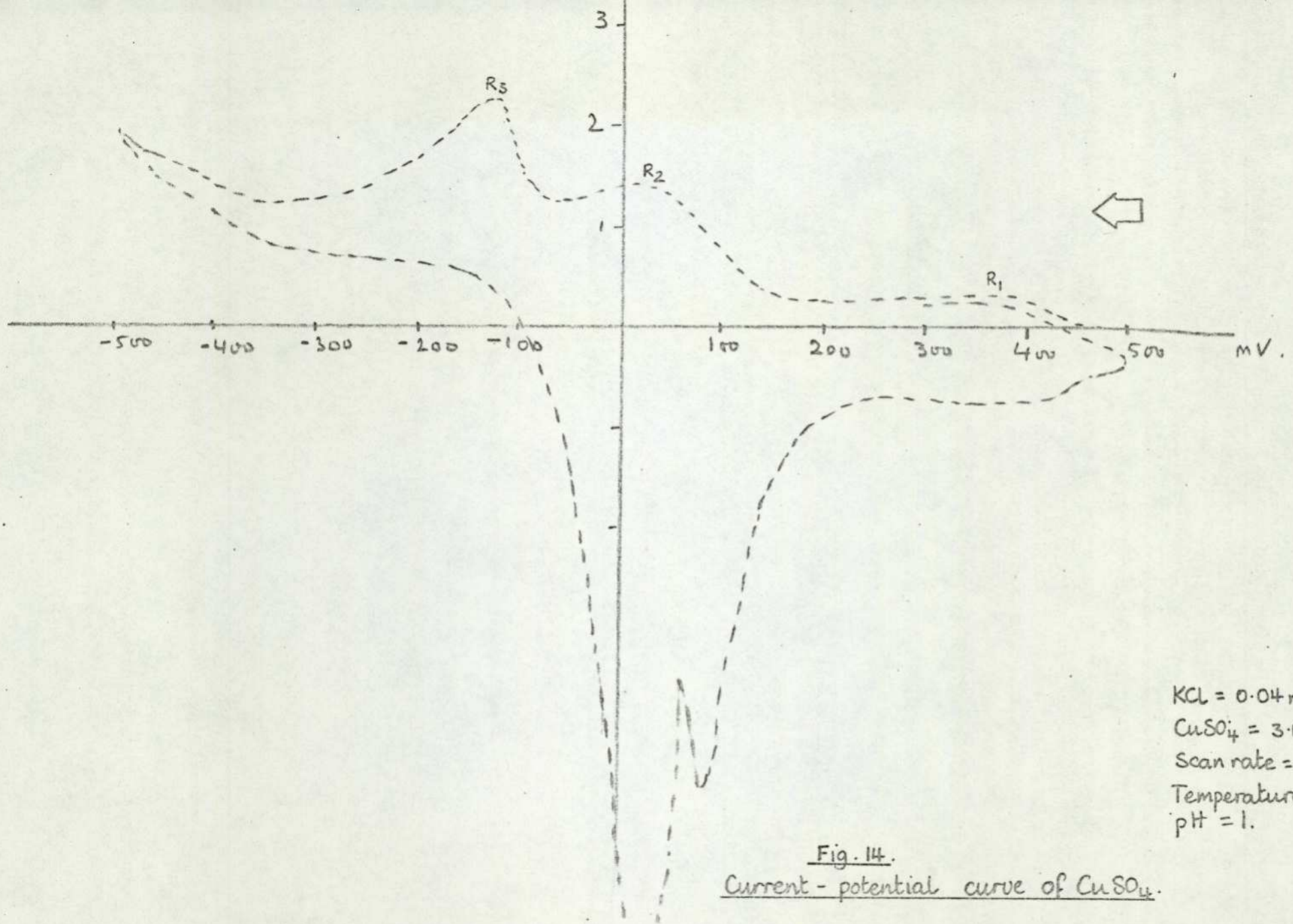


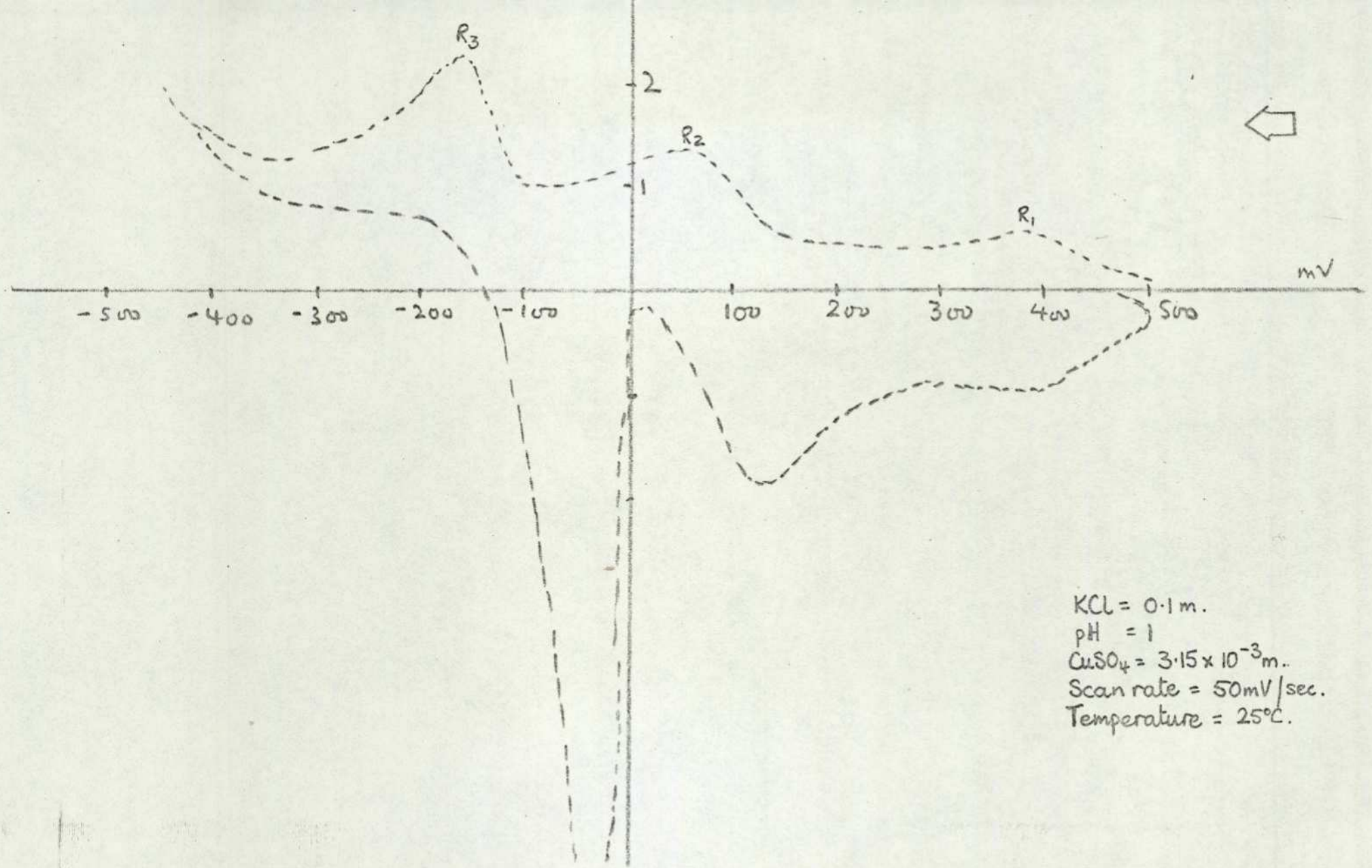
Fig. 13.

Current - potential curve of $CuSO_4$.



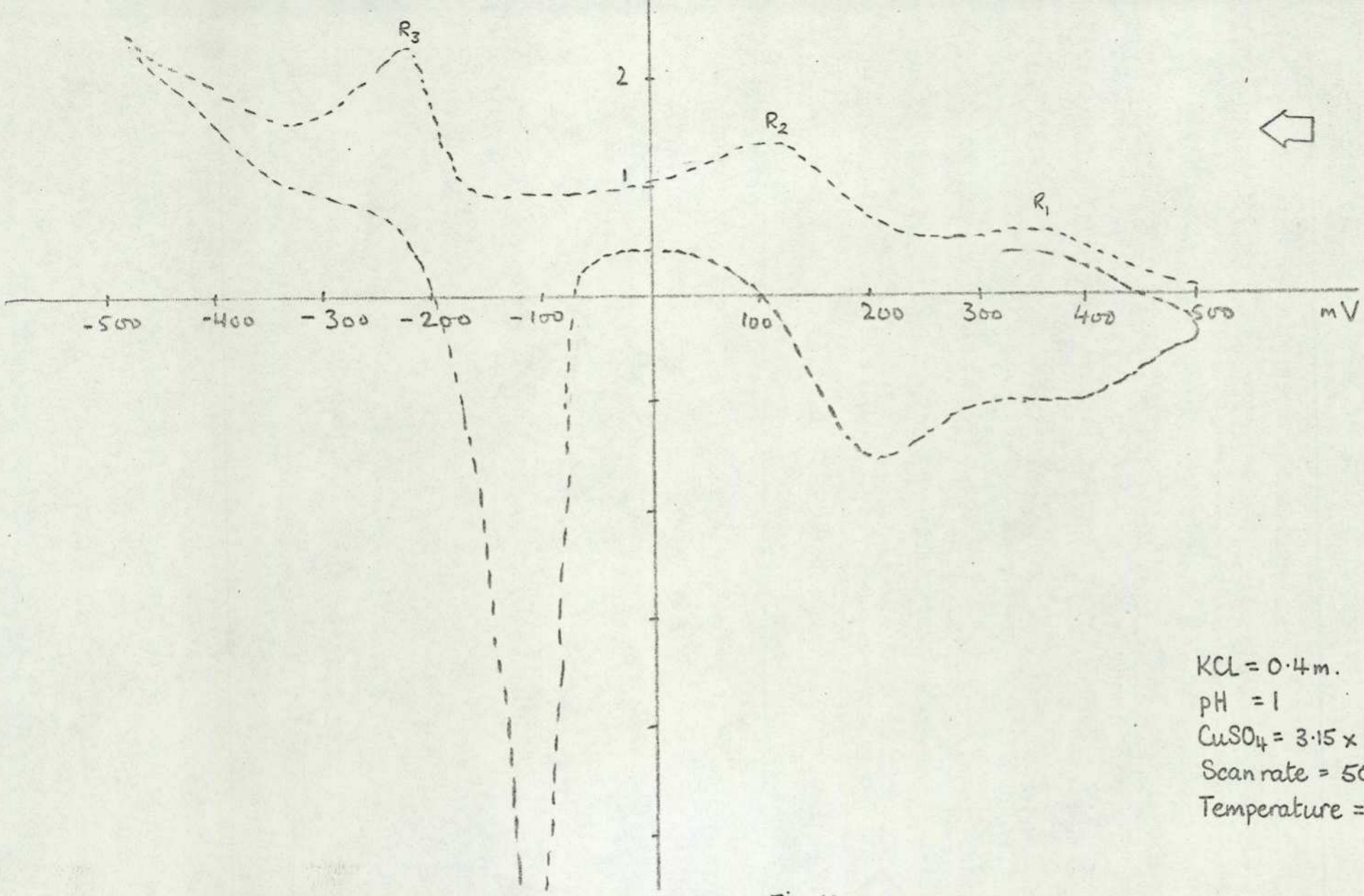
KCL = 0·04 m.
$CuSO_4$ = 3.15×10^{-3} m.
Scan rate = 50 mV/sec.
Temperature = 25°C.
pH = 1.

Fig. 14.
Current - potential curve of $CuSO_4$.



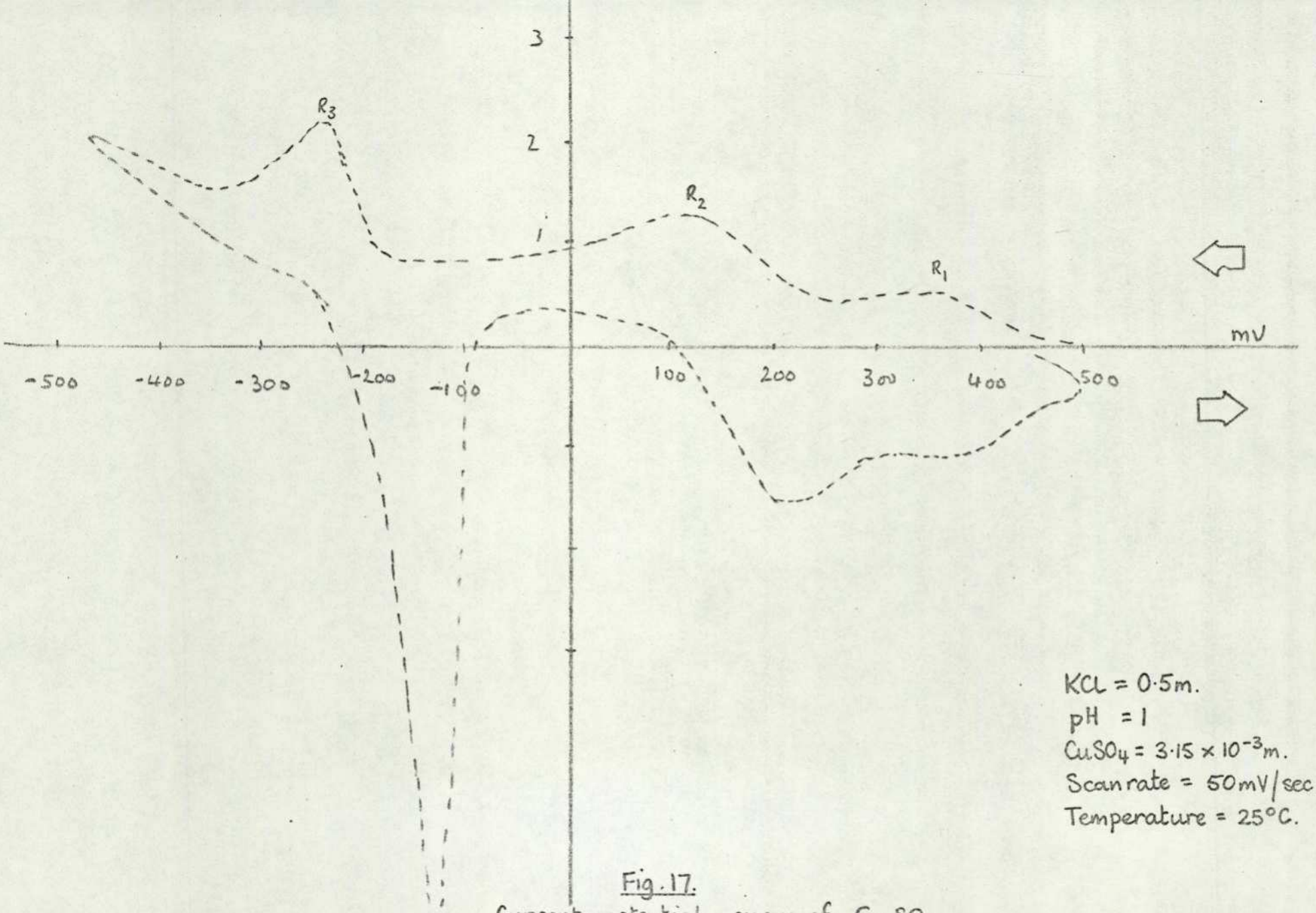
KCl = 0·1 m.
pH = 1
$CuSO_4 = 3{\cdot}15 \times 10^{-3}$ m.
Scan rate = 50mV/sec.
Temperature = 25°C.

Fig. 15.
Current - potential curve of $CuSO_4$.



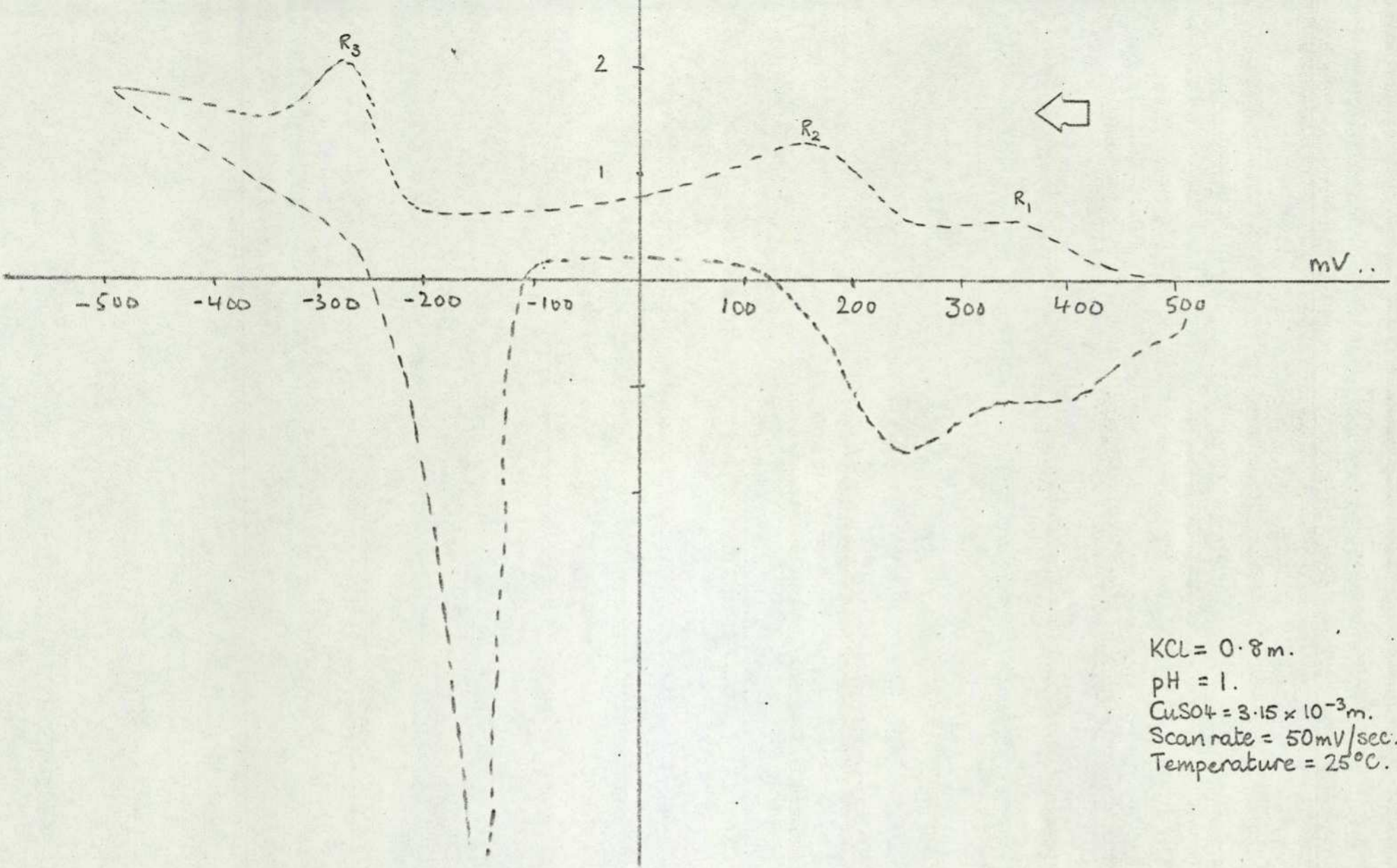
KCl = 0·4 m.
pH = 1
$CuSO_4$ = $3{\cdot}15 \times 10^{-3}$ m.
Scan rate = 50 mV/sec.
Temperature = 25°C.

Fig. 16.
Current - potential curve of $CuSO_4$.



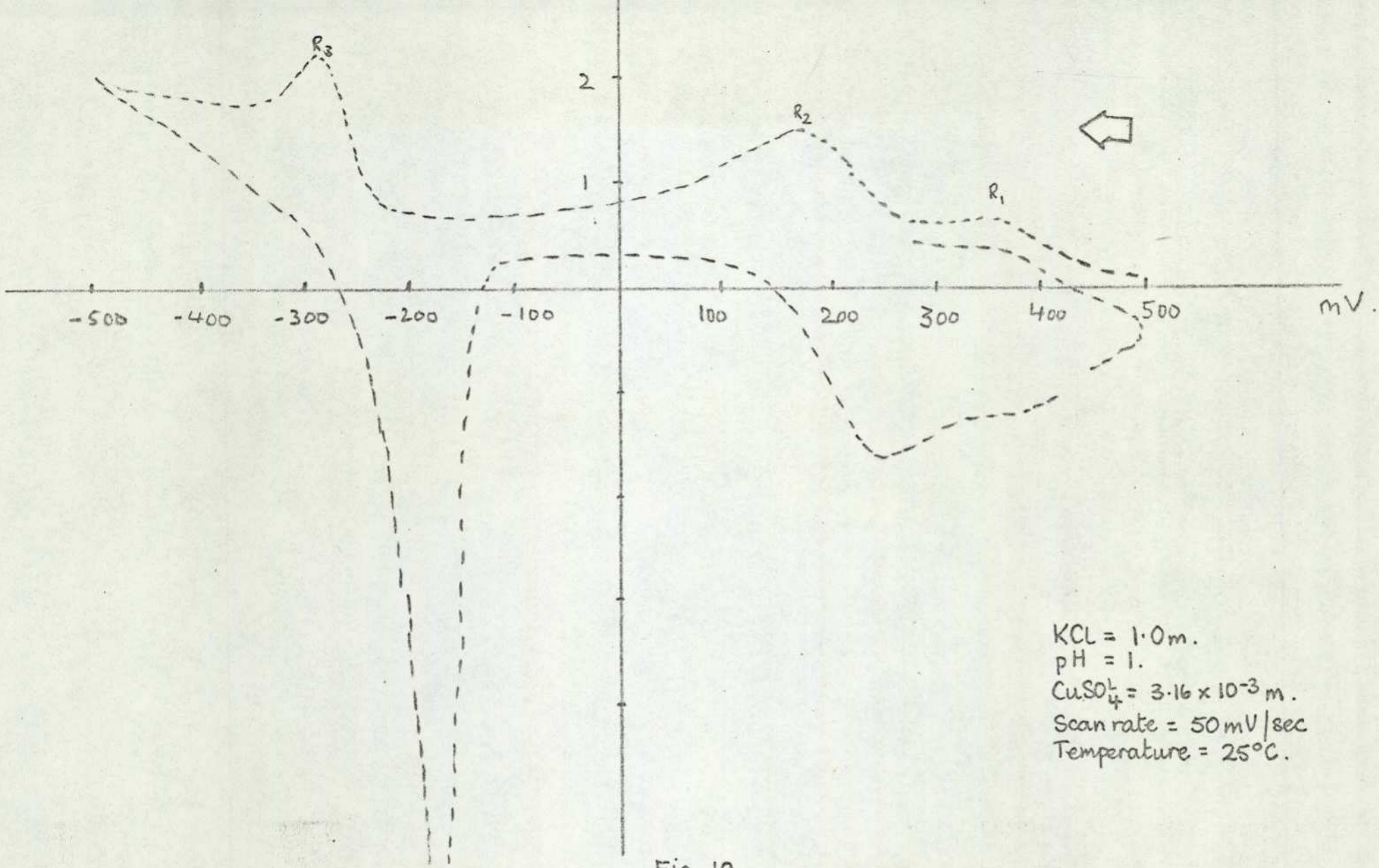
KCl = 0·5m.
pH = 1
$CuSO_4 = 3{\cdot}15 \times 10^{-3}$m.
Scan rate = 50mV/sec.
Temperature = 25°C.

Fig. 17.
Current-potential curve of $CuSO_4$.



KCL = 0·8m.
pH = 1.
$CuSO_4 = 3.15 \times 10^{-3}$m.
Scan rate = 50mV/sec.
Temperature = 25°C.

Fig. 18.
Current potential curve of $CuSO_4$



KCL = 1·0m.
pH = 1.
$CuSO_4$ = 3.16×10^{-3} m.
Scan rate = 50 mV/sec
Temperature = 25°C.

Fig. 19.
Current - potential curve of $CuSO_4$.

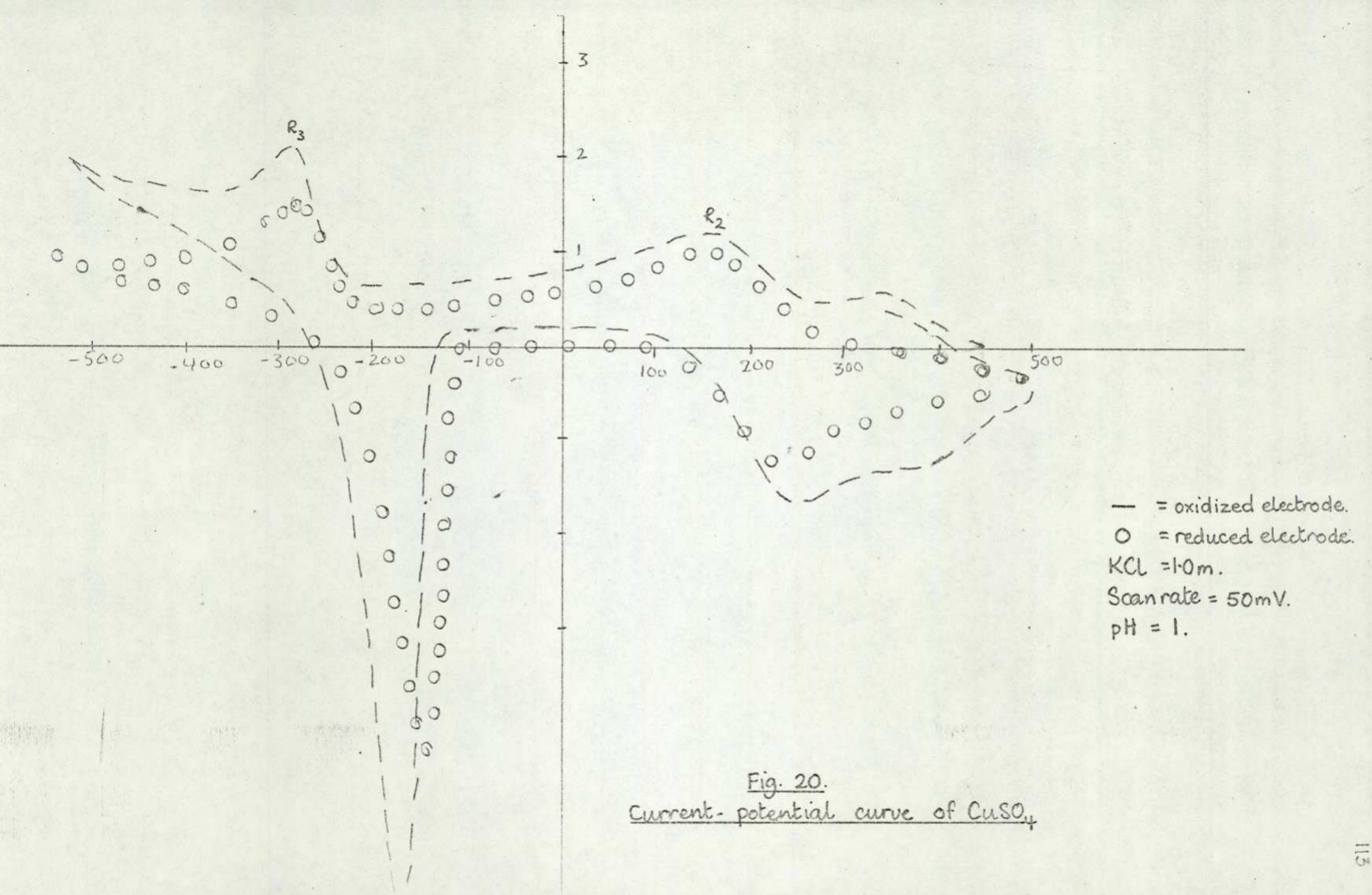


Fig. 20.
Current-potential curve of $CuSO_4$

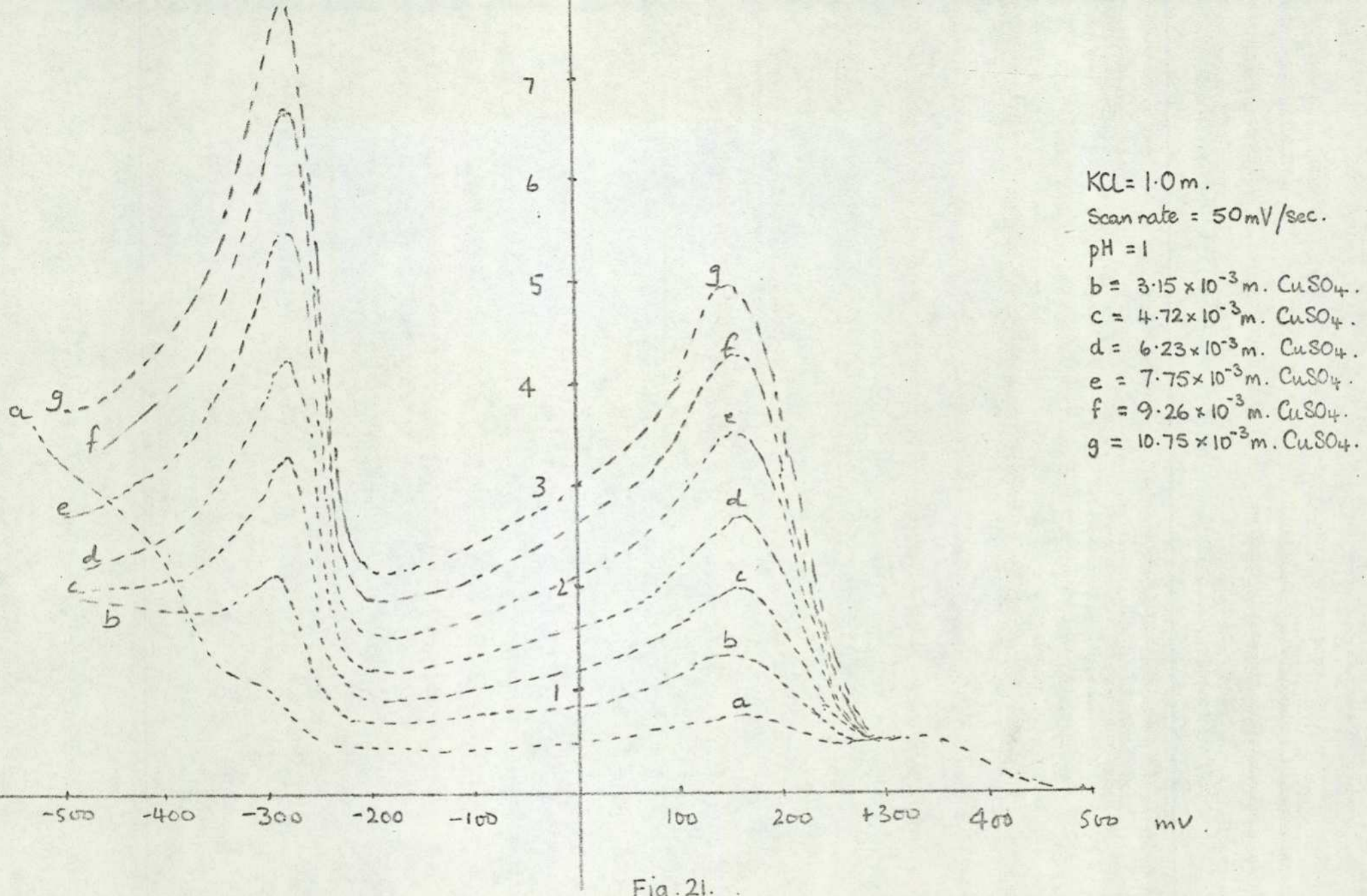


Fig. 21.

Variation of peak current with $CuSO_4$ concentration.

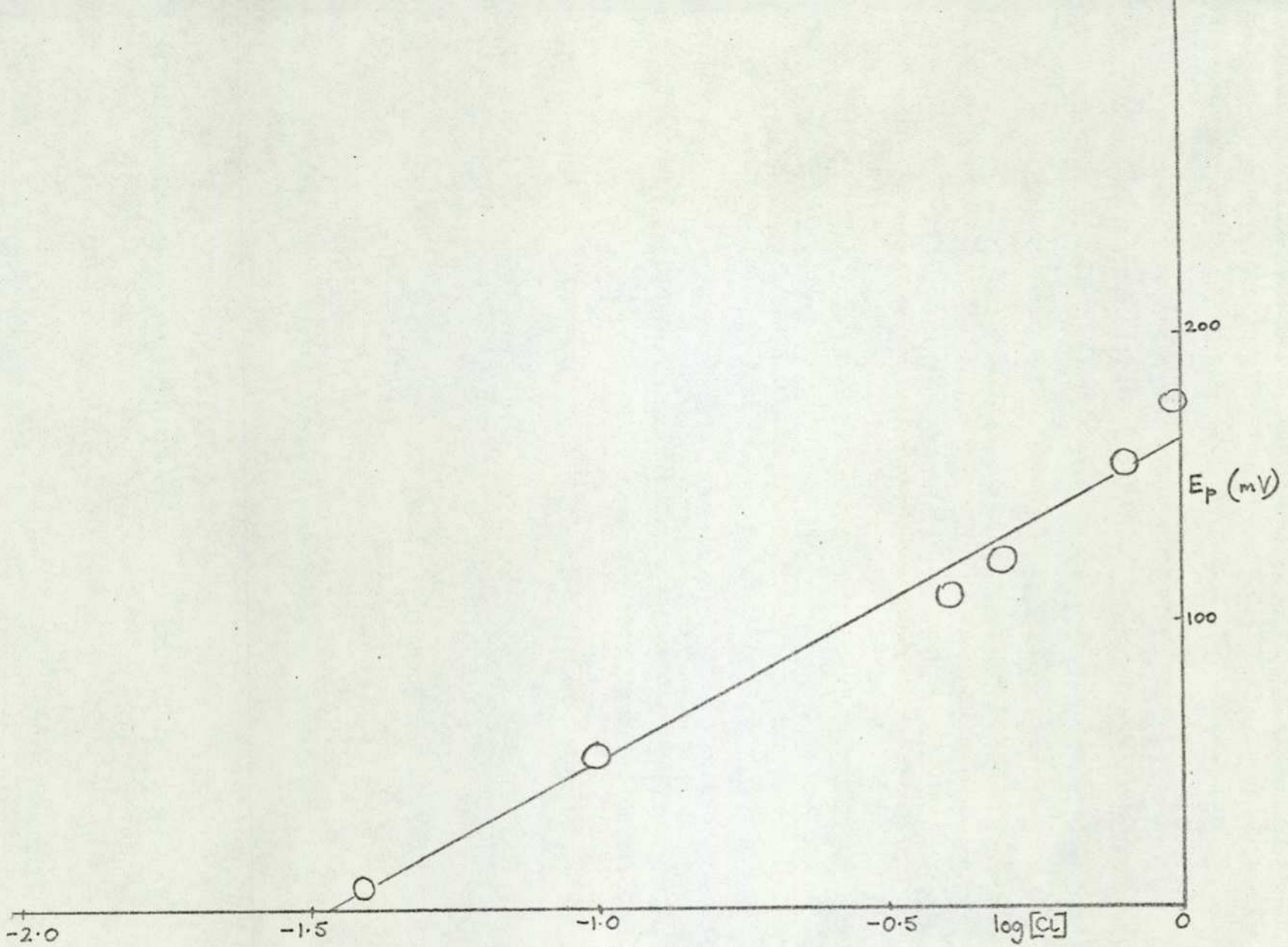


Fig. 22.

Variation of peak potential of peak R_2 with Chloride Ion concentration.

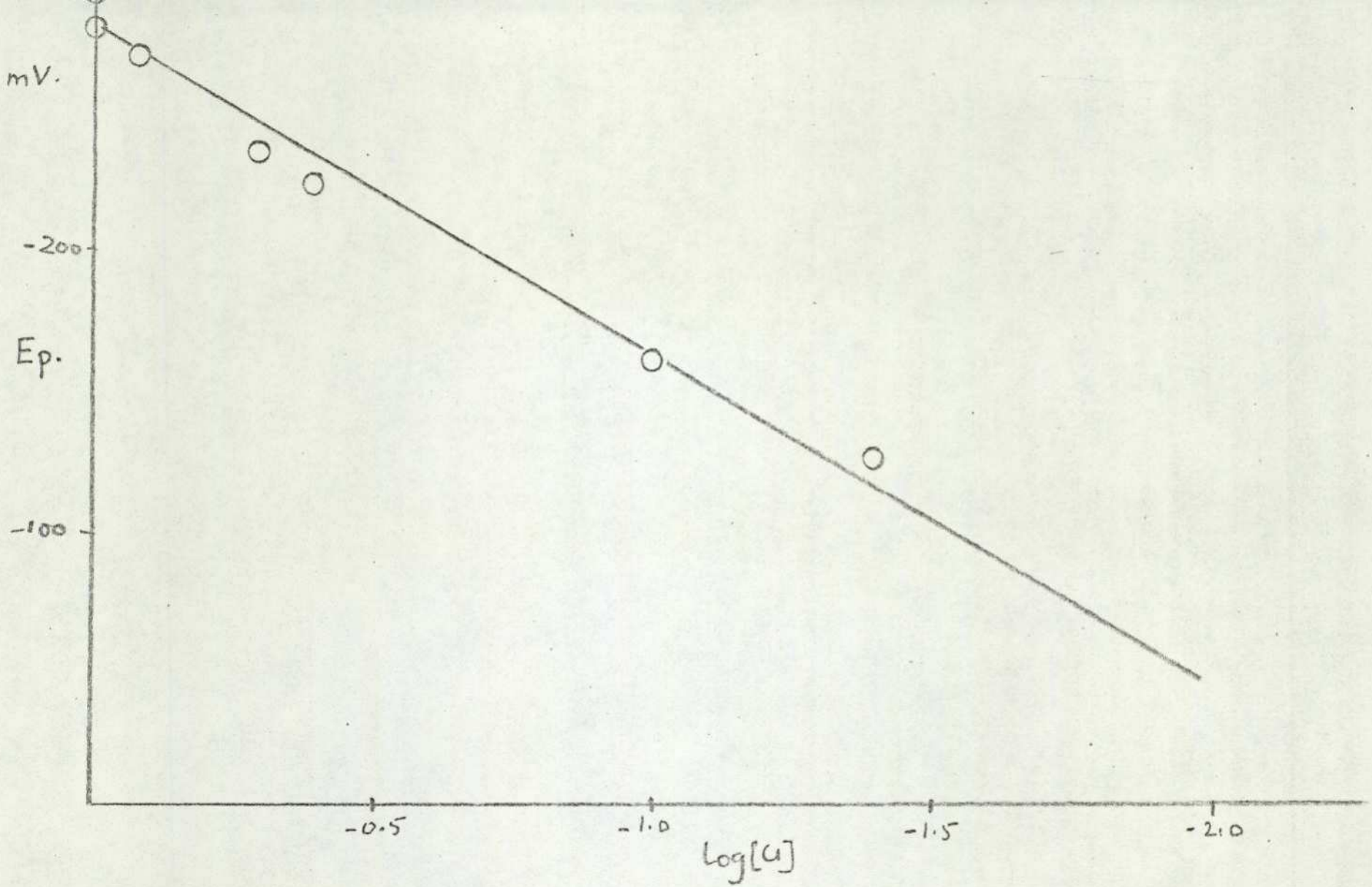


Fig. 23.

Variation of peak potential of peak R_2 with Chloride ion concentration.

REFERENCES FOR CHAPTER (3)

(1) Electroanalytical Chemistry, by J.J. Ligane, Interscience, 1958, pp 639 - 651

(2) M. Pourbaix, Atlas of Electrochemical Equilibria in Aqueous Solutions, Pergamon Press, 1966

(3) O. Gatty and E.C.R. Spooner. the Electrode potential behaviour of corroding metals in aqueous solutions, Clarendon Press, Oxford, 1938

(4) Ref. 2, page 387

(5) E. Mattson, Svensk Kemisk Tidskrift, 1962, 74, 76.

(6) J. Bjerrum, G. Schwarzenbach and L.G. Sillen. Stability Constants, Special Publication No. 17, The Chemical Society, London, 1964.

(7) W.M. Latimer, Oxidation Potentials, 2nd Ed., Prentice Press, New York, 1952.

(8) E. Mattron and J. O'M. Bockris, Trans. Faraday Soc., 1959, 1586.

(9) J. O'M. Bockris and M. Enyo, Trans. Faraday Soc., 1962, 1187.

(10) O.R. Brown and H.R. Thirsk, Electrochim Acta, 1965, 10, 383

(11) Mehl and Bockris, J. Chem. Phys., 1957, 27, 818.

(12) Mehl and Bockris, Can. J. Chem, 1959, 37, 190

(13) R.G. Pearson, Chem. in Britain, 1967, 104

(13a) R. Pearson, J. Chem. Educ, 1968, 45, 581

(14) S. Ahrland, Structure and Bonding, 1966, 1, 207

(15) S. Ahrland, Structure and Bonding, 1968, 5, 118

(16) J.C. Reeve, Ph.D. Thesis, University of London, 1971, and references therein.

(17) J. Heyrovsky, Disc. Faraday Soc., 1947, 1, 212

(18) L.E. Orgel, An Introduction to Transition metal chemistry, 2nd Ed., Methuen and Co., 1966

(19) H.J. Emeleus and A.G. Sharpe, Modern Aspects of Inorganic Chemistry, page 502 - 503, Pub. Routledge and Regan Paul, London, Fourth Edition, 1973.

(20) L.I. Gurevich and A.V. Pomosov, Electrokhimiya, 1971, 7, 158.

(21) A.V. Pomosov and A.I. Levin, Transactions of Conference on the Effects of Surface-Active agents on the Electrodeposition of Metals (in Russian), Gospolitauchizdat Vilnyus, 1957, p 227

(22) A.T. Kuhn, Chemistry and Industry, 1971, 473.

*(24) L.N. Nekrasov and N.P. Berezina, Dokl, Akad. Nauk SSSR (in Russian) 1962, 142, 855

(25) W.J. Albery and M.L. Hitchman, Ring-Disc Electrodes, Clarendon Press, 1971, page 78.

(26) D.G. Peters and S.A. Gruser, J. Electroanal. Chem., 1965, 9, 27.

(27) D.G. Peters and L.A. Franklin, J. Electroanal. Chem., 1965, 9, 385

(28) Determination of pH by R.G. Bates, John Wiley, 1964.

(29) A. Meyer, Galvanotechink and Oberflacheuscutz, 1961, 2, 91.

(30) N. Ibl in Advances in Electrochemistry and Electrochemical Engineering, Ed. C.W. Tobias, Interscience, 1962, Chapter 2.

(31) N. Ibl, J. Electrochem. Soc., 1967, 144, 1288.

*(23) New Instrumental Methods in Electrochemistry, by P. Delahay, Interscience, 1961, Ch. 8.

(32) C. Wagner, in Advances in Electrochem. and Electrochemical Engineering, Ed. C.W. Tobias, Interscience, 1962, Chapter I.

(33) C. Wagner, J. Electrochem. Soc., 1951, 96, 116.

(34) N. Ibl, PH. Javet and F. Stahel, Electrochemica Acto, 1972, 17, 733.

(35) G.W. Tindal and S. Bruckenstein, Anal, Chem., 1968, 40, 1051

(36) M.W. Breiter, J. Electrochem. Soc., 1967, 114, 1125

(37) G. Bates, in Techniques of Electrochem. Ed. E. Yeager and A.J. Salkind, Chapter One, Volume One, Wiley-Interscience, 1972.

(38) M. Stiulikova and F. Vydra, J. Electroanal. Chem., 1973, 44, 117.

CHAPTER 4

ELECTROLYSIS IN THE PRESENCE OF A REDUCING AGENT

4.1.a. Introduction

It was shown in Chapter 3 that the reduction of cupric ions to the metal takes place in a chloride medium via the following reactions; (pot. V. S. C. E.)

$$Cu^{2+} + 2Cl^{-} + e \rightleftharpoons Cu\,Cl_2^{1-} \qquad (4.1)$$

$$E^{o} = 0.165 + 0.114 \log \left[Cl^{-}\right] \qquad (4.1a)$$

$$Cu\,Cl_2^{1-} + e \rightleftharpoons Cu + 2Cl^{1-} \qquad (4.2)$$

$$E^{o} = -0.280 - 0.118 \log \left[Cl^{-}\right] \qquad (4.2a)$$

Therefore, if one could increase the cuprous ion concentration, the reaction should be more efficient and proceed at a faster rate than in solutions with much less cuprous ion concentrations. This is because of the following:-

(i) Since the reaction is,

$$Cu^{2+} \rightarrow Cu^{1+} \rightleftharpoons Cu \qquad (4.3)$$

then the cuprous ion is an intermediate ion in the reaction. It is a fact widely accepted in chemical kinetics that any increase in the reaction intermediate concentration should result in an increase in the rate of the overall reaction.

(ii) The cuprous complex formed has a higher diffusion coefficient than the cupric ions. Therefore, the mass transport of the electroactive species to the cathode is improved and, consequently, the rate and efficiency of the overall reaction are improved.

In general, the reduction of the cupric to the cuprous state can be achieved by using a reducing agent. The fundamental condition which a substance must satisfy in order to function as a reducing agent for a certain species is that the reversible potential of its electrode reaction be less positive (more reducing) than the potential of the species to be reduced. The electrode potentials may be computed from the standard electrode potential or other appropriate thermodynamic data of the substance concerned (1), with appropriate allowances for pH and other influencing factors.

If such a calculation shows that the reversible electrode potential occurs at more oxidizing potentials than that of the species to be reduced, then the substance definitely cannot function as a reducing agent. On the other hand, if the foregoing thermodynamic condition is fulfilled, the substance may or may not actually function as a reducing agent depending on the kinetic factors as reflected in the overvoltage.

Hydrazine is one of the most commonly known reducing agents used. Therefore, the author chose hydrazine to study the possibility of the partial chemical reduction of the cupric to the cuprous state, followed by an electrochemical reduction of the copper ions to the metallic state.

The half reaction for the oxidation of hydrazine, as is shown in Appendix One, is

$$N_2H_5^+ \rightarrow N_2 + 5H^+ + 4e \qquad (4.4)$$

$$E = -0.44 - 0.075pH - 0.015 \log \left[N_2H_5^+\right] \qquad (4.4a)$$

Table II in Appendix One shows that hydrazine should be able to reduce the cupric state to the cuprous and the metal state.

The results of table II Appendix One are presented in table 4.1.

Table 4.1

Variation of electrode potential of reaction 4.4 with pH

pH	Standard Electrode potential (referred to S.C.E.) mV
2	-590
3	-665
4	-740
5	-815
6	-890

4.2.a. Electrolysis at low pH, using hydrazinium sulphate as the reducing agent

Tables 4.2 to 4.5 show the results of the current efficiencies of copper deposition in solutions using hydrazinium sulphate as the reducing agent under varying conditions. All solutions using hydrazinium sulphate were freshly prepared.

Table 4.2

Potassium chloride	= 0.100 m
pH	= 2.0
Cu^{2+}	= 200 p.p.m.
Temperature	= $25^{o}C$
Current	= 15 mA

Electrode area = $7cm^2$

Time of electrolysis = 120 minutes

Volume of solution = 150 ml

$N_2H_4H_2SO_4$	Final p.p.m.	% efficiency
0.0m	18	76.8
0.002m	18	76.8
0.005m	16	77.6
0.01m	18	76.8
0.02m	16	77.6

Table 4.2a shows the effect of changing the chloride ion concentration on the current efficiency in the presence of 0.01m. hydrazinium sulphate.

Table 4.2.a

$N_2H_4H_2SO_4$ = 0.01m

Cu^{2+} = 200 p.p.m.

Temperature = 25^oC

pH = 2

Current = 15 mA

Electrode area = $7cm^2$

Time of electrolysis = 120 min

Volume of solution = 150 ml

KCl	Final p.p.m.	% efficiency
0.0m	50	63.3
0.003m	16	77.6
0.005m	18	76.8
0.01m	16	77.6
0.02m	18	76.8
0.1m	18	76.8

Table 4.3 shows the effect of varying the pH on the current efficiency.

Table 4.3

$N_2H_4H_2SO_4$ = 0.01 m

Cu^{2+} = 200 p.p.m.

KCl = 0.1m

Temperature = $25^{o}C$

Current = 15mA

Electrode area = $7cm^2$

Time of electrolysis= 60 min

Volume of solution = 150 ml

pH	final p.p.m.	% efficiency
1	95	88.6
2	95	88.6
3	95	88.6

In order to work at pH $\geq$ 4 it is necessary to use a buffer, therefore the results of electrolysis at pH $\geq$ 4 will be discussed in Section 4.2.b.

Table 4.4 shows the effect of varying the temperature on the current efficiency.

Table 4.4

$N_2H_4H_2SO_4$	= 0.01m
KCl	= 0.1m
Cu^{2+}	= 200 p.p.m.
pH	= 2
Current	= 15 mA
Electrode area	= 7 cm^2
Time of electrolysis	= 60 min.
Volume of solution	= 150 ml

Temperature	Final p.p.m.	% efficiency
25°C	95	88.6
37°C	92	91.1
45°C	90	92.8
53°C	90	92.8

Table 4.5 shows the variation of current efficiency with time during the electrolysis.

Table 4.5

$N_2H_4H_2SO_4$	= 0.01m
KCl	= 0.1m
Cu^{2+}	= 200 p.p.m.
pH	= 2
Temperature	= 25°C
Current	= 15 mA
Electrode area	= 7cm^2
Volume of Solution	= 150 ml

Time (min)	Final p.p.m.	% efficiency
0	200	-
30	155	75.9
60	95	88.6
90	47	86.6
120	18	76.8

Results in tables 4.2 - 4.5 show that the addition of hydrazinium sulphate to the solution at pH $\leq$ 3 does not improve the efficiency of the electrolysis as compared with the results shown in chapter three section 3.1.b.

These results indicate that although thermodynamically hydrazine should be able to reduce the cupric state to the metallic state, there must be a kinetic factor which hinders the reduction.

Lingane (3) found that hydrazine is oxidized electrochemically with an overpotential ranging from 600 to 900 mV. This is to be expected since the oxidation of hydrazine occurs via the formation of free radicals and unstable ions (4, 5, 15, 16, 17).

Other workers (6, 7, 8, 9, 10) have studied the chemical oxidation of hydrazine and came to the same conclusions. Cahn and Co-workers (6), and Rosseinsky (10) have found that hydrazine is not oxidized by cupric ions in acidic medium in agreement with the results obtained above.

4.2.b. Electrolysis at pH range 4 - 5.

Since the results in section 4.2.a. show that the electrolysis in the pH range 1 - 3 resulted in no significant

improvement in the current efficiencies, it was decided to carry out the electrolysis at higher pH. The buffer capacity of water and ordinary salts is low at pH 4 or more. (11) It was, therefore, decided to use buffers to control the pH. Lingane (12) in a similar set of experiments, but using constant potential electrolysis, employed a potassium tartrate buffer. In the following experiments, 0.02m potassium tartrate was used as a buffer. The pH of the solution was adjusted to the required value by the dropwise addition of sulphuric acid or potassium hydroxide solution.

Polarisation curves

Fig. 4.1 shows the steady state current potential curve of copper sulphate solution containing 0.1m potassium chloride and 0.02m potassium tartrate.

Curve A in Fig. 4.1 corresponds to a solution free of hydrazinium sulphate at pH 5, whereas curve B corresponds to the current-potential curve of a solution containing 0.01m hydrazinium sulphate. As can be seen from the curves, the presence of hydrazinium sulphate increases the limiting current of the system.

Table 4.6 and fig. 4.2 show the effect of varying the pH on the result of constant current electrolysis.

Table 4.6

Potassium chloride	= 0.1m
Potassium tartrate	= 0.02m
Hydrazinium sulphate	= 0.01m
Temperature	= $25^{o}C$
Cu^{2+}	= 200 p.p.m.

Current = 15 mA

Electrode area = 7cm^2

Time of electrolysis = 90 min

Volume of solution = 150 ml

pH	final p.p.m.	% efficiency
1	65	75.9
1.5	66	75.4
3	80	67.5
4	80	67.5
4.5	72	72.0
5	50	84.4

Tables 4.7, 4.8 and figures 4.3 and 4.4 show the effect of varying the concentration of hydrazinium sulphate and potassium chloride respectively.

Table 4.7

Potassium chloride = 0.1 molar

Potassium tartrate = 0.02 molar

Temperature = 25^{o}C

Initial Copper = 200 p.p.m.

Current = 15 mA

Electrode area = 7 cm^2

Time of Electrolysis = 90 minutes

pH = 5

Volume of solution = 150 ml.

Hydrazinium sulphate (molar)	Final Copper Concentration p.p.m.	% efficiency
0	80	67.5%
0.002	78	68.6
0.005	50	84.4
0.01	52	83.2
0.015	50	84.4
0.02	50	84.4
0.05	50	84.4

Table 4.8

Hydrazinium sulphate	= 0.01 molar
Potassium tartrate	= 0.02 molar
pH	= 5
Temperature	= $25^{\circ}C$
Electrode area	= $7cm^2$
Current	= 15 mA
Time of Electrolysis	= 90 minutes
Initial copper concentration	= 200 p.p.m.
Volume of solution	= 150 ml.

KCl (molar)	Final copper concentration p.p.m.	% efficiency
0.0	A precipitate of copper metal was formed and the magnetic stirrer was plated with copper	
0.005	48	85.5

Table 4.8 continued

KCl (molar)	Final copper concentration p.p.m.	% efficiency
0.01	49	84.9
0.015	52	83.3
0.020	50	84.4
0.10	50	84.4

The results in table 4.8 show that the presence of chloride ions is essential in order to stabilize the intermediate cuprous ions formed and prevent their disproportionation and the formation of the copper metal. The results of table 4.7 show that the presence of hydrazine improves the efficiency of deposition of a tartrate solution. These results are also confirmed by the current potential curves shown in figure 4.1 where it was observed that the limiting current for the hydrazine solution was 8.5 mA as compared with a value of 5.5 mA for hydrazine free solution. However the value of 8.5 mA is still lower than the value 10 mA obtained in chapter three for the unbuffered hydrazine free solution. This can be explained in terms of the higher diffusion coefficient of the copper tartrate complexes as compared with the diffusion coefficient of the hydrated cupric ion.

Results in table 4.7 show that there is partial reduction of the cupric-tartrate complexes (Appendix two) to the cuprous state. This was confirmed by measuring the concentration of the cuprous state formed by the chemical reduction of the cupric state with hydrazine. This was effected by reducing the unreacted cupric ions completely to the cuprous state at a controlled potential of

-100 mV against the S.C.E. The results of these experiments will be discussed in section 4.4.a.

It suffices to mention that the degree of the chemical conversion of the cupric state to the cuprous state under the conditions of table 4.7 was found to be 35%.

Using the result of 35% conversion and the data shown in table 4.9 it can be shown that the limiting current of solutions containing hydrazine should be higher than those in which hydrazine is absent.

Table 4.9

Species	Diffusion Coefficient	Reference
Cu^{2+}	7.8×10^{-6} cm^2. s^{-1}	13
$Cu\,Cl_2^{1-}$	13.3×10^{-6} cm^2. s^{-1}	13
$Cu(Tartrate)_2$	3.8×10^{-6} cm^2. s^{-1}	12

Now

$$i_l = \frac{nFDAC}{\delta} \qquad (4.5)$$

where

C = 3.15×10^{-6} mole. cm^{-3} of cupric ion

A = 7cm^2

F = 96490 coul (g.eq)$^{-1}$

i_l = Limiting current, A

δ = Nerst diffusion layer, cm

n = number of electrons.

Substituting the value of the limiting current observed for copper solution (Chapter three, i_l = 10 mA) in equation 4.5, the value of δ was found to be 3.3×10^{-3} cm.

Since the degree of chemical reduction of the cupric to the cuprous state ($CuCl_2^{1-}$) is 35%, the concentration of the cuprous state equals 1.103×10^{-6} g. ion. cm^{-3} and the concentration of the cupric complexes (Appendix two) is 2.047×10^{-6} g. ion cm^{-3}.

In a solution containing both cupric and cuprous complexes, the resulting limiting current is the sum of the currents due to the cuprous and cupric states,

i.e.

$$i_T = \frac{n_1 D_1 FAC_1}{\delta} + \frac{n_2 D_2 FAC_2}{\delta} \qquad (4.6)$$

where

i_T = The total limiting current.

Subscripts 1 and 2 refer to the cuprous and cupric states respectively.

Using the value of the limiting current for hydrazine free, buffered solution, i_l = 5.5 mA, (Fig. 4.1), the value of D_2 was found to be 4.26×10^{-6} $cm^2 . s^{-1}$. Substituting the value of D_2 in equation 4.2, the value of i_T is found to be 6.6 mA. This compares well with the observed value (8.5 mA).

The calculated value is lower than the observed value for the following reasons:

(a) There is a range in the limiting current observed in curve A figure 4.1, therefore the calculated value of D_2 is not accurate.

(b) As is shown in Appendix two, there are two main cupric species, namely $Cu(Tartrate)_1$ (43.8% of the total cupric ions), and $Cu(Tartrate)_2$ (54.3% of the total cupric ions). The diffusion coefficient of the bulkier ditartrate complex is expected to be smaller than that of the monotartrate complex.

For example, the value of the diffusion coefficient of the cupric complexes found by Lingane (12), Table 4.9, is lower than the value calculated by the author. This is because the composition of the cupric complexes used by Lingane was $Cu(Tartrate)_1$ = 5%, $Cu(Tartrate)_2$ = 87% and $Cu(Tartrate)_3$ = 8%. Therefore the value of 4.26×10^{-6} $cm^2 . s^{-1}$ for D_2 used by the author is not an accurate value because there are two cupric species in the solution as shown in Appendix two.

Since less charge is needed to reduce the cuprous state, the efficiencies quoted in tables 4.2 - 4.8 are all apparent efficiencies because they were calculated on the assumption that the overall electrochemical reduction is a two electron process. In fact later on in this chapter apparent efficiencies of over 100% will be quoted.

It must be mentioned that if a solution containing potassium chloride, potassium tartrate, hydrazinium sulphate and copper sulphate is left overnight, copper metal is deposited. But it was found that if potassium chloride is replaced by potassium bromide no precipitate is formed when the solution is left overnight.

Some experiments were repeated using potassium bromide instead of potassium chloride. Table 4.10 shows the result of varying the hydrazinium sulphate concentration on the result of electrolysis.

Table 4.10

Potassium bromide	= 0.1 molar
Potassium tartrate	= 0.02 molar
Initial Copper	= 200 p.p.m.

pH = 5

Temperature = 25°C

Current = 15 mA

Electrode area = 7cm^2

Time of electrolysis = 90 minutes

Volume of solution = 150 ml

$N_2H_4H_2SO_4$ (molar)	Final p.p.m.	% efficiency
0.005	50	84.4
0.01	40	90
0.02	43	88.3
0.05	40	90

Table 4.11 shows the effect of varying the potassium bromide concentration.

Table 4.11

Hydrazinium sulphate = 0.01 molar

Potassium tartrate = 0.02 molar

Initial copper concentration = 200 p.p.m.

pH = 5

Temperature = 25°C

Current = 15 mA

Time of electrolysis = 90 minutes

Electrode area = 7 cm^2

Volume of Solution = 150 ml

KBr molar	Final p.p.m.	% efficiency
0.0	Copper metal precipitated	
0.005	A green precipitate of cuprous bromide was formed	
0.02	40	90
0.04	43	88.3
0.06	40	90
0.10	40	90

One concludes from the above results that the introduction of potassium bromide does not improve the results sufficiently to warrant its use. Its main advantage is that it stabilizes the solution over a long period. But as will be seen later the use of a weaker reducing agent will obviate the necessity of using potassium bromide.

4.3.a. Electrolysis at Higher Temperatures

Table 4.12 and figure 4.5 show the effect of increasing the temperature upon the result of electrolysis.

Table 4.12

Potassium Tartrate	=	0.02 molar
Potassium Chloride	=	0.1 molar
pH	=	5
Initial Copper concentration	=	200 p.p.m.
Current	=	15 mA
Time of electrolysis	=	60 minutes
Hydrazinium Sulphate	=	0.01 molar

Electrode area = 7 cm^2

Volume of Solution = 150 ml

Temperature	Final p.p.m.	% efficiency (apparent)
25	95	88.6
35	75	105.5
45	53	124
53	40	135

As expected, raising the temperature improves the apparent efficiency of deposition because the chemical conversion of the cupric to the cuprous state is increased. In fact, as will be shown later, controlled potential reduction of cupric to cuprous state shows that about 50% of the cupric ions were reduced to the cuprous state at 45°C. Furthermore figures 4.6 and 4.7 are current potential curves for tartrate solutions without and with hydrazinium sulphate. It can be seen that the limiting current at 45°C in the presence of hydrazine is approximately 13.5 mA whereas in the absence of hydrazine it is roughly 11 mA. Again the increase in the limiting current is due to the presence of the cuprous complex in solution.

Tables 4.13, 4.14 and figures 4.8 and 4.9 show the effect of varying the pH and hydrazinium sulphate concentration on the result of electrolysis respectively at 45°C.

Table 4.13

Potassium tartrate = 0.02 molar

Potassium Chloride = 0.1 molar

Initial Copper concentration = 200 p.p.m.

Hydrazinium sulphate = 0.01 molar

Current = 15 mA

Temperature = 45°C

Time of electrolysis = 60 minutes

Electrode area = 7 cm^2

Volume of solution = 150 ml.

pH	Final Copper p.p.m.	Apparent Efficiency
4	93	90.3
4.5	85	97.0
5.0	53	124
5.4	41	135

Table 4.14

Potassium Tartrate = 0.02 molar

Potassium Chloride = 0.1 molar

Initial Copper concentration = 200 p.p.m.

pH = 5

Temperature = 45°C

Current = 15 mA

Time of electrolysis = 60 minutes

Electrode area = 7 cm^2

Volume of solution = 150 ml

Hydrazinium sulphate (molar)	Final Copper p.p.m.	Apparent efficiency
0	113	73.4
0.0025	80	100
0.005	60	118
0.01	53	124
0.015	38	134

Figures 4.10 and 4.11 show the variation of the electrode potential of the working electrode during the electrolysis in solutions with and without hydrazinium sulphate respectively. Again the figures show that the electrode potential is more positive during the electrolysis in the presence of hydrazine. This is of course due to the improved efficiency of deposition.

Table 4.15 and figures 4.12 and 4.13 show the results of electrolysis at different currents.

Table 4.15

Potassium Tartrate	= 0.02 molar
Potassium Chloride	= 0.1 molar
Initial copper concentration	= 200 p.p.m.
pH	= 5
Temperature	= $45^{o}C$
Volume of solution	= 150 ml
Electrode area	= 7 cm^2

Current mA	Time (min)	p.p.m.	Apparent efficiency
15			
	0	200	-
	15	153	158.6
	30	120	134.5
	60	53	124
	90	9.5	107.2
21			
	0	200	-
	15	143	137.4
	30	105	114.5
	45	49	124.5
	60	20	108.5
30			
	0	200	-
	15	138	104
	30	70	109
	45	40	90
	60	12	79

As can be seen, at very high current densities (30 mA), the efficiency of deposition decreases because the mass transport effect becomes significant at higher currents and lower concentrations.

The tartrate ion forms relatively strong complexes with the cupric ions. The complexes formed are shown below (14).

More detailed information is presented in Appendix two.

$$M + L \rightleftharpoons ML \qquad \beta 1 = \frac{[ML]}{[M][L]} = 10^{3.2} \qquad (4.7)$$

$$M + 2L \rightleftharpoons ML_2 \qquad \beta_2 = \frac{[ML_2]}{[M][L]^2} = 10^{5.11} \qquad (4.8)$$

$$M + 3L \rightleftharpoons ML_3 \qquad \beta_3 = \frac{[ML_3]}{[M][L]^3} = 10^{4.77} \qquad (4.9)$$

$$M + 4L \rightleftharpoons ML_4 \qquad \beta_4 = \frac{[ML_4]}{[M][L]^4} = 10^{6.5} \qquad (4.10)$$

where

M = metal ion

L = ligand

[ ] = concentration

In the above equations signs were omitted for convenience.

If a salt used to buffer the solutions forms weaker complexes with the cupric ions, then the efficiency of deposition should be increased because it would be easier to reduce such complexes.

One such salt is potassium acetate. The stability constants of the acetate-cupric complexes are (14)

$$M + L \rightleftharpoons ML \qquad \beta_1 = 10^{1.7} \qquad (4.11)$$

$$M + 2L \rightleftharpoons ML_2 \qquad \beta_2 = 10^{2.7} \qquad (4.12)$$

$$M + 3L \rightleftharpoons ML_3 \qquad \beta_3 = 10^{3.0} \qquad (4.13)$$

Equations 4.11, 4.12 and 4.13 show that the stability constants of the acetate complexes are two orders of magnitude less than those of the tartrate complexes and therefore the efficiency of copper deposition should be improved in an acetate solution.

Table 4.16 confirms the above conclusion. Comparisons of results using acetate and tartrate buffers are shown in table 4.16.

Table 4.16

Hydrazinium Sulphate	= 0.1 molar
Initial Copper Concentration	= 200 p.p.m.
Potassium Chloride	= 0.1 molar
Current	= 15 mA
Time of electrolysis	= 60 minutes
Volume of solution	= 150 ml
Electrode area	= 7 cm^2

Salt (0.02 molar)	pH	Final p.p.m	Apparent Efficiency
Potassium Acetate			
	4.0	76	104
	4.5	50	126·5
	5.0	25	147·6
Potassium Tartrate			
	4.0	93	90·27
	4.5	85	97
	5.0	53	124

4.3.b. Using Sulphite As a Reducing Agent

It was necessary to try another reducing agent since hydrazine is an expensive chemical. The most obvious other choice is the sulphite ion.

Figure 4.14 shows the current potential curve for an acetate solution containing 200 p.p.m. copper and 0.005 molar sodium sulphite at 45°C.

The limiting current for the above system is roughly 17 mA. This value of the limiting current is higher than any obtained during the course of this research.

Table 4.17 shows the result of varying the concentration of sodium sulphite upon the efficiency of electrolysis.

Table 4.17

Potassium Acetate	= 0.02 molar
Potassium Chloride	= 0.1 molar
Initial Copper Concentration	= 200 p.p.m.
pH	= 5
Temperature	= 45°C
Current	= 30 mA
Electrode Area	= 7 cm^2
Time of electrolysis	= 30 minutes
Volume of solution	= 150 ml

Sodium Sulphite (molar)	Final p.p.m.	Apparent Efficiency
o	94	87.7
0.002	61	117.3
0.0035	54	122.3
0.005	54	122.3

Table 4.18 shows the result of electrolysis at a current density of 4.28 mA/cm^2 at 45°C.

Table 4.18

Potassium Acetate	= 0.02 molar
Potassium Chloride	= 0.1 molar

Sodium Sulphite	= 0.005 molar
pH	= 5
Current	= 30 mA
Electrode area	= 7cm^2
Temperature	= 45^{o}C
Volume of Solution	= 150 ml

Time (minutes)	p.p.m.	Apparent Efficiency
0	200	-
15	121	131.6
30	54	122.3
34	40	119.3
40	20	113.9

Table 4.19 shows the effect of increasing the temperature upon the efficiency of deposition.

Table 4.19

Potassium Acetate	= 0.02 molar
Potassium Chloride	= 0.1 molar
Initial Copper Concentration	= 200 p.p.m.
Sodium Sulphite	= 0.005 molar
pH	= 5
Current	= 15 mA
Time of electrolysis	= 60 minutes
Volume of Solution	= 150 ml

Temperature (^{o}C)	Final p.p.m.	Apparent Efficiency
25	68	111.3
45	32	141.7

As can be seen from table 4.19 electrolysis at room temperature gives very encouraging results.

It must be pointed out that after adding the sodium sulphite, copper sulphate, buffer, and adjusting the pH to 5, the colour of the resulting solution is light green. On leaving the solution overnight, no precipitate was formed. In the case of hydrazine and tartrate the colour of the resulting solution was dark blue initially but changed to green and finally to light yellow.

4.4.a. Controlled Potential Electrolysis

This technique was used to estimate the percentage conversion of the cupric ions to cuprous ions. Since reducing agents were present in the solution it was decided to estimate the concentration of the cuprous ions indirectly by reducing the remaining cupric ions to the cuprous state and measuring the quantity of electricity required to complete the reduction.

If

Q_o = measured quantity of electricity required to complete the reduction of the cupric ions to the cuprous ions.

Q_c = measured quantity of electricity in the absence of a reducing agent, required to completely reduce the cupric state to the cuprous state.

then

$$\% \text{ conversion} = \frac{Q_c - Q_o}{Q_c} \times 100$$

Figures 4.16 and 4.15 are potential-current curves for stirred solutions with and without hydrazinium sulphate. A small platinum electrode, area 3.2 cm^2, was used as the cathode. Both curves show two waves, the first one starting at -100 mV, is due to the reduction of the cupric to the cuprous state.

Therefore, -100 mV (against S.C.E.) was chosen as the control potential for estimating the degree of conversion. The theory and experimental of controlled potential electrolysis have been explained in Chapter two, section

Tables 4.20 - 4.24 and figures 4.17 to 4.21 and 4.17a to 4.21a show the results of controlled potential electrolysis.

Table 4.20

Control Potential	= -100 mV against S.C.E.
Potassium Tartrate	= 0.02 molar
Potassium Chloride	= 0.1 molar
Copper sulphate	= 3.15×10^{-3} molar
pH	= 5
Temperature	= $45^{\circ}C$
Platinum Electrode area	= 38 cm^2
Volume of Solution	= 150 ml

Time (sec)	Current A x 10^{-3}	log (current)
120	35	-1.456
300	29	-1.538
480	25	-1.602
600	22.5	-1.648
720	20	-1.699
900	17	-1.769
1080	14.5	-1.839
1200	13.0	-1.886
1320	11.5	-1.939
1440	10.5	-1.979

$\therefore$ i_o = 38 x 10^{-3}A (intercept of figure 4.17a)

k = 3.92 x 10^{-4} sec^{-1} (slope of figure 4.17a)

$$\therefore \mathbb{Q}_c = \frac{0.038}{2.303 \times 3.92 \times 10^{-4}}$$

= 42.14 coul.

The theoretical value of $\mathbb{Q}_c$ is 45.6 coul. The difference between the observed and the theoretical value can be explained in terms of the diffusion of the cupric ions to the anode compartment.

Table 4.21

Control Potential	= -100 mV vs S.C.E.
Potassium tartrate	= 0.02 molar
Potassium chloride	= 0.1 molar
Hydrazinium sulphate	= 0.01 molar
Copper sulphate	= 3.15 x 10^{-3} molar
pH	= 5

Temperature = 25°C

Platinum Electrode area = 38 cm^2

Volume of solution = 150 ml

Time (sec)	Current (A)	log (current)
180	9.6×10^{-3}	-2.018
300	9.2×10^{-3}	-2.036
480	8.43×10^{-3}	-2.074
600	8.0×10^{-3}	-2.097
780	7.5×10^{-3}	-2.125
900	7.25×10^{-3}	-2.140
1080	6.7×10^{-3}	-2.174
1200	6.5×10^{-3}	-2.187
1500	5.9×10^{-3}	-2.229

Hence, $i_o = 10 \times 10^{-3}$A (intercept of figure 4.18a)

$k = 1.46 \times 10^{-4} sec^{-1}$ (slope of figure 4.18a)

$Q_o = i_o/2.303k = 29.7$ coul.

Therefore % conversion of tartrate solution containing 0.01 molar hydrazine at room temperature is given by

$$\% \text{ conversion} = \frac{42.14 - 29.7}{42.14} \simeq 30\%$$

using the theoretical value of Q_c, then

$$\% \text{ conversion} = \frac{45.6 - 29.7}{45.6} = 35\%$$

Table 4.22

Control Potential	= -100 mV vs S.C.E.
Potassium Tartrate	= 0.02 molar
Potassium Chloride	= 0.1 molar
Hydrazinium Sulphate	= 0.01 molar
Copper sulphate	= 3.15×10^{-3} molar
pH	= 5
Temperature	= $45^{o}C$
Electrode area	= 38 cm^2
Volume of solution	= 150 ml

Time (sec)	Current (A)	log (current)
240	12.4×10^{-3}	-1.910
300	11.9×10^{-3}	-1.924
360	11.38×10^{-3}	-1.944
420	10.8×10^{-3}	-1.967
480	10.13×10^{-3}	-1.994
600	9.5×10^{-3}	-2.022
720	8.63×10^{-3}	-2.064
900	8.0×10^{-3}	-2.097
1140	7.0×10^{-3}	-2.155

Hence

$i_o = 15.1 \times 10^{-3}$A (from intercept of figure 4.19a)

$k = 3.3 \times 10^{-4} sec^{-1}$ (slope of figure 4.19a)

$\therefore \quad Q_o = 19.9$ coul $= i_o/2.303\ k$

$\therefore$ % conversion of tartrate solution containing hydrazine at $45^{o}C$ is given by

$$\% \text{ conversion} = \frac{42.14 - 19.9}{42.14}$$

$$= 52{\cdot}7 \ \%$$

Table 4.23

Potassium Acetate	= 0.02 molar
Potassium Chloride	= 0.1 molar
Hydrazinium sulphate	= 0.01 molar
Copper sulphate	= 3.15×10^{-3} molar
pH	= 5
Temperature	= $45^{o}C$
Electrode area	= 38 cm^2
Control Potential	= -100 mV against S.C.E.
Volume of Solution	= 150 ml

Time sec.	Current A	Log (current)
180	6.2×10^{-3}	-2.208
240	5.65×10^{-3}	-2.248
300	5.40×10^{-3}	-2.268
360	5.10×10^{-3}	-2.290
420	4.90×10^{-3}	-2.310
540	4.6×10^{-3}	-2.340

Hence

$$i_o = 9.25 \times 10^{-3} A \text{ (intercept of figure 4.20a)}$$

$$k = 3.6 \times 10^{-4} \text{ sec}^{-1} \text{ (slope of figure 4.20a)}$$

$$\therefore \quad Q_o = \frac{i_o}{2.303k}$$

$$= 11.2 \text{ coul.}$$

Therefore, percentage conversion in acetate solution containing 0.01 molar hydrazinium sulphate at 45°C is given by

$$\% \text{ conversion} = \frac{42.14 - 11.2}{42.14} = 71\ \%$$

As was expected the use of acetate buffer has increased the extent of the chemical reduction of the cupric ions as compared with tartrate buffer.

Table 4.24

Potassium Acetate	= 0.02 molar
Potassium Chloride	= 0.1 molar
Sodium sulphite	= 0.005 molar
Copper sulphate	= 3.15×10^{-3} molar
pH	= 5
Temperature	= 45°C
Electrode area	= 38 cm^2
Control Potential	= -100 mV against S.C.E.
Volume of solution	= 150 ml.

Time sec.	Current A	Log (current)
120	14.75×10^{-3}	-1.831
300	12.1×10^{-3}	-1.917
420	11.0×10^{-3}	-1.959
480	10.4×10^{-3}	-1.983
600	9.6×10^{-3}	-2.018
720	8.6×10^{-3}	-2.066
900	7.8×10^{-3}	-2.108
1200	6.5×10^{-3}	-2.187

From intercept of figure 4.21a, $i_o = 15.85 \times 10^{-3}$A

From slope of figure 4.21a, $k = 3.6 \times 10^{-4}$sec^{-1}

$\therefore \quad Q_o = i_o/2.303k = 19.1$ coul.

Therefore percentage of conversion in acetate solution containing 0.005 molar sodium sulphite at 45°C is given by

$$\% \text{ conversion} = \frac{42.14 - 19.1}{42.14}$$

$$= 54.6\%$$

It must be emphasized that during the course of these experiments about 10 p.p.m. or less of copper diffused to the anode compartment. This introduces an error of about 1 coulomb. Furthermore the background current, current due to supporting electrolyte only, was found to be less than 0.2 mA; therefore it was not found necessary to take the background current into account. The percentages of conversion quoted above were reproducible to within less than 4%. It must be pointed out that the possibility of deposition of Cu_2O does not exist under the conditions of the experiment, since there was no visual evidence for its deposition during the controlled potential electrolysis experiments conducted.

As can be seen from the results above, the cupric ions are partially chemically reduced to the cuprous state. The degree of chemical reduction increases by raising the temperature.

4.4.b Linear Sweep Voltammetry

Figures 4.22 and 4.23 show the potential-current curve of the background electrolyte used. It is clear from the figures that there is no electrochemical reduction of hydrazine or sulphate in the region of copper deposition.

Figure 4.24 shows two current-potential curves of a tartrate solution at different pH in the absence of a reducing agent. Curve A, pH 1.7, is similar to the curve in figure 3.15 chapter three. Curve B, pH 5, has the second peak shifted to a more cathodic region because the cupric ions are complexed with the tartrate ions (appendix three). The third peak position has not changed. This indicates that the reaction corresponding to the third peak (R_3) is still

$$Cu\,Cl_2^{1-} + e \rightleftharpoons Cu + 2Cl^-$$

In appendix two it is shown that 44.8% of the cupric ions are complexed to one tartrate ion and 54.3% are complexed to two tartrate ions. Therefore, it is difficult to assign an exact reaction to peak R_2, but it must be due to a reduction of the cupric to the cuprous state.

Addition of a reducing agent (at pH 5) shifts peak R_2 back to the value at pH 1.7 in figure 4.24, while peak R_3 position remains unchanged, as shown in figures 4.25 and 4.26. These results seem to indicate that the cuprous state does not form complexes with the tartrate and acetate ions or it forms very weak complexes. In any case these results indicate that the cuprous state is present as $Cu\,Cl_2^{1-}$ ion and not Cu Cl (s). These results are also confirmed by results in section 4.4a where there was no visual evidence for either Cu_2O(s) or Cu Cl (s).

4.5.a Conclusion

Results in chapter three show that copper is deposited more efficiently in the presence of chloride ions. The improvement in current efficiency of copper deposition in the presence of a

chloride ion could be due to the chloride bridge mechanism outlined in Chapter three, section 3.1.a . Furthermore results in Chapter three show that carrying out the electrolysis at currents higher than the limiting current results in the formation of powdery deposits which have high surface area. The higher surface area will decrease the polarization of the copper electrode and hence add to the improvement of current efficiency.

Linear voltammetric work has shown that copper deposition takes place via the following electrochemical reactions in a chloride medium

$$Cu^{2+} + 2Cl^{1-} + e \rightleftharpoons Cu\,Cl_2^{1-}$$

$$CuCl_2^{1-} + e \rightleftharpoons Cu + 2Cl^{1-}$$

Partial chemical reduction of the cupric ion to the cuprous state followed by electrochemical reduction to the copper metal results in higher current efficiency even at current densities higher than the limiting current densities. The presence of chloride ions is essential in the integrated chemical-electrochemical process because it stabilizes the cuprous ions formed during the chemical reduction.

Hydrazine and sodium sulphite are two reducing agents that can be used to achieve the partial chemical reduction of the cupric ions to the cuprous ions under right conditions of pH and temperature.

The integrated chemical-electrochemical process results in a higher rate of production of copper metal in a shorter time. Therefore, this process is time and power saving.

Furthermore, if the electrolysis is carried out in a one compartment cell, the power consumption will be further reduced because the reducing agent will act as an anodic depolarizer. For example the average cell voltage during two hours electrolysis of a chloride-free, buffer-free and hydrazine-free solution containing 200 p.p.m. copper at pH 2 at 15 mA was found to be 2.90V; whereas the average cell voltage of a similar solution containing 0.01m hydrazinium sulphate during electrolysis at the same current and for the same period of time was 1.1 V.

Finally the author does not think that the integrated chemical-electrochemical method can be used for the recovery of other common divalent, trivalent, or hexavalent metal ions like Ni(11) and Cr(VI) since this would involve the production of very unstable low valency ions like Ni(1)

4.5.b Suggestionsfor future work

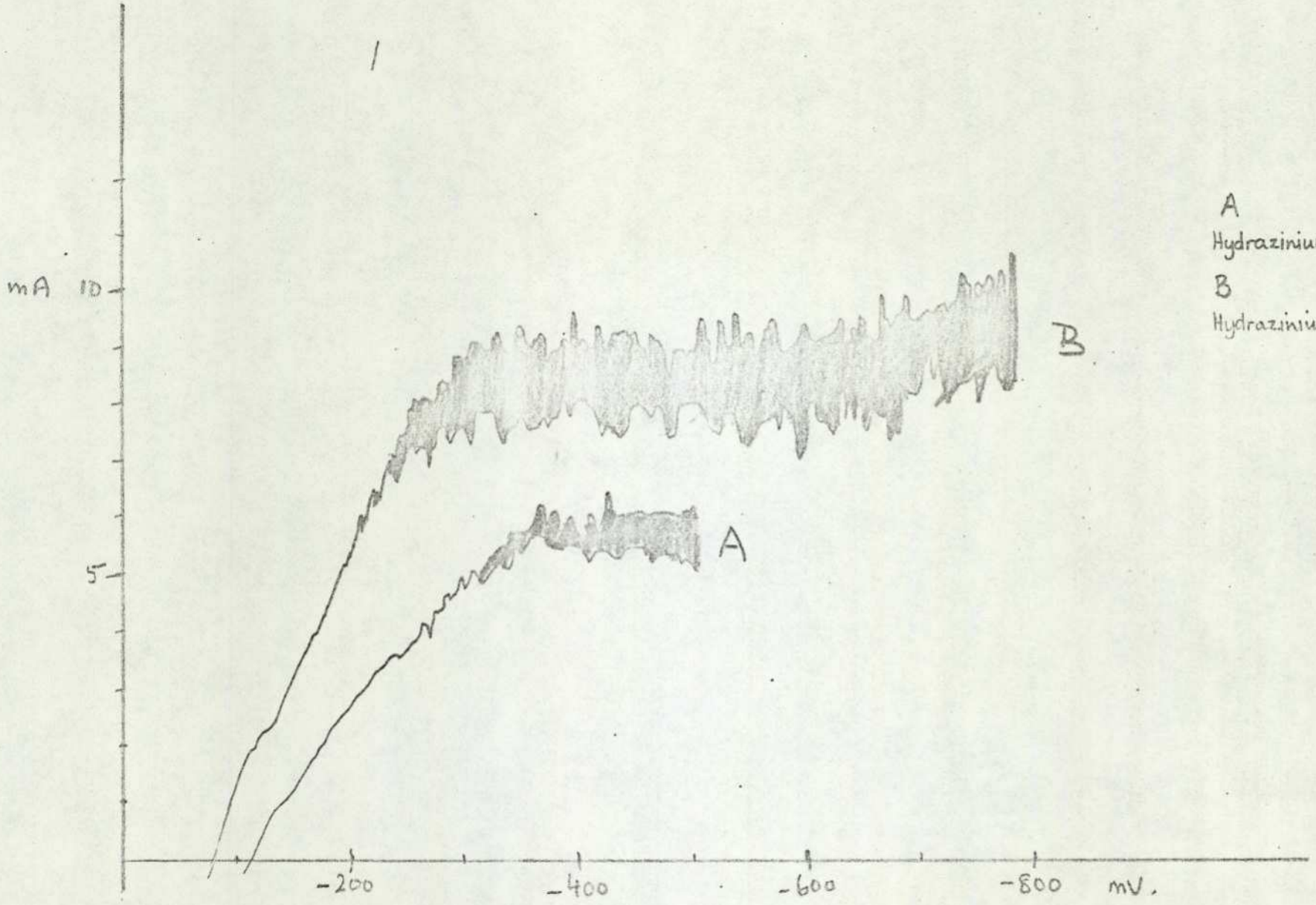
The author suggests the following projects for further research.

(a) The use of sulphur dioxide as a reducing agent since it is much cheaper than Hydrazine or Sodium sulphite.

(b) The effect of ions like Ferric, Ferrous, Chromate, and Nickel on the efficiency of copper deposition in the presence of reducing agents.

(c) Study of the mechanism of copper deposition in chloride and bromide media.

(d) The application of the Integrated Chemical-Electro-Chemical method to newly designed cells like the fluidized bed electrode, etc. mentioned in Chapter one.



A
Hydrazinium sulphate = 0·0 molar.
B
Hydrazinium sulphate = 0·01 molar.

Fig. 4.1. Steady state current-potential curve for $CuSO_4$ (stirred solution),

T = 25°C, pH = 5, Cu^{2+} = 200 p.p.m.; KCl = 0·1 molar, potassium tartrate = 0·02 molar.

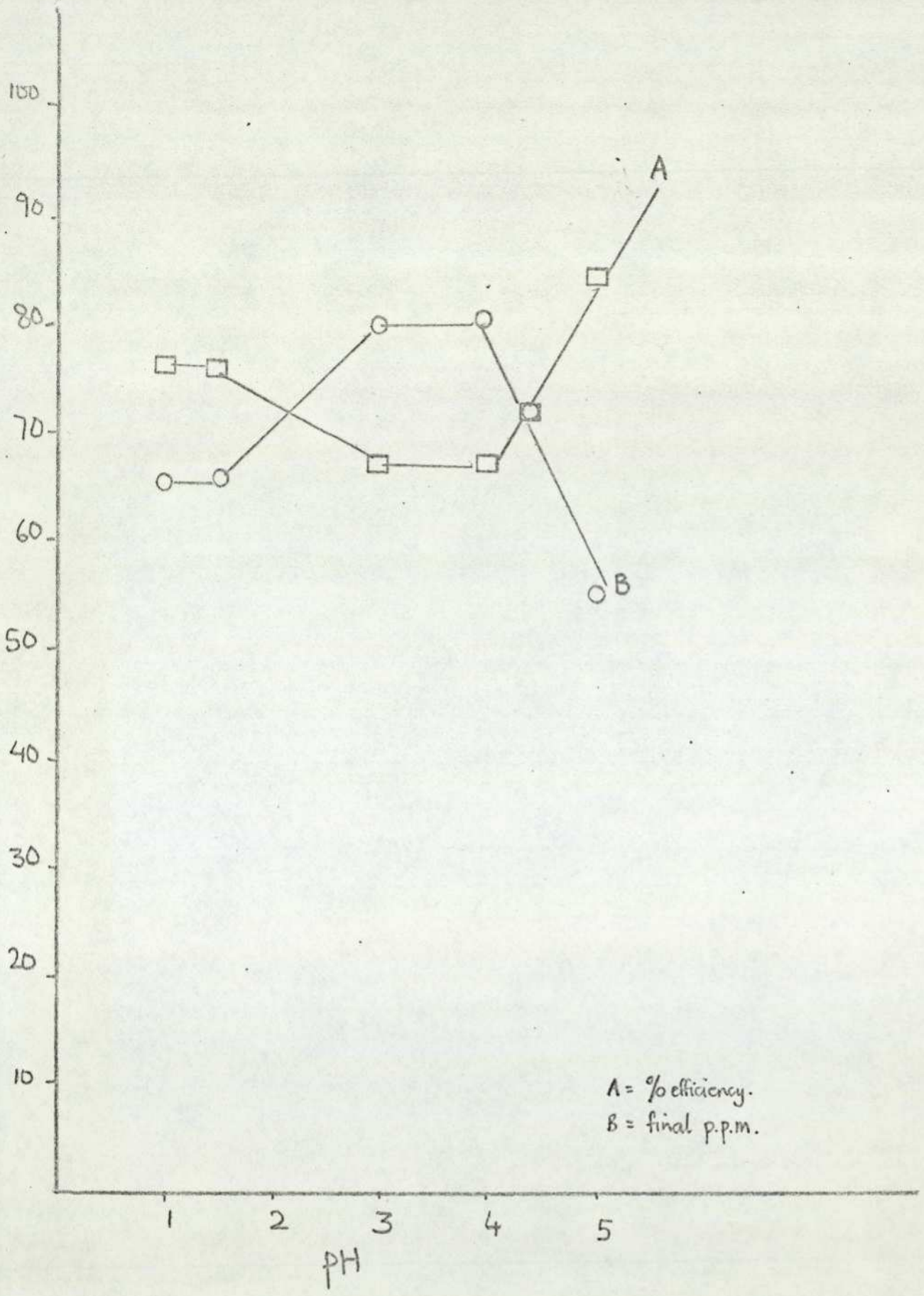


Fig. 4.2. Effect of varying pH on copper deposition.

Cu^{2+} = 200 p.p.m; KCL = 0·1 molar, potassium tartrate 0·02 molar, hydrazinium sulphate 0·01 molar, T = 25°C, time of electrolysis 90 min, c.d. = 4·12 mA/cm^2.

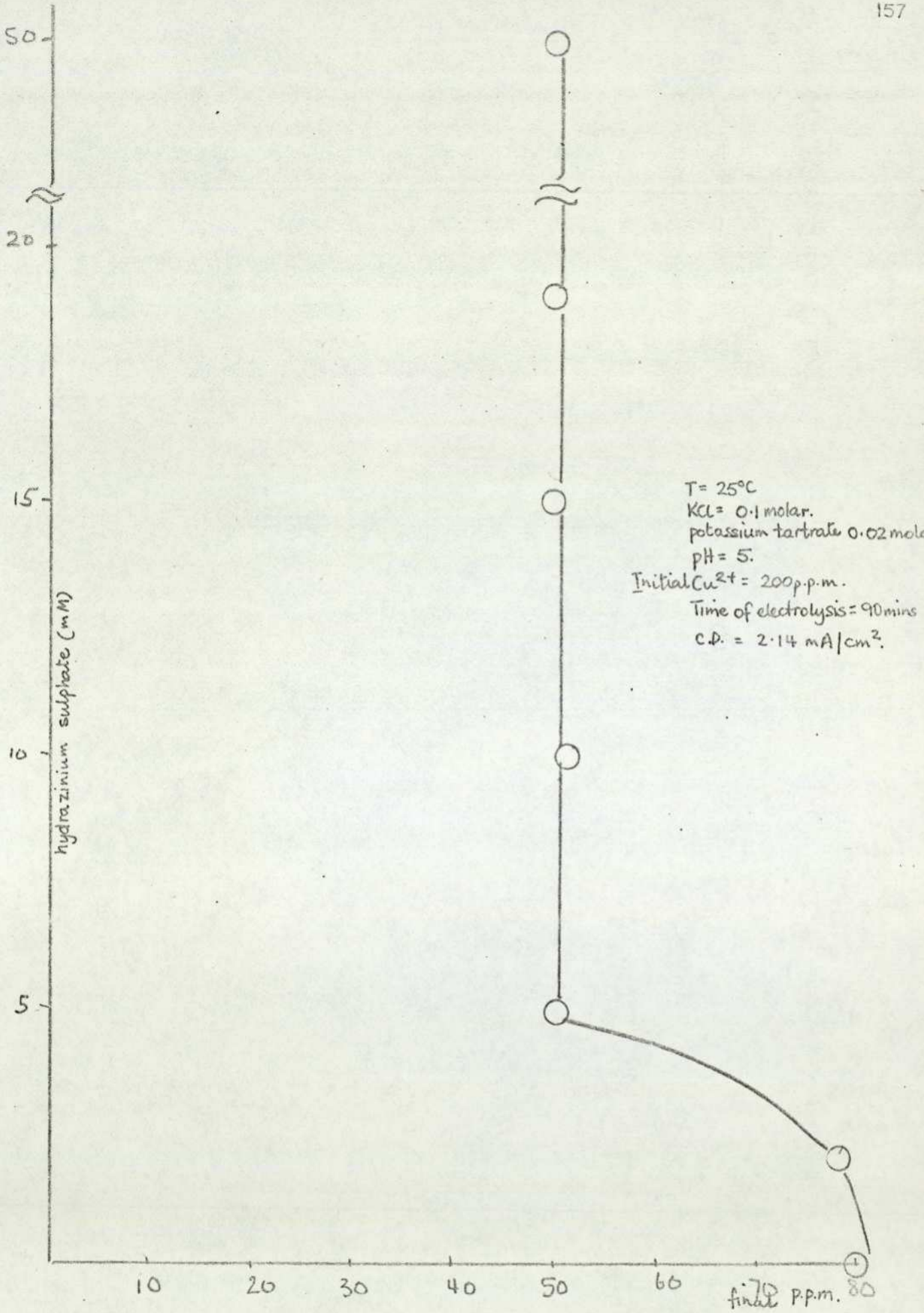


Fig 4.3. Effect on efficiency of copper deposition, caused by varying concentration of hydrazinium sulphate.

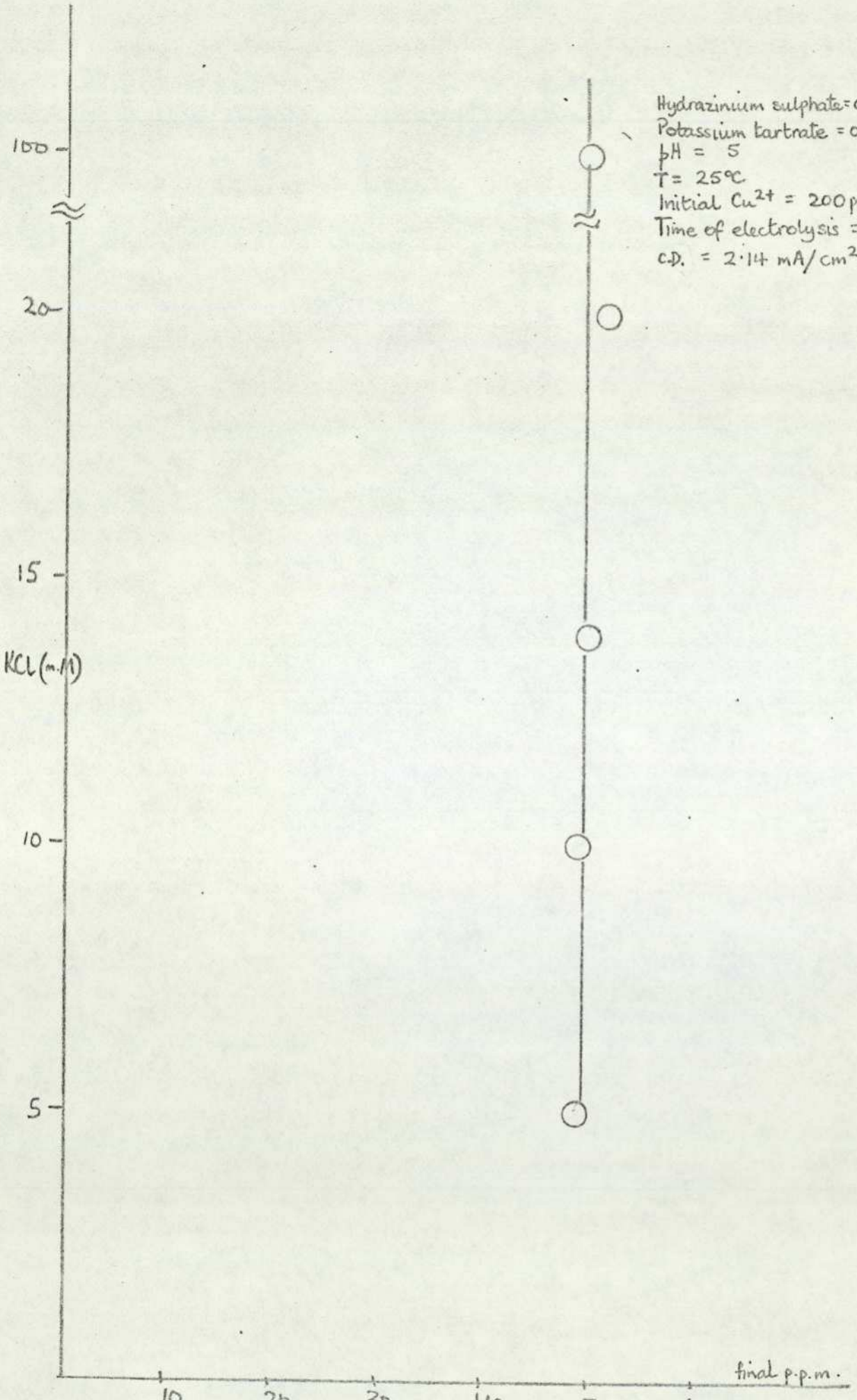


Fig 4.4. Effect on efficiency of copper deposition caused by varying the concentration of potassium chloride.

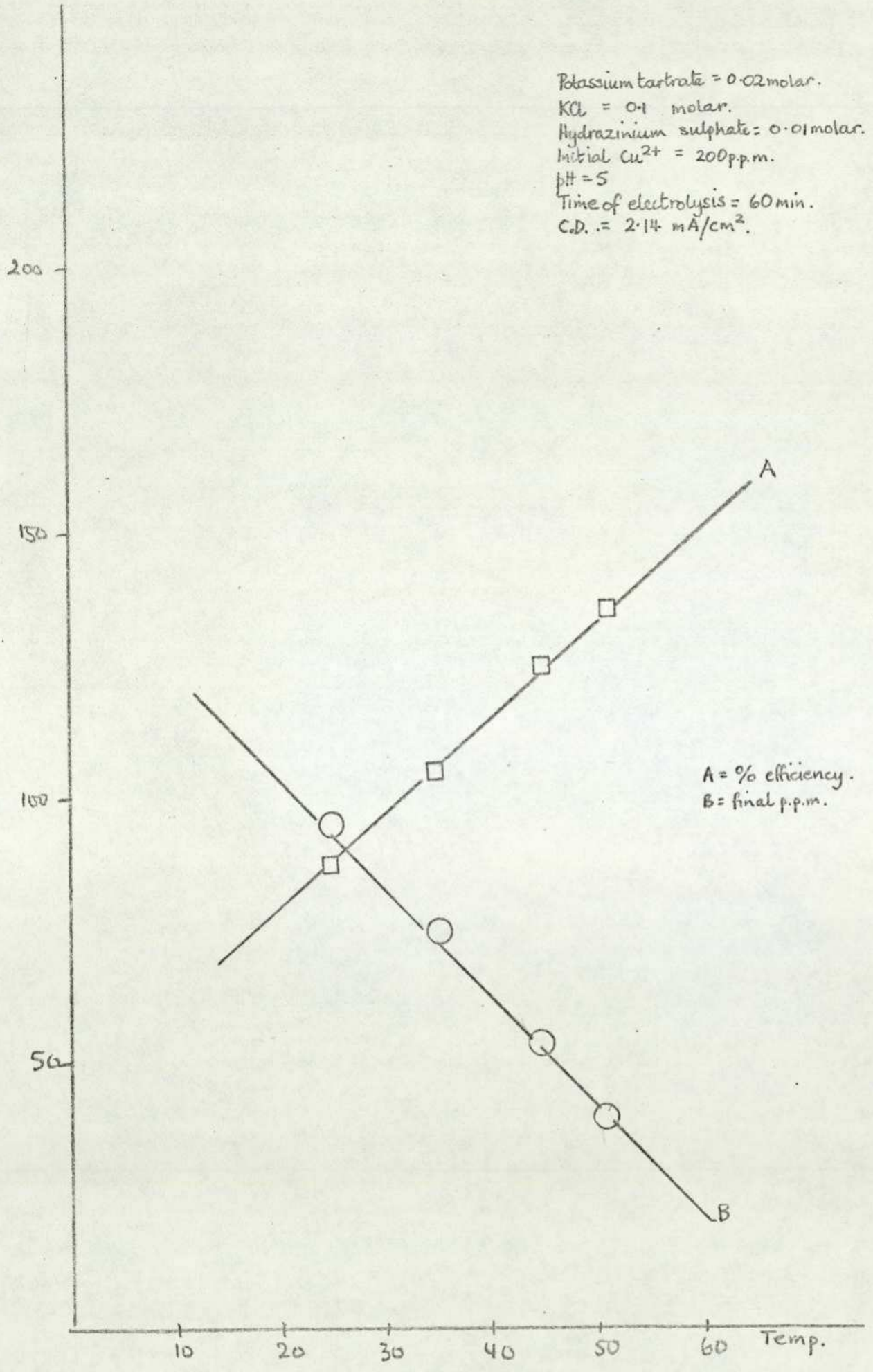


Fig. 4·5. Effect on efficiency of copper deposition caused by varying the temperature.

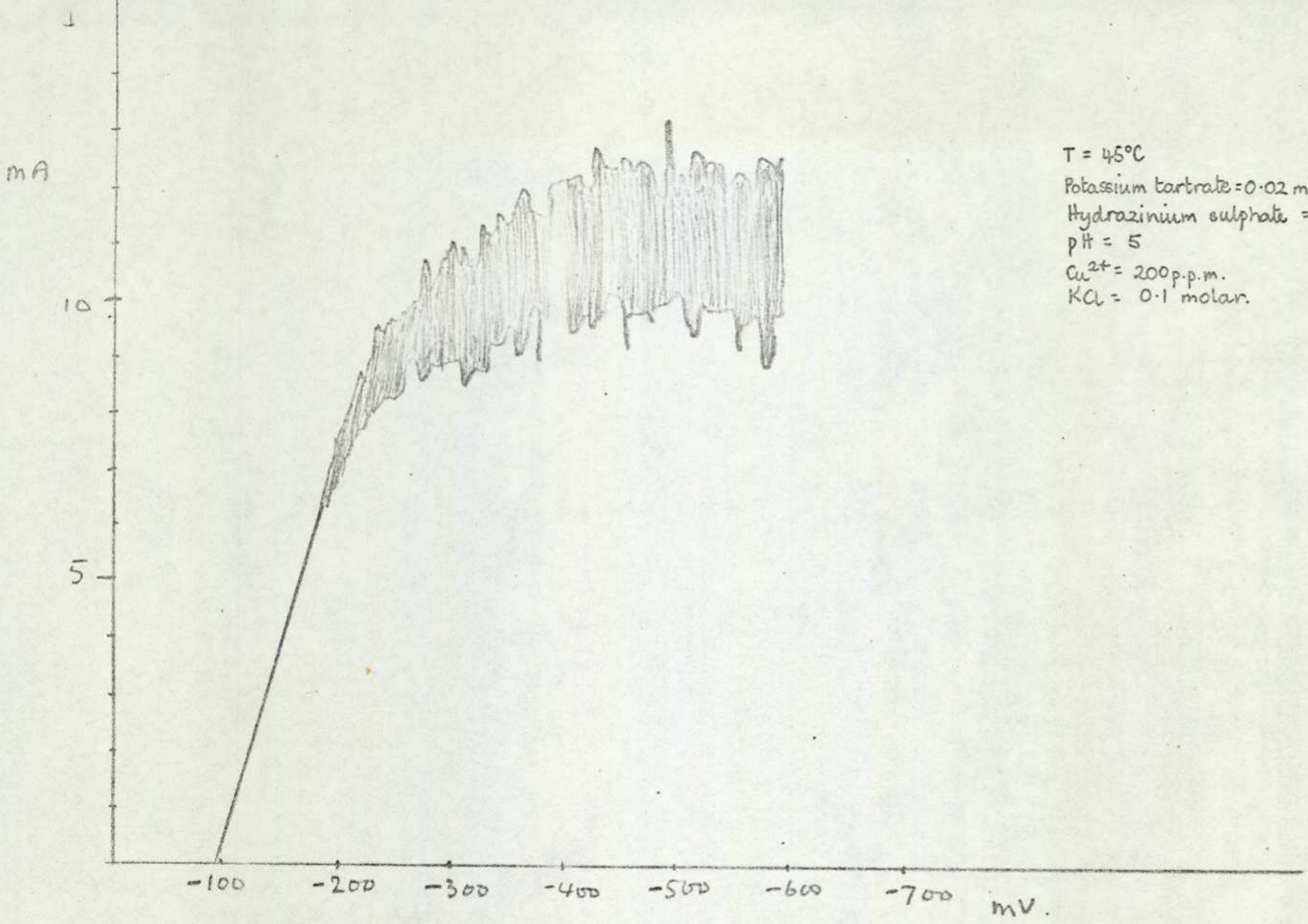
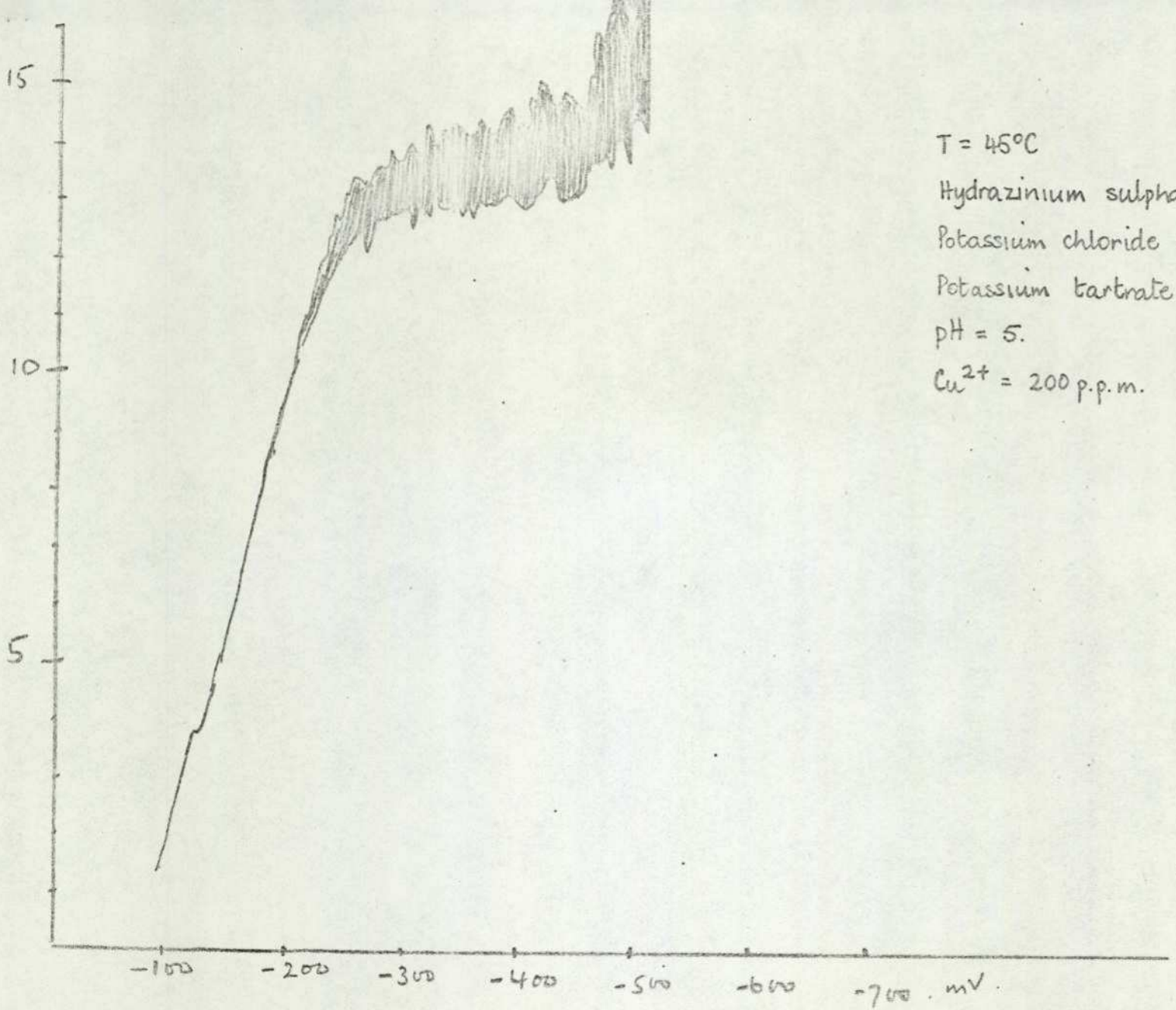


Fig. 4.6. Steady state current-potential curve for $CuSO_4$ (stirred solution)



T = 45°C

Hydrazinium sulphate = 0·01 molar.

Potassium chloride = 0·1 molar.

Potassium tartrate = 0·02 molar

pH = 5.

Cu^{2+} = 200 p.p.m.

Fig. 4.7. Steady state current-potential curve for $CuSO_4$ (stirred solution)

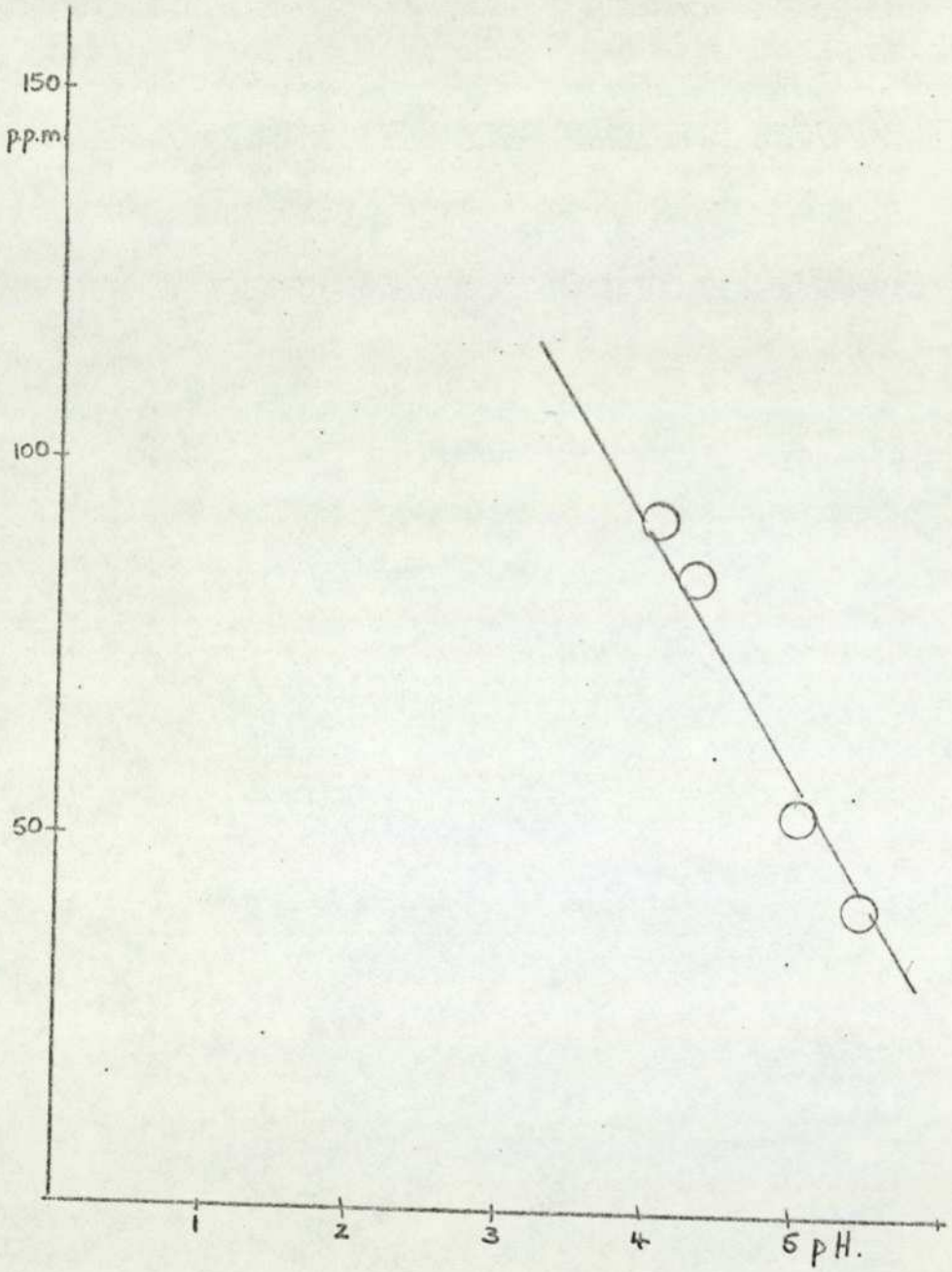
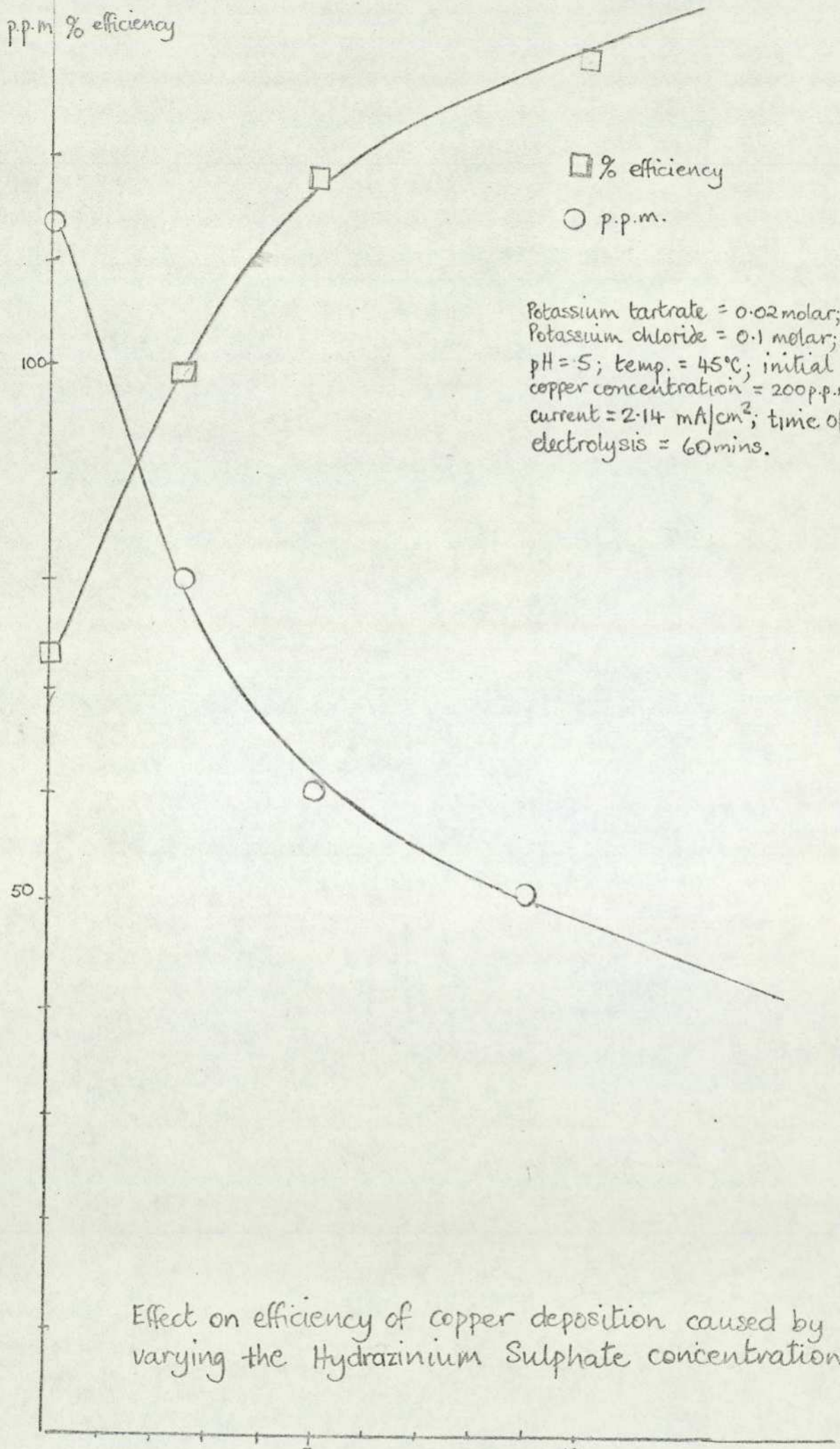


Fig. 4.8. Effect of varying pH on copper deposition.
Temp. = 45°C; Potassium tartrate = 0·02 molar;
Potassium chloride = 0·1 molar;
Hydrazinium sulphate = 0·01 molar; c.d. = 2·14 mA/cm^2;
time of electrolysis = 60 mins; initial copper
concentration = 200 p.p.m.



Effect on efficiency of copper deposition caused by varying the Hydrazinium Sulphate concentration.

Fig. 4.9.

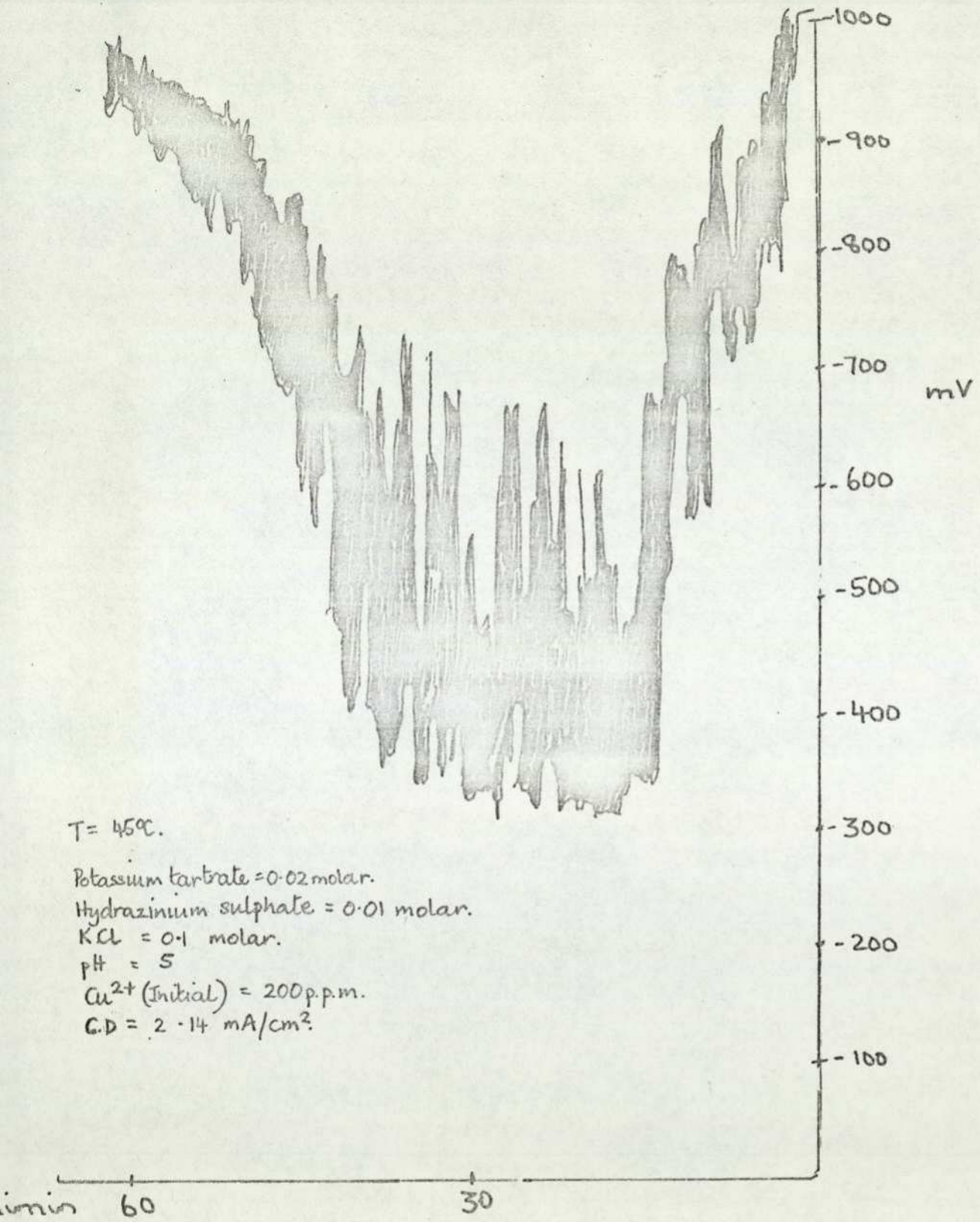


Fig. 4.10 Potential - time curve during constant current electrolysis.

T= 45°C.
Potassium tartrate = 0·02 molar.
Hydrazinium sulphate = 0·0 molar.
Potassium chloride = 0·1 molar
pH = 5.
Cu^{2+} = 200 p.p.m. (Initial)
C.D = 2·14 mA/cm².

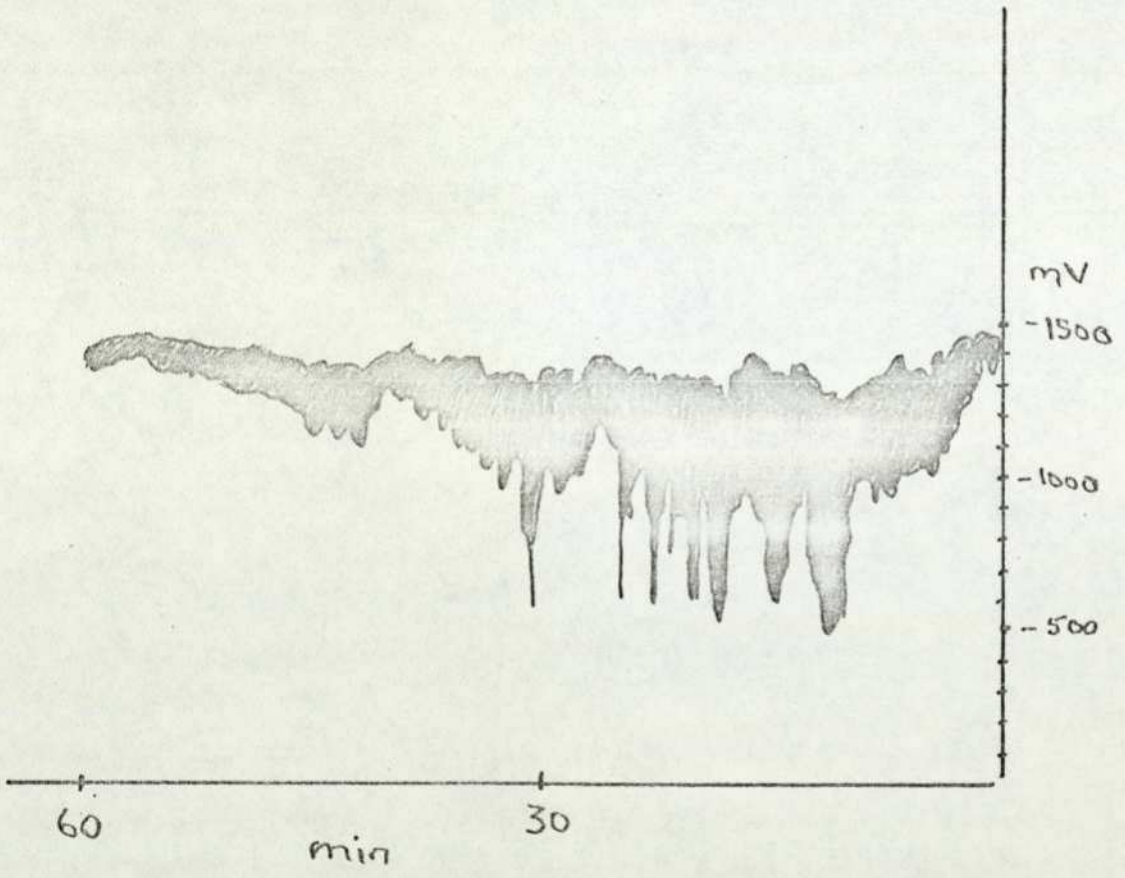


Fig. 4.11. Potential - time curve during constant current electrolysis.

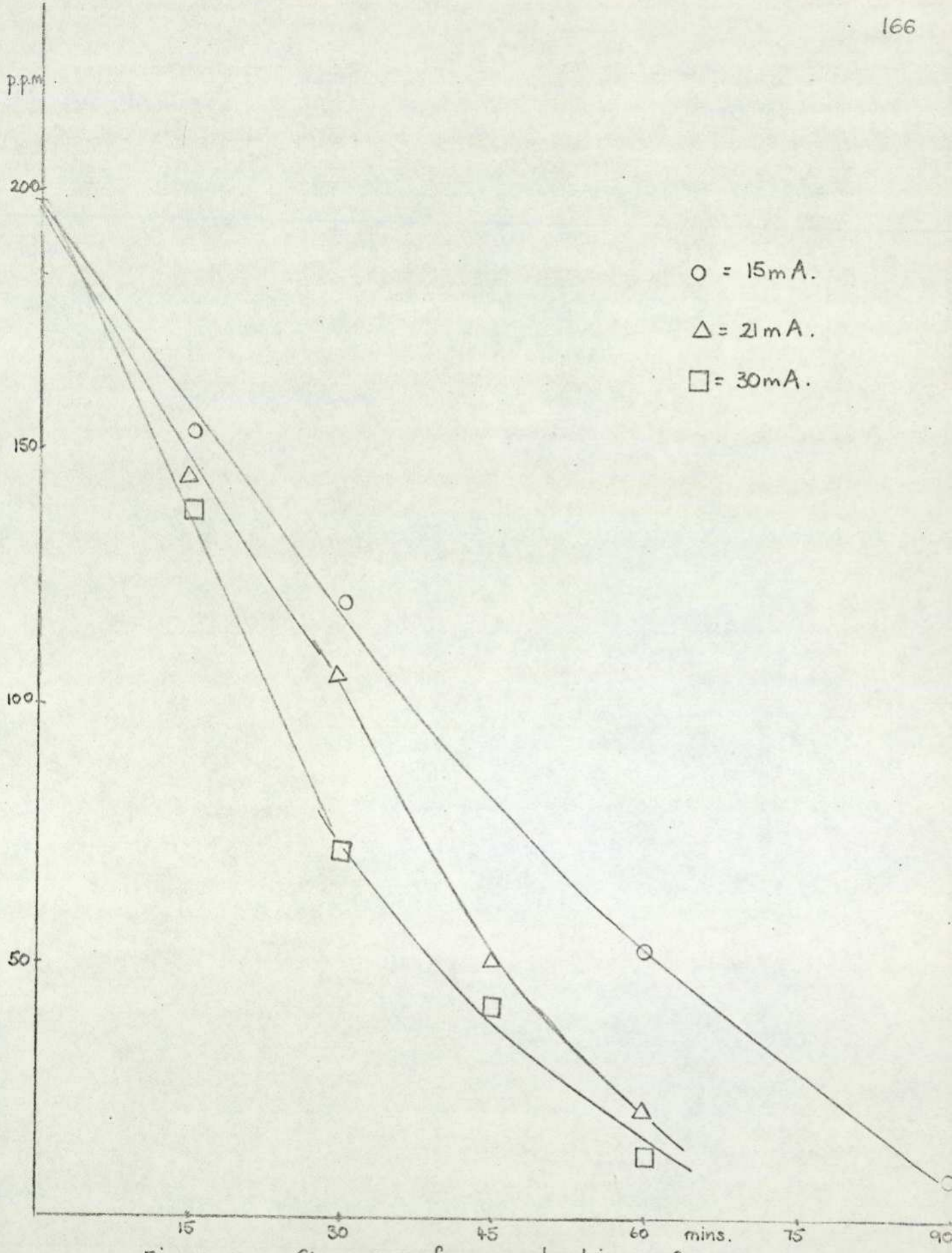


Fig. 4.12 Change of concentration of copper with time at constant current electrolysis.
Temp. = 45°C; potassium tartrate = 0·02 molar; potassium chloride = 0·1 molar; pH = 5; electrode area = 7cm^2.

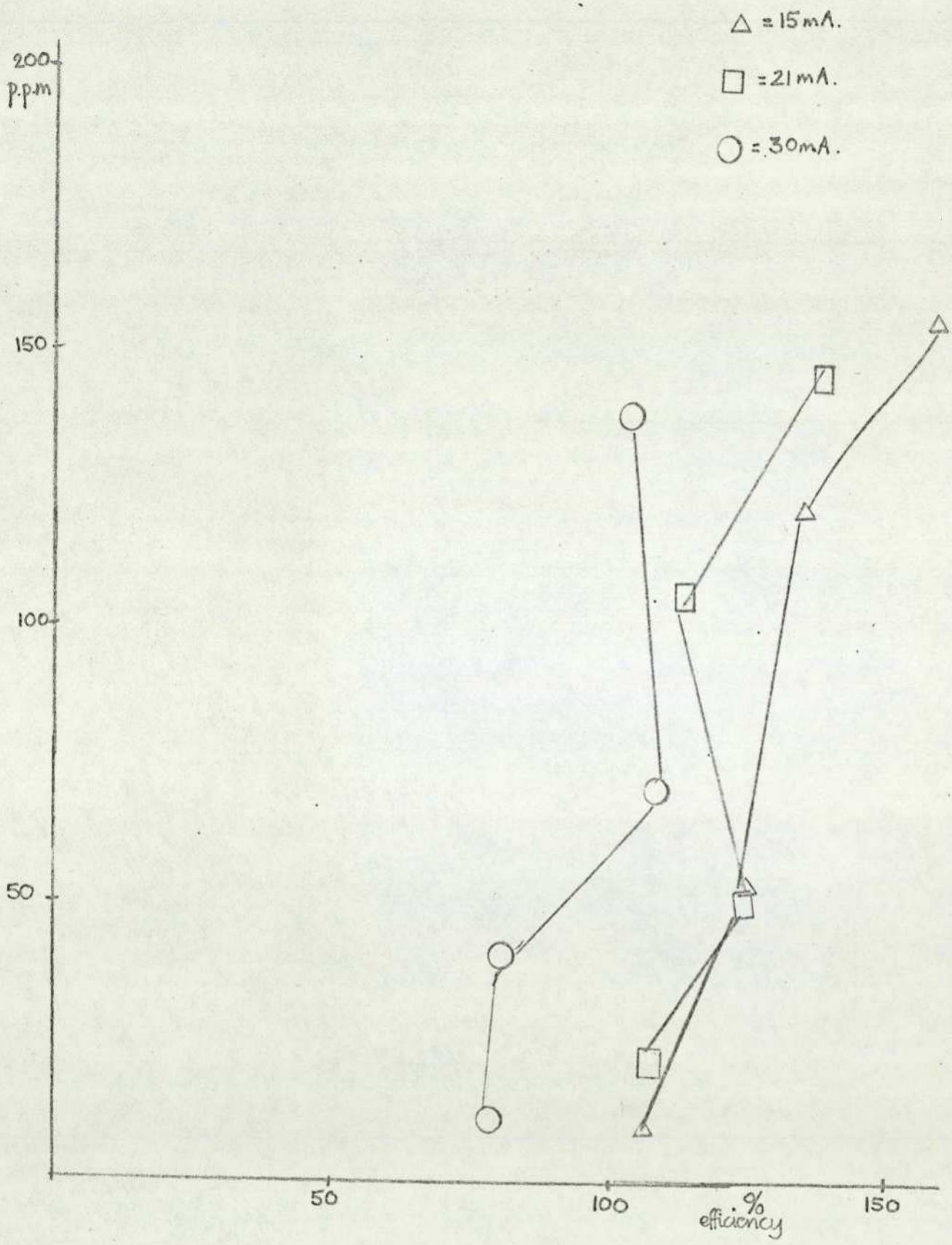


Fig. 4.13. Variation of efficiency of copper deposition during constant current electrolysis.
(Experimental conditions the same as in Fig. 4.12.)

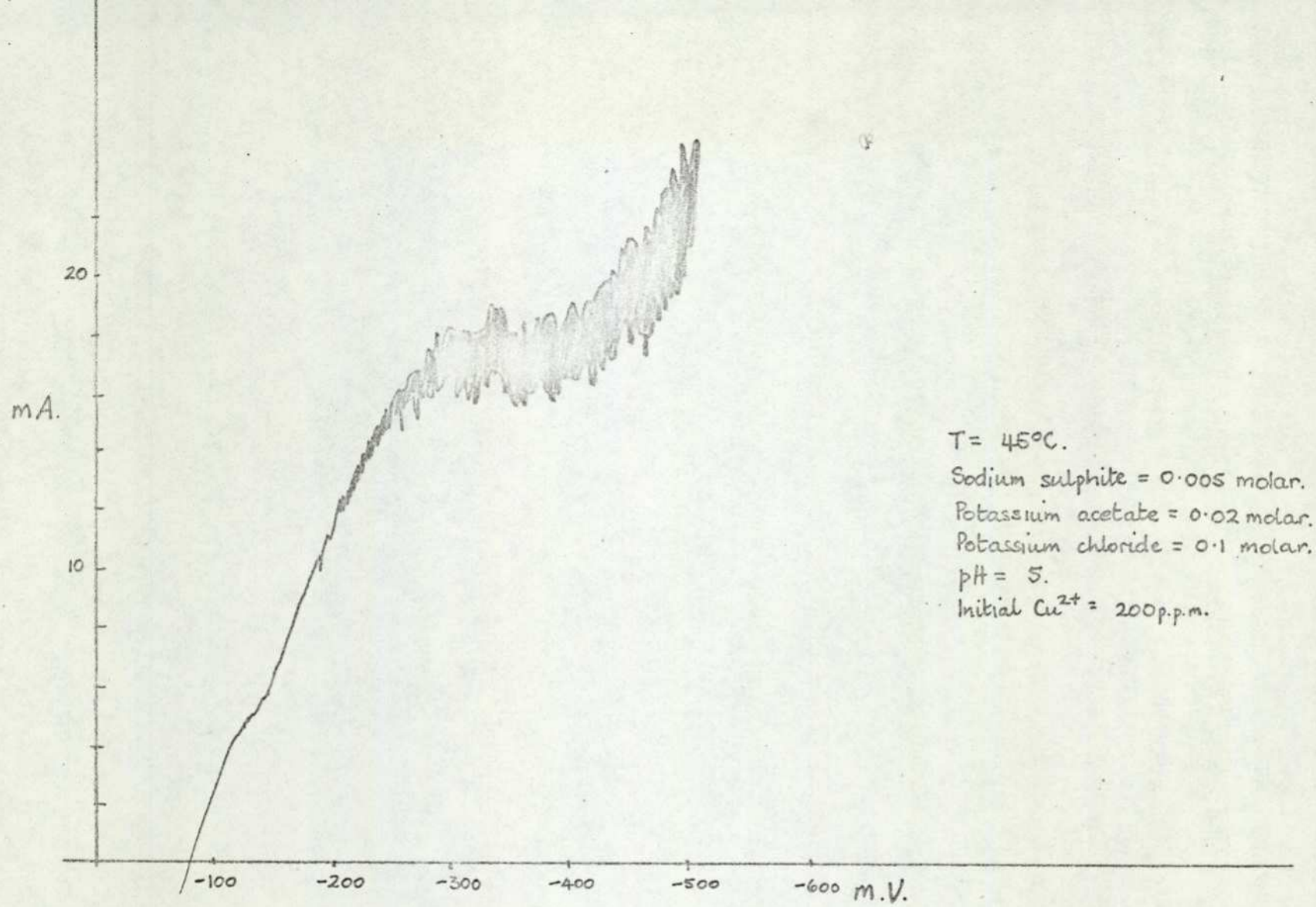
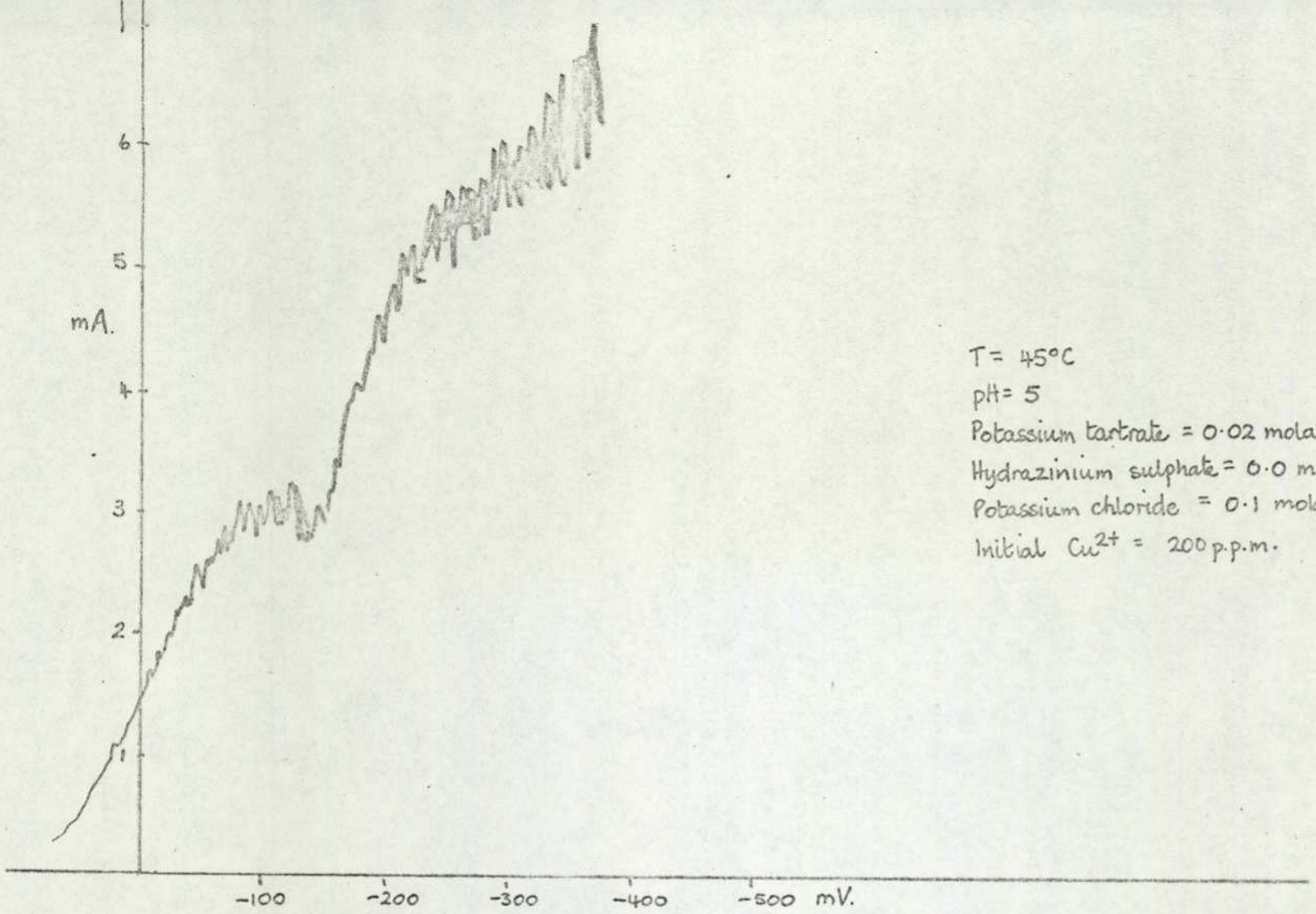


Fig. 4.14. Steady state current-potential curve for CuSO4 (stirred solution)



T = 45°C
pH = 5
Potassium tartrate = 0·02 molar.
Hydrazinium sulphate = 0·0 molar.
Potassium chloride = 0·1 molar.
Initial Cu^{2+} = 200 p.p.m.

Fig 4.15. Steady state current - potential curve for $CuSO_4$ (stirred solution) using small platinum electrode (3·2 cm^2).

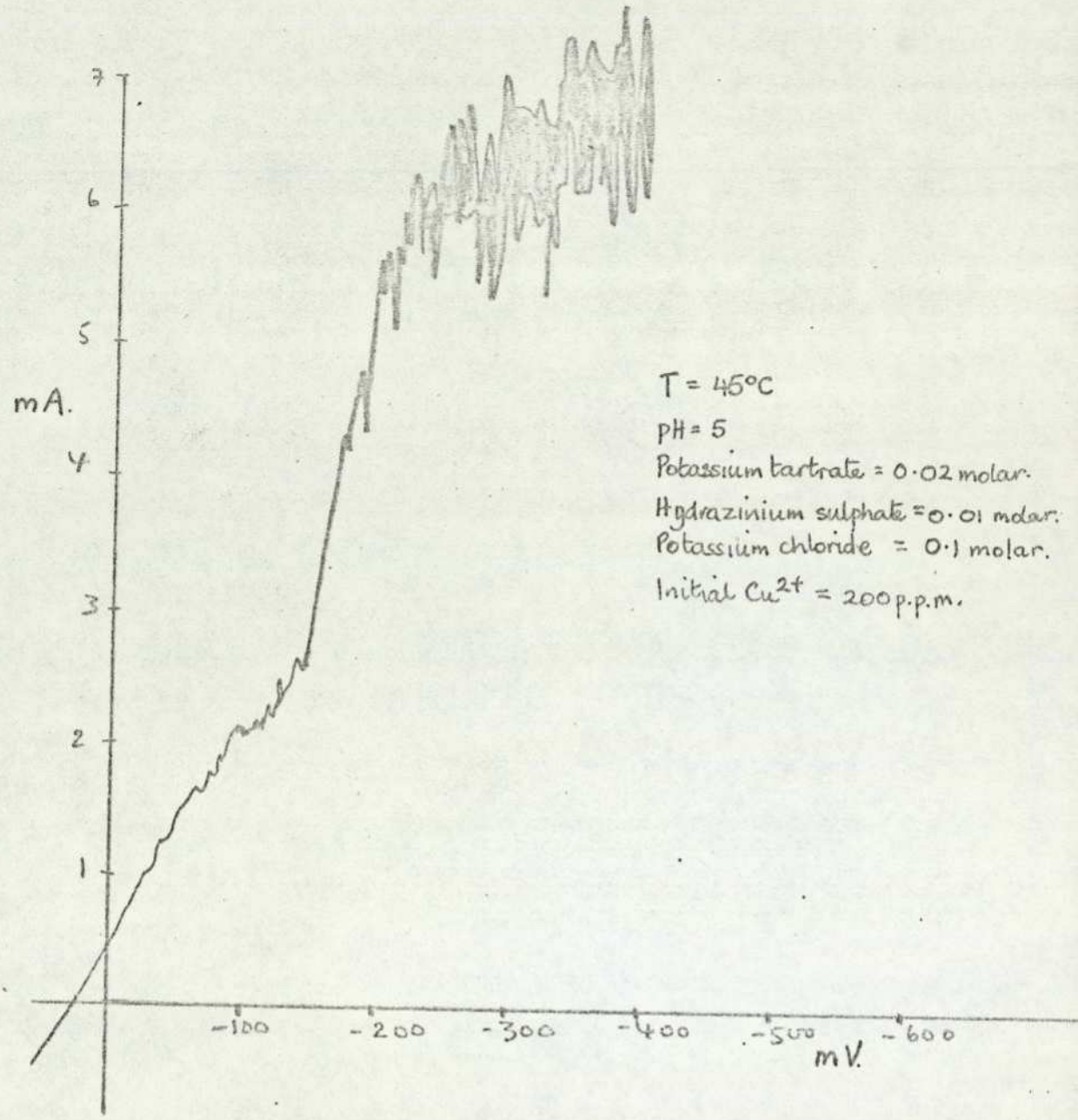


Fig. 4.16. Steady state current-potential curve for $CuSO_4$ (stirred solution) using small platinum electrode (3·2 cm^2)

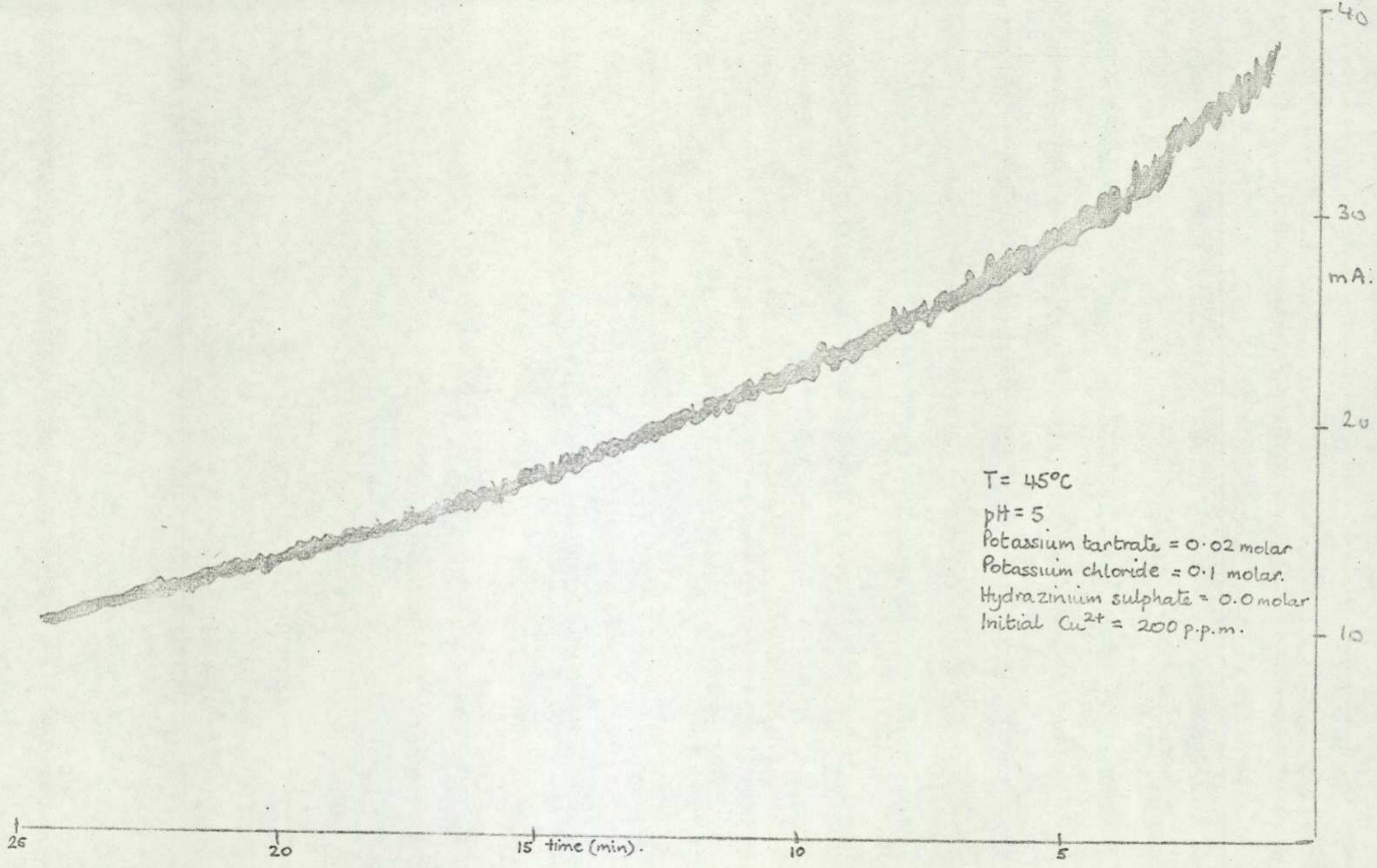
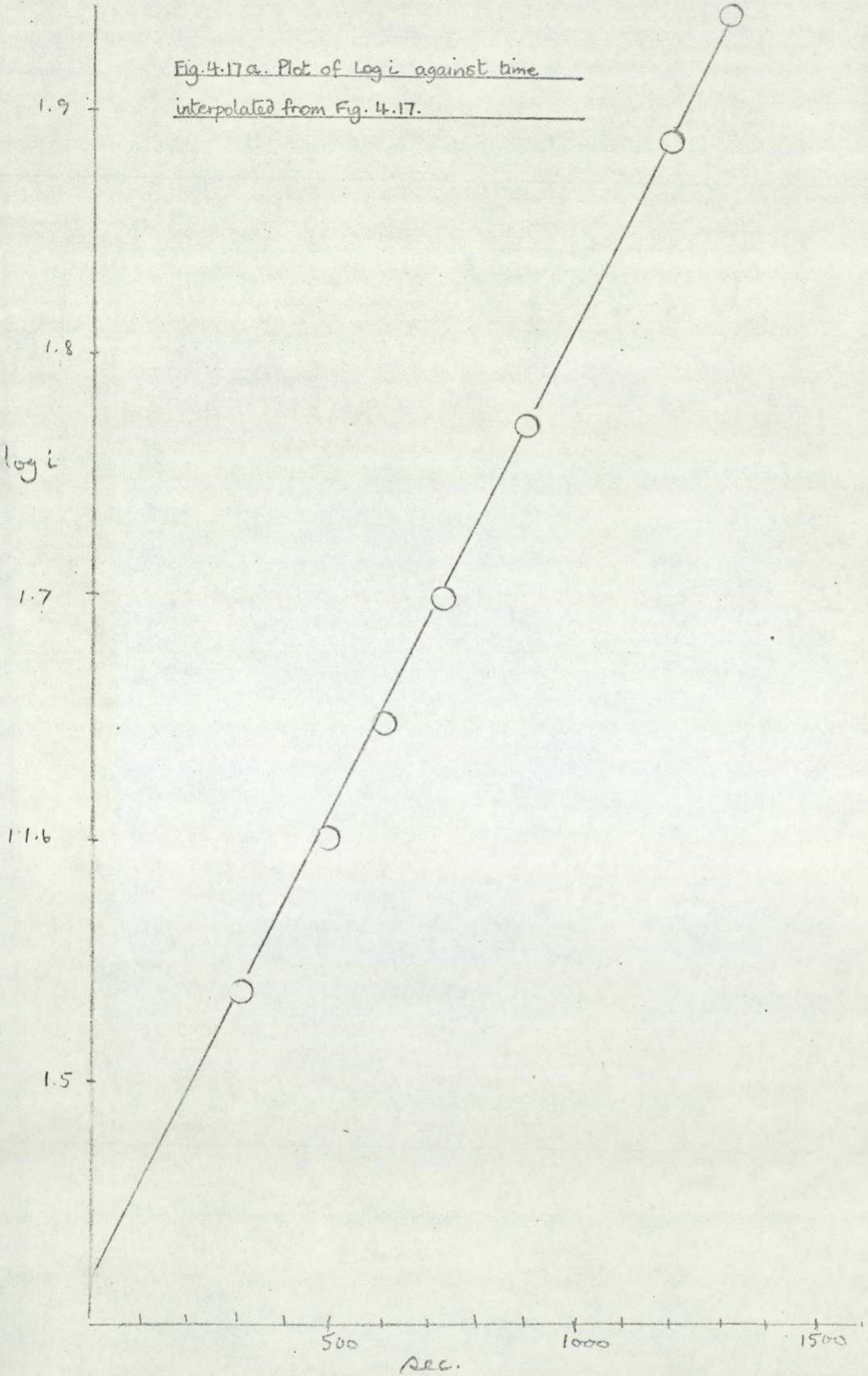


Fig.4.17 Current-time curve during constant potential electrolysis (-100mV against S.C.E.)

Fig. 4.17a. Plot of Log i against time interpolated from Fig. 4.17.



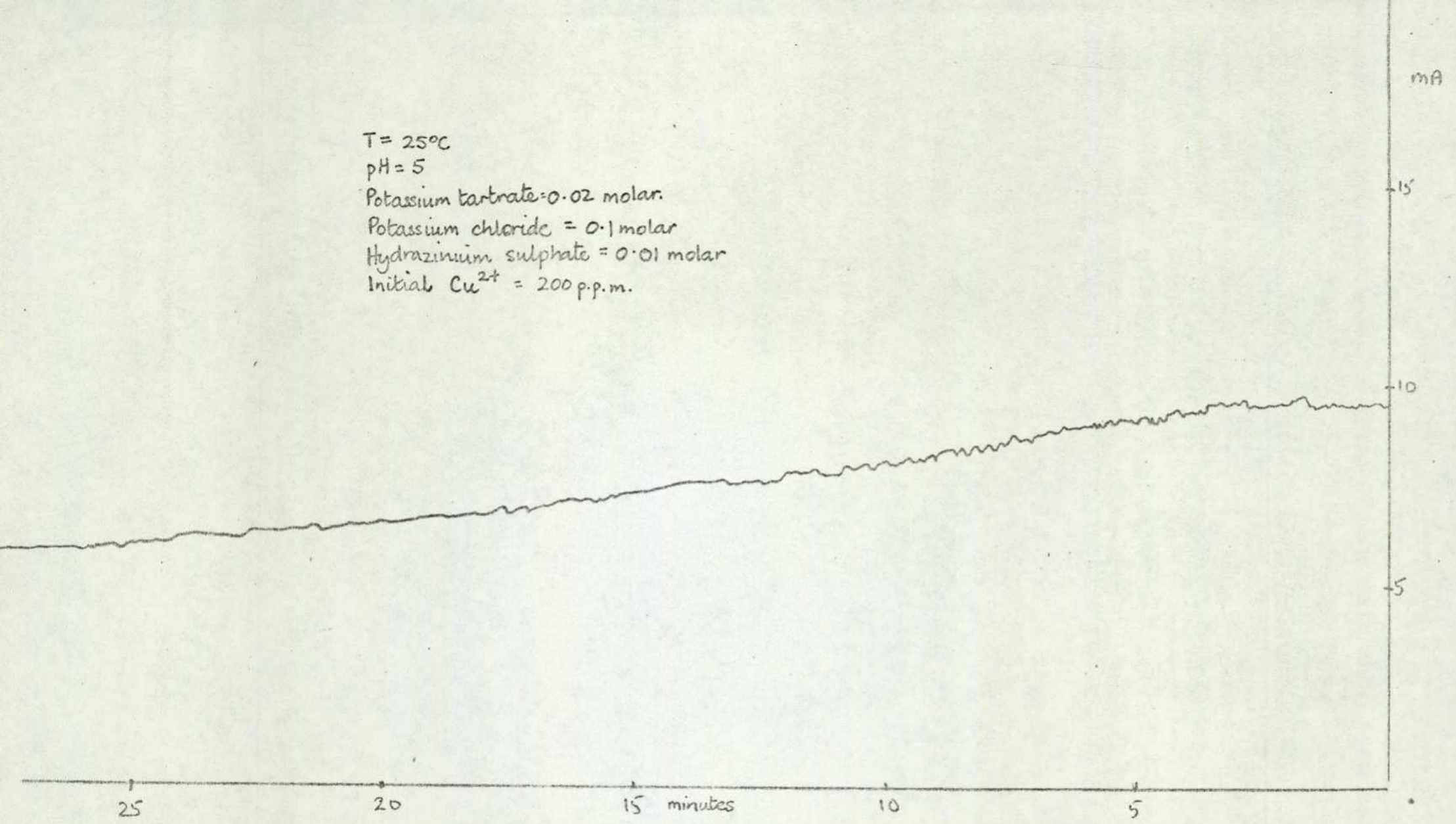


Fig. 4.18. Current - time curve during controlled potential electrolysis (-100mV against S.C.E.)

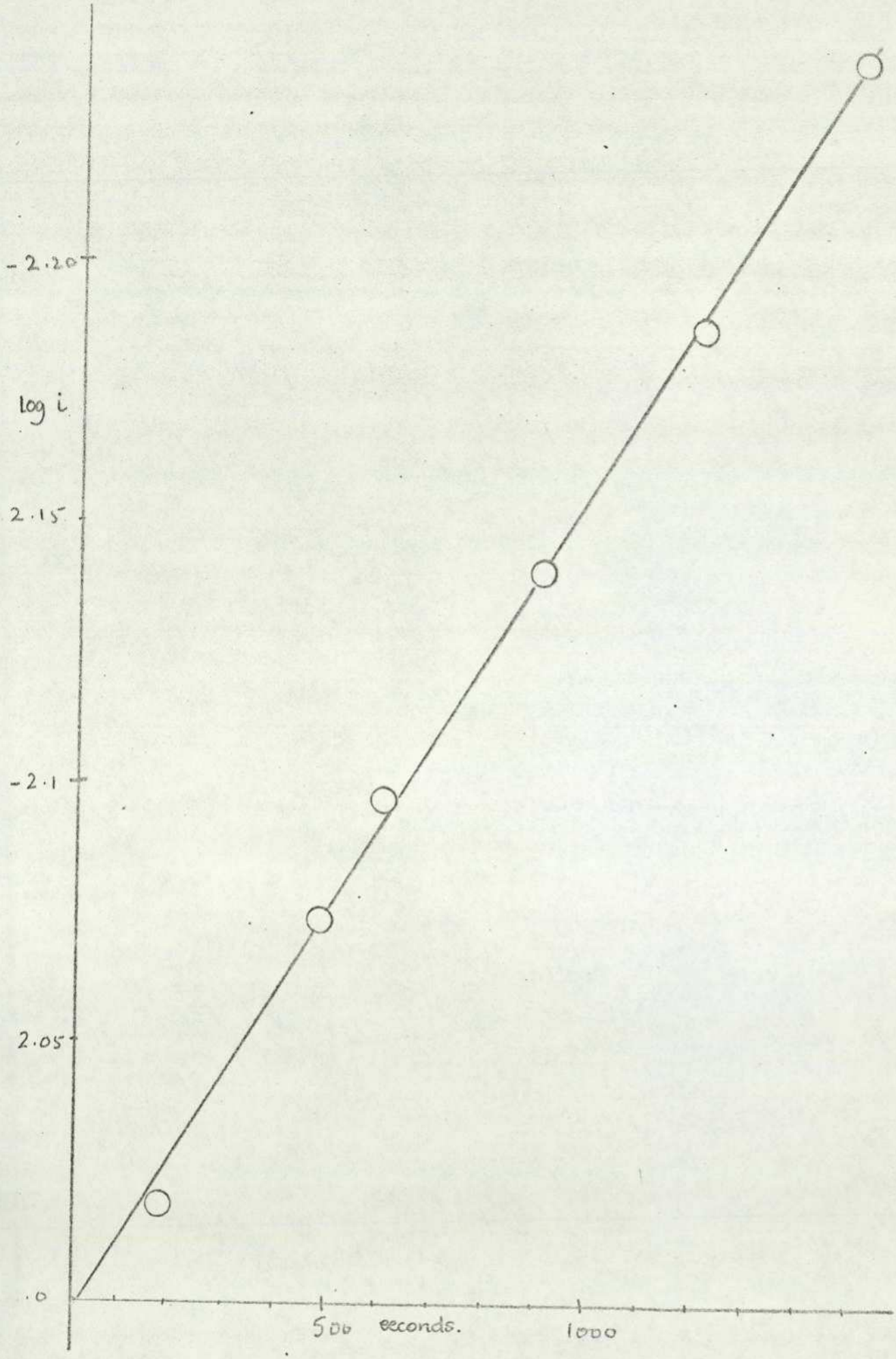


Fig 4.18a. Plot of log i against time, interpolated from Fig. 4.18.

T = 45°C.
pH = 5
Potassium tartrate = 0·02 molar.
Potassium chloride = 0·1 molar.
Hydrazinium sulphate = 0·01 molar.

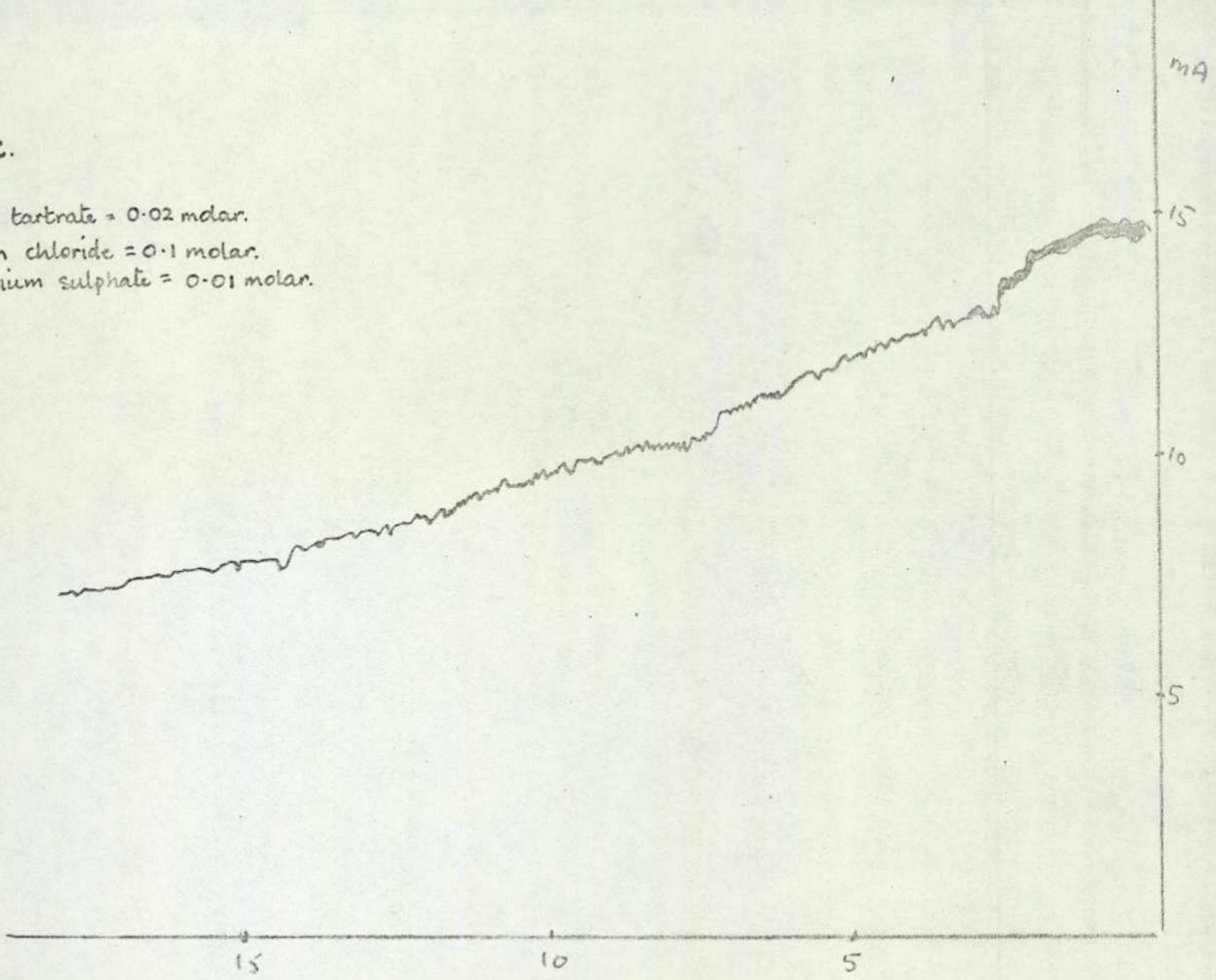


Fig 4.19. Current - time curve during controlled potential electrolysis (-100mV against S.C.E.)

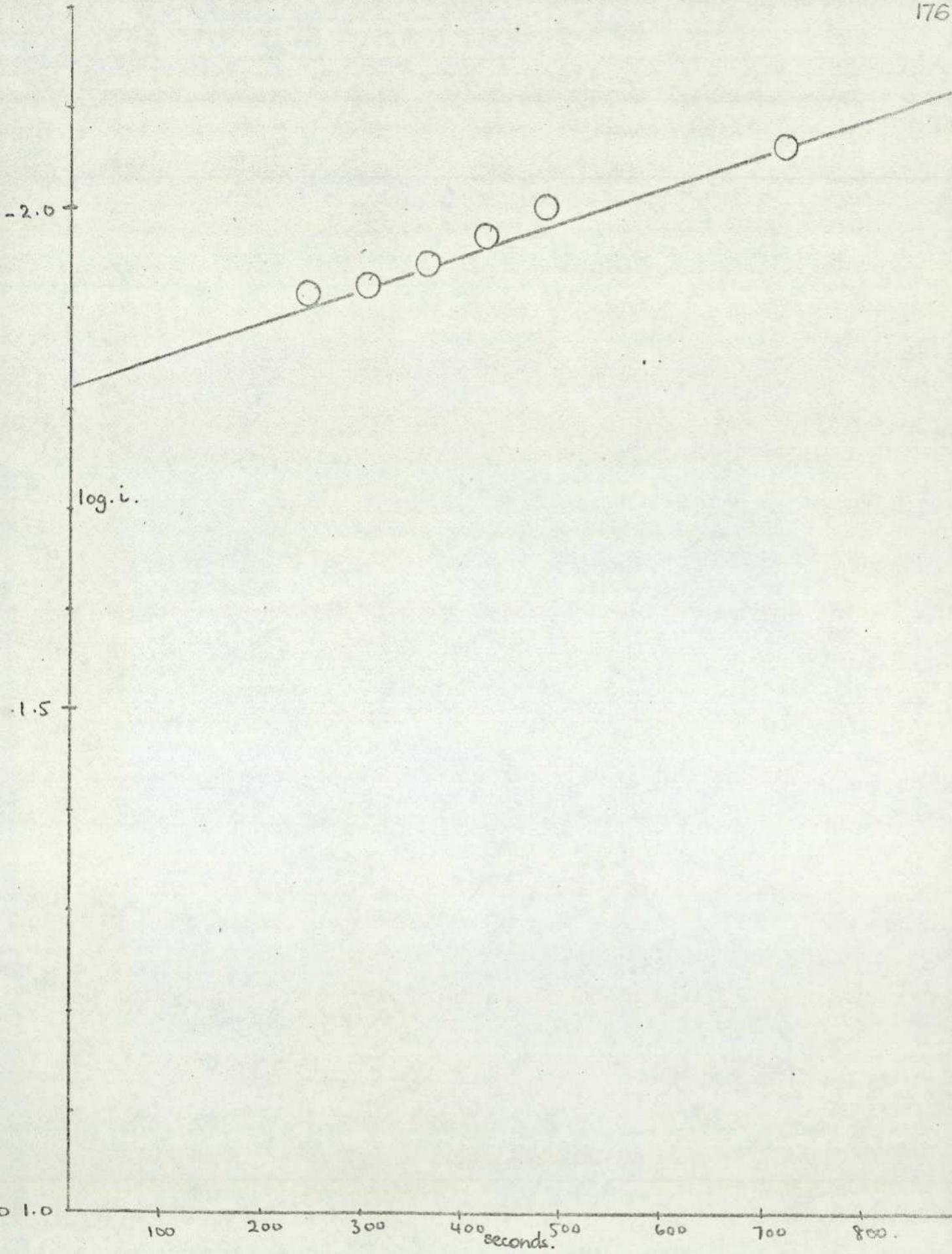
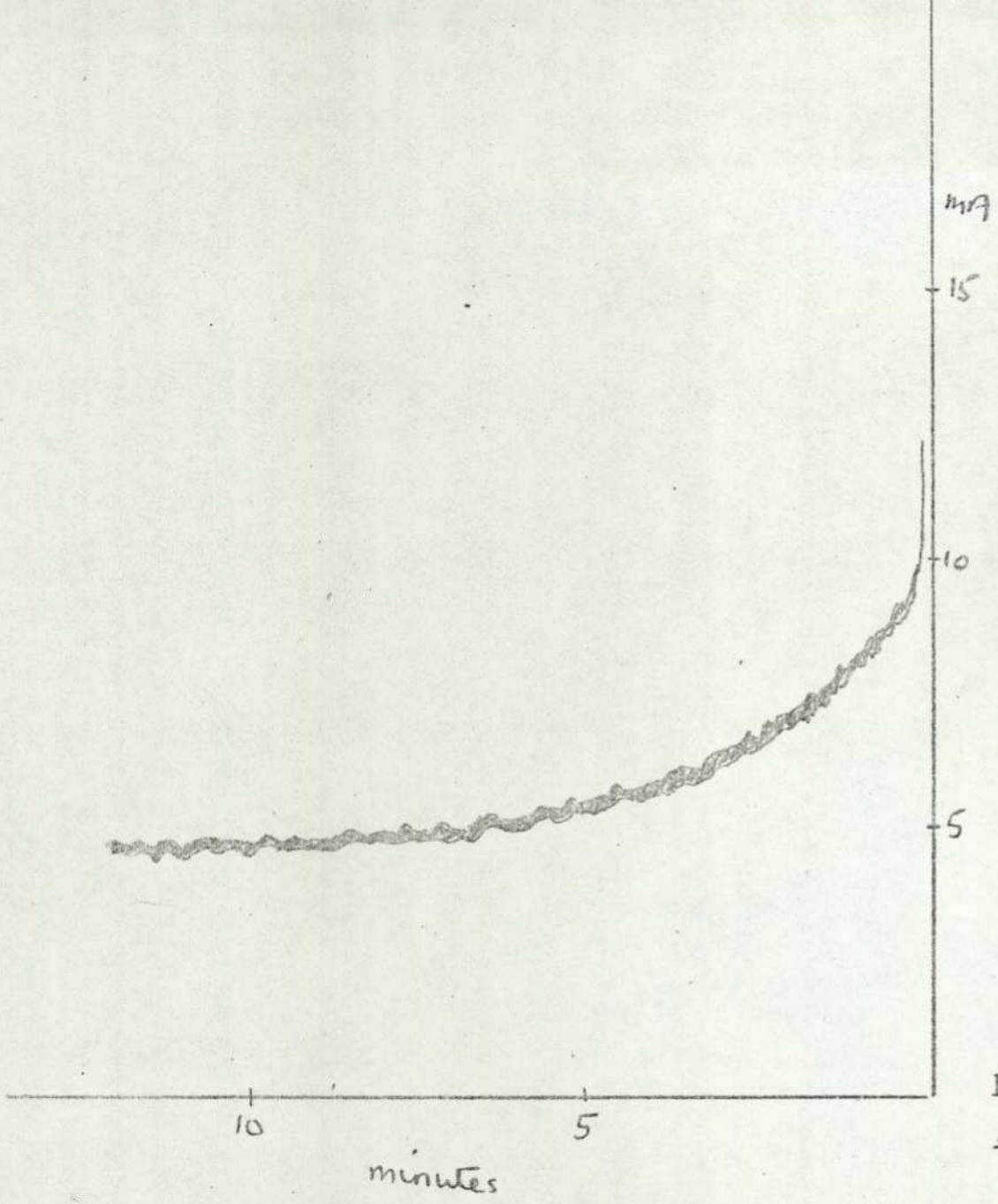


Fig 4.19 a. Plot of log i against time, interpolated from Fig. 4.19.



T = 45°C.
pH = 5
Potassium acetate = 0·02 molar.
Hydrazinium sulphate = 0·01 molar.
Potassium chloride = 0·1 molar.

Fig. 4.20. Current - time curve during controlled potential electrolysis (−100 mV against S.C.E)

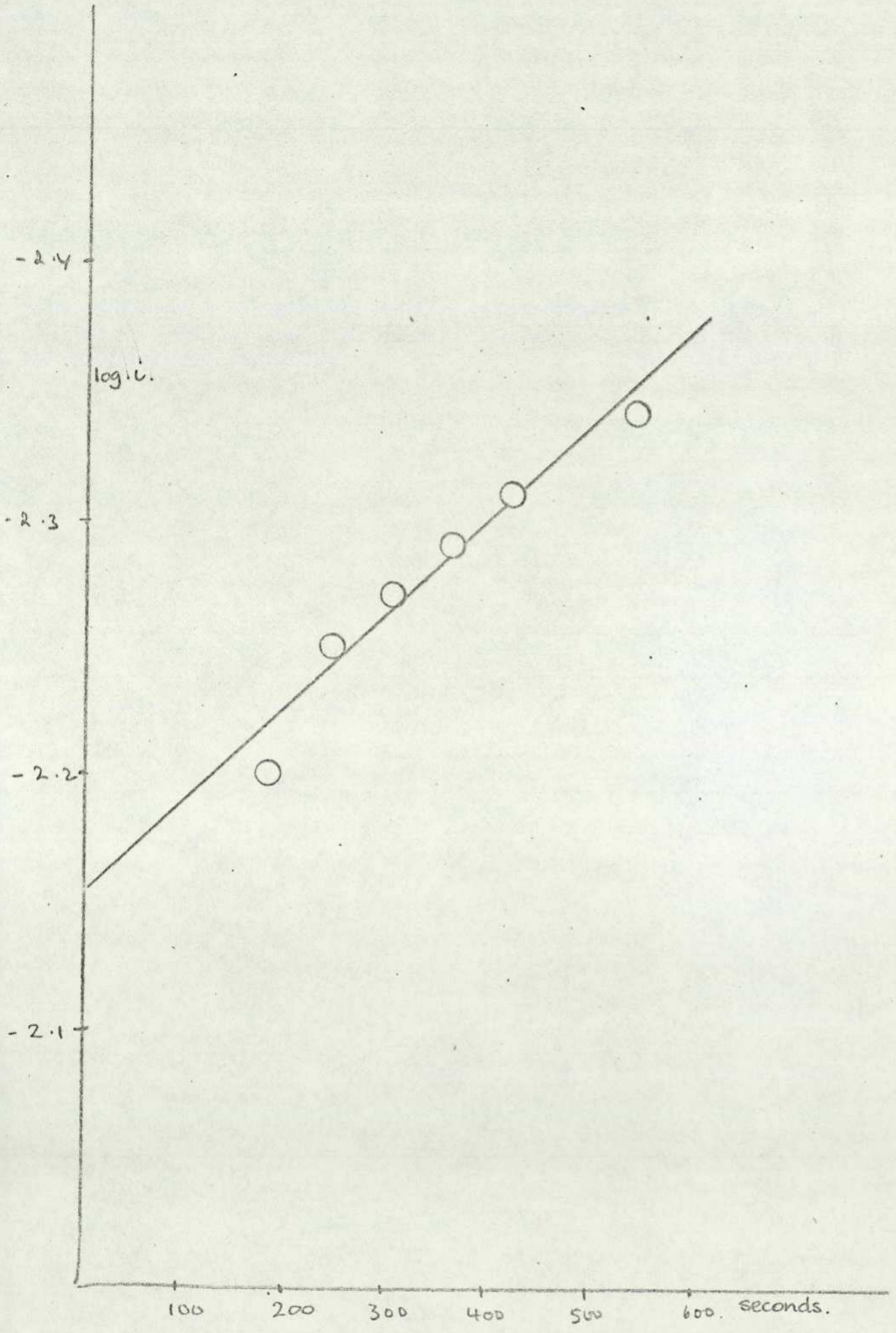


Fig. 4.20a. Plot of log i against time, interpolated from Fig 4.20.

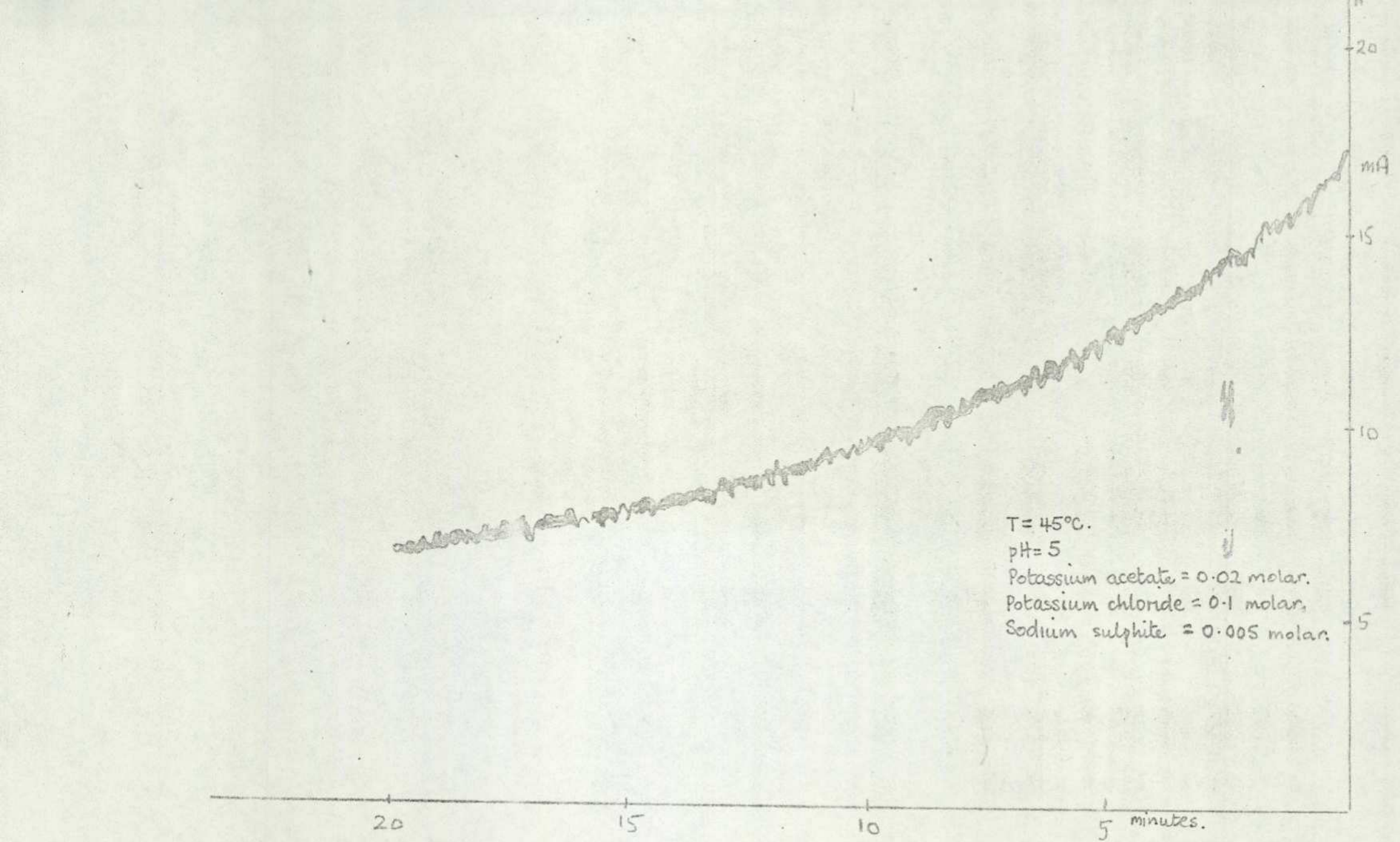


Fig 4.21. Current-time curve during controlled potential electrolysis (−100 mV against S.C.E.)

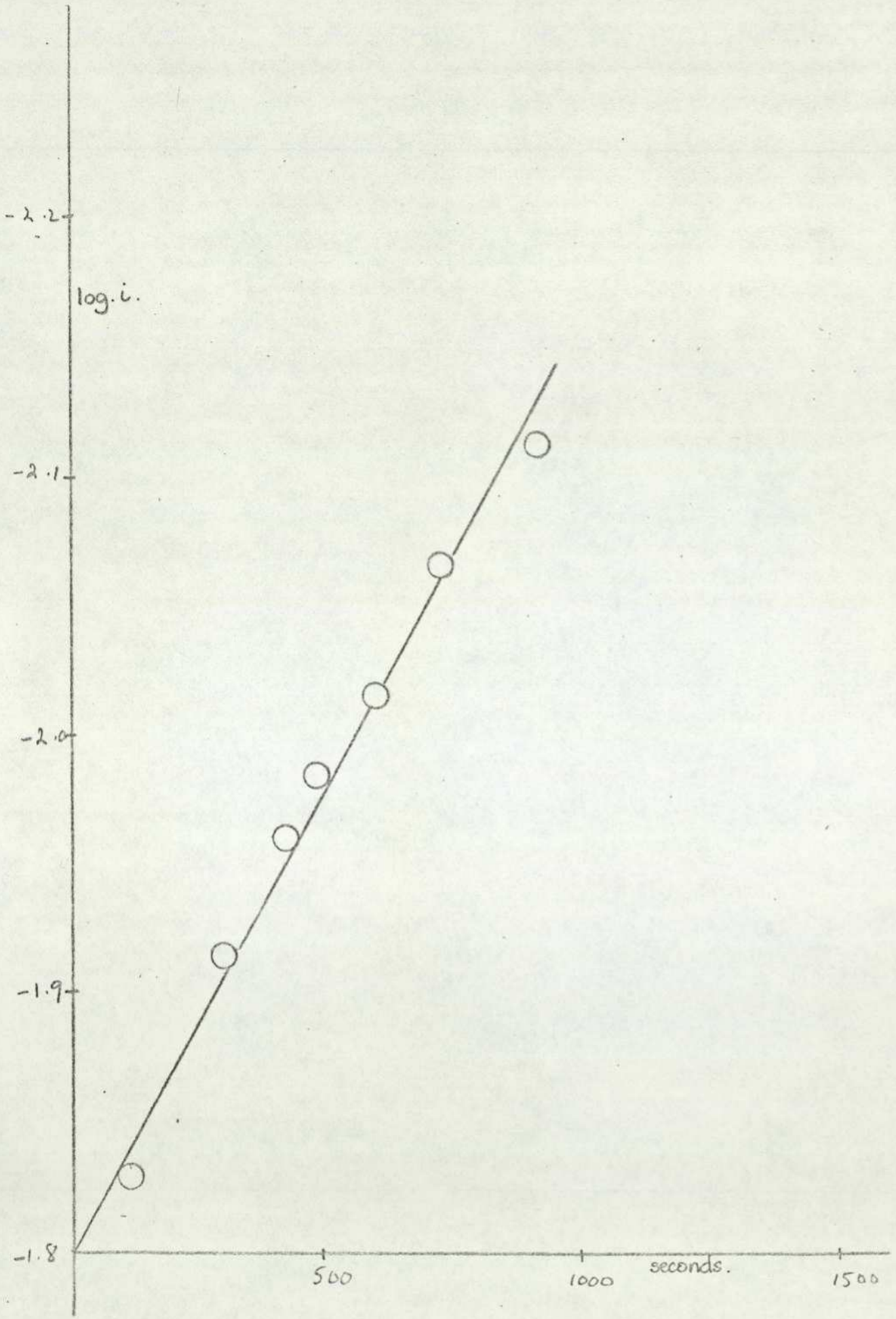


Fig. 4.21a Plot of log i against time interpolated from Fig. 4.21

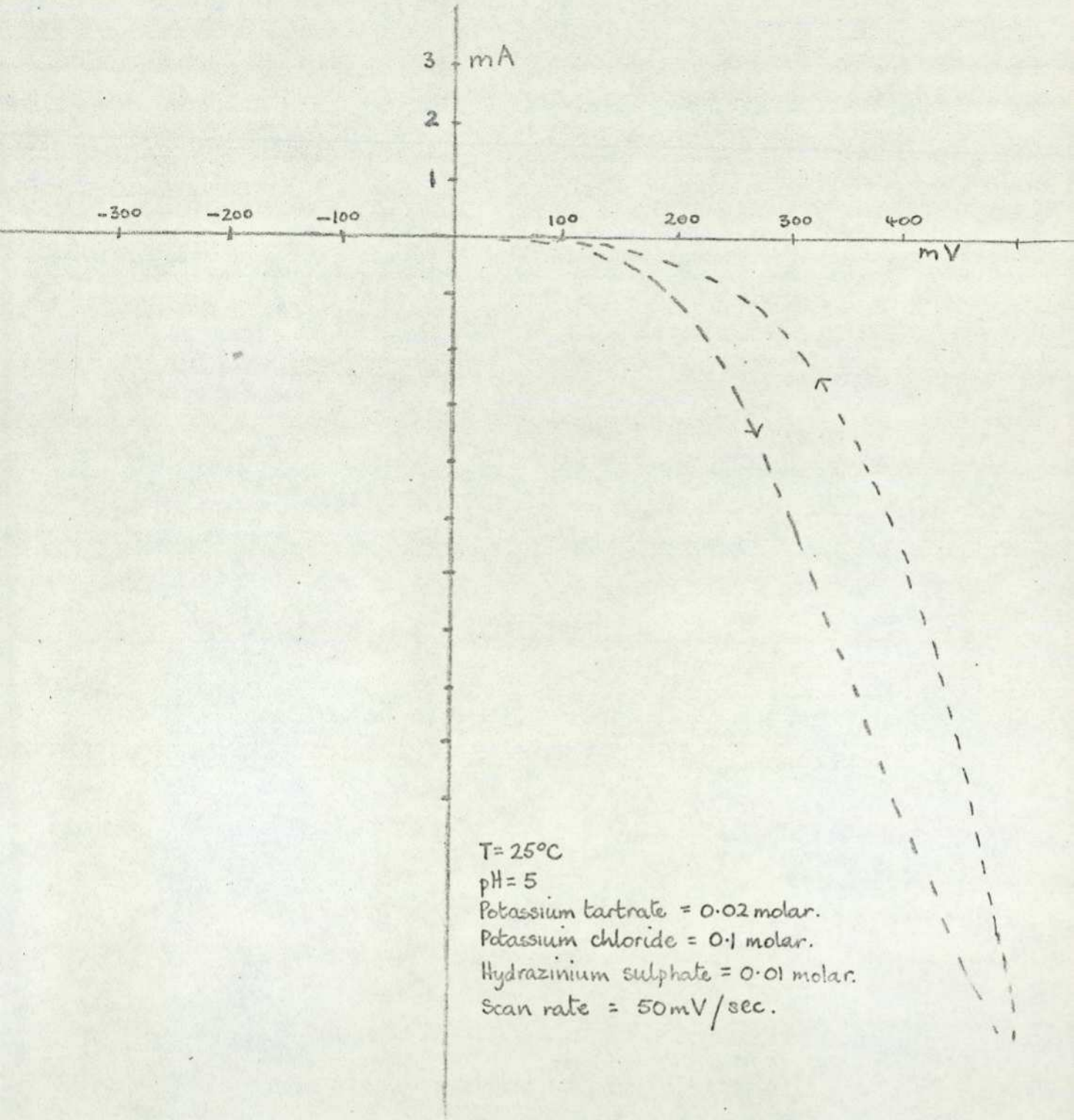


Fig 4.22. Current - potential curve of background electrolyte (unstirred solution) using platinum electrode (3·2cm²)

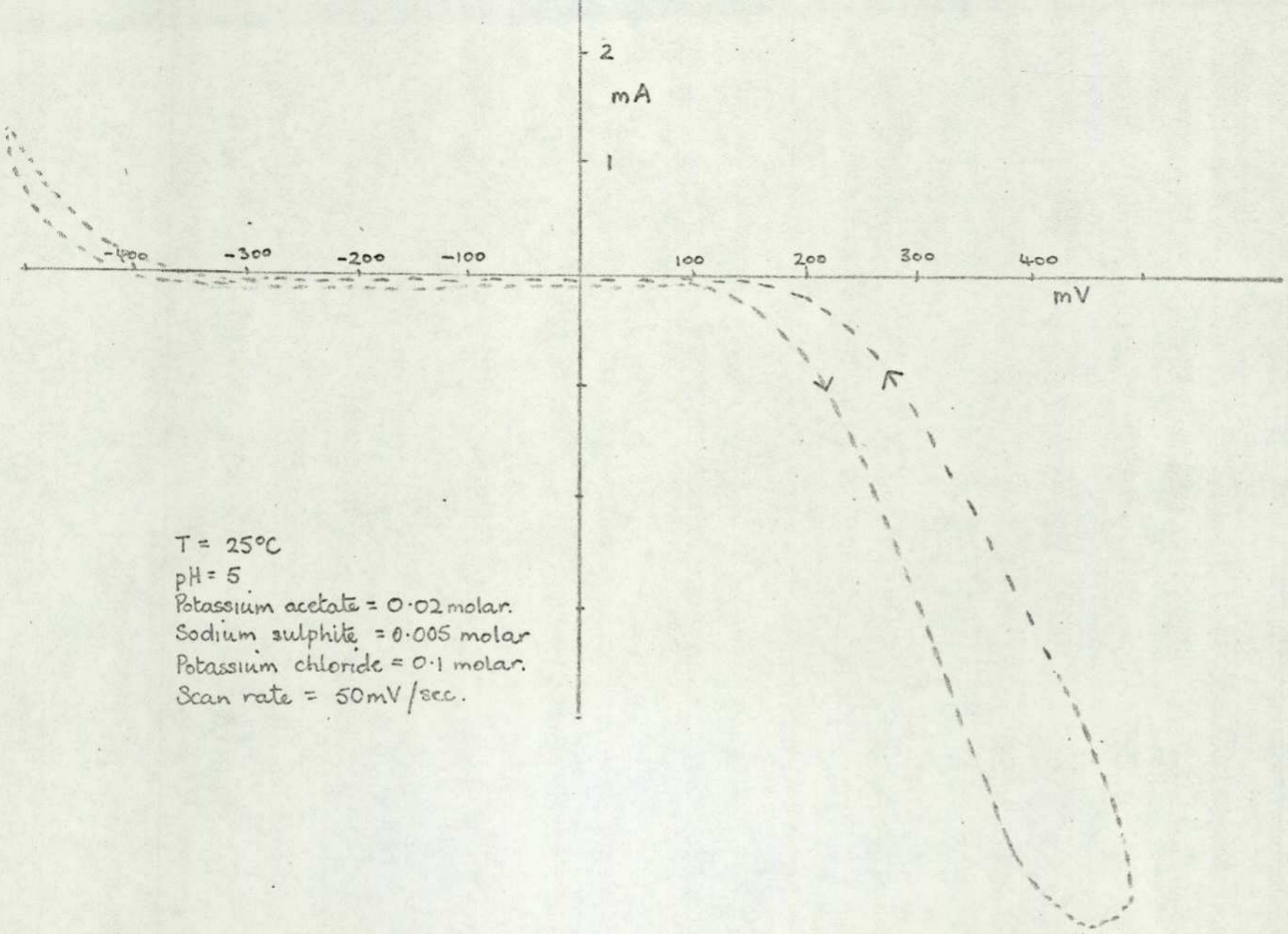


Fig. 4.23. Current-potential curve of background electrolyte (unstirred solution) using platinum electrode ($3{\cdot}2 cm^2$)

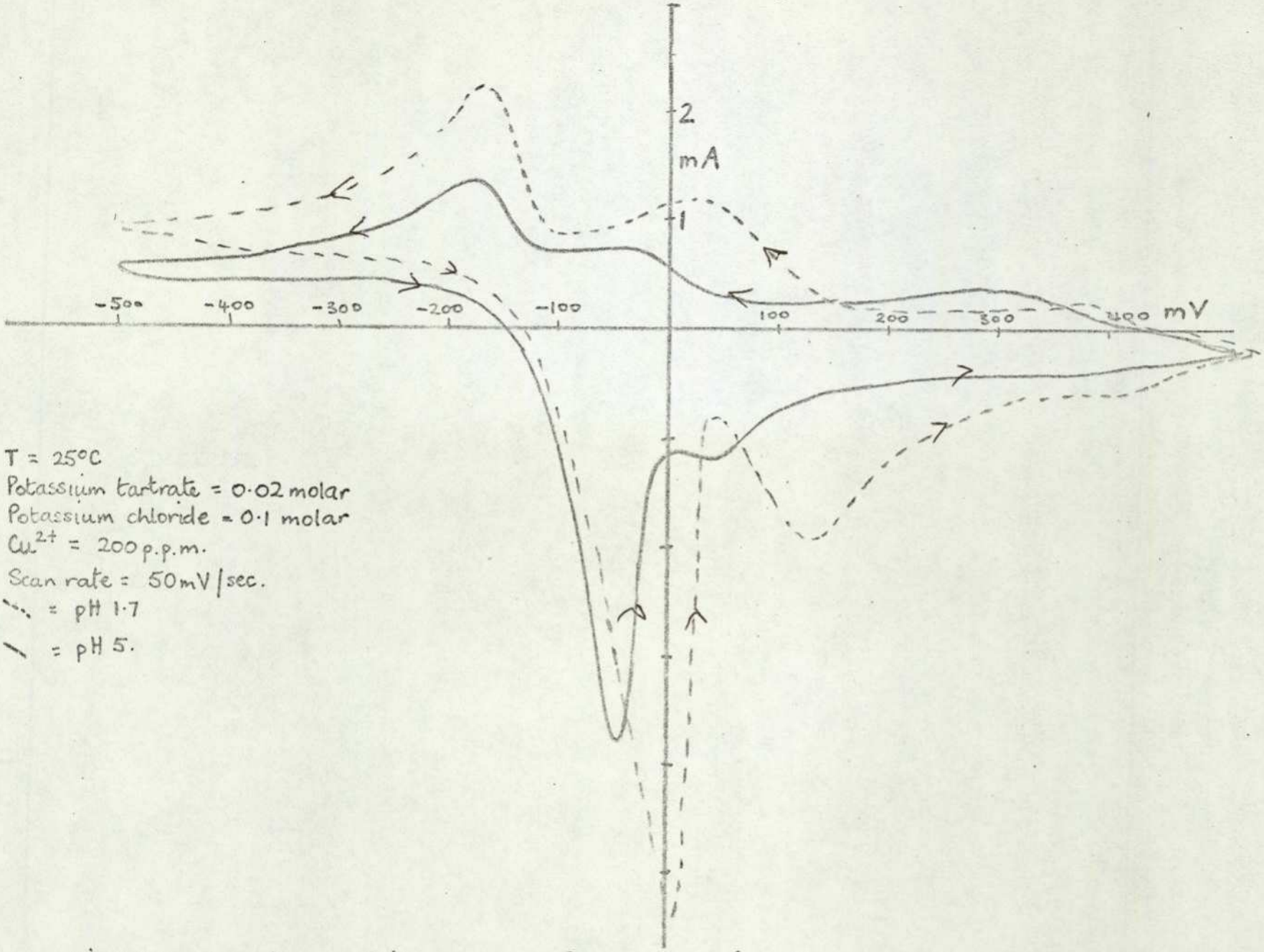


Fig. 4.24. Current-potential curve of Cu SO4 (unstirred solution) using

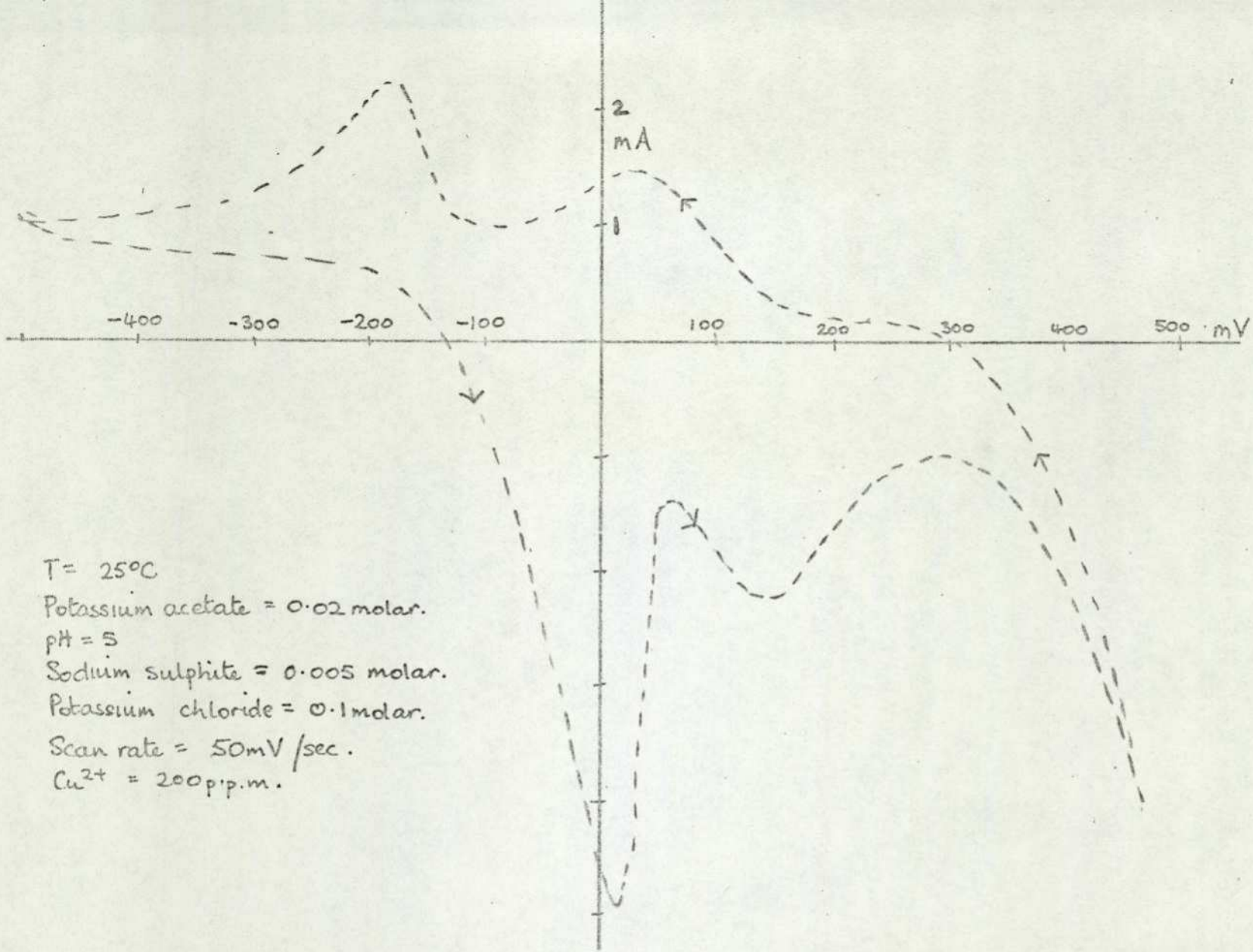


Fig 4.25. Current-potential curve of $CuSO_4$ (unstirred solution) using platinum electrode (3.2 cm^2)

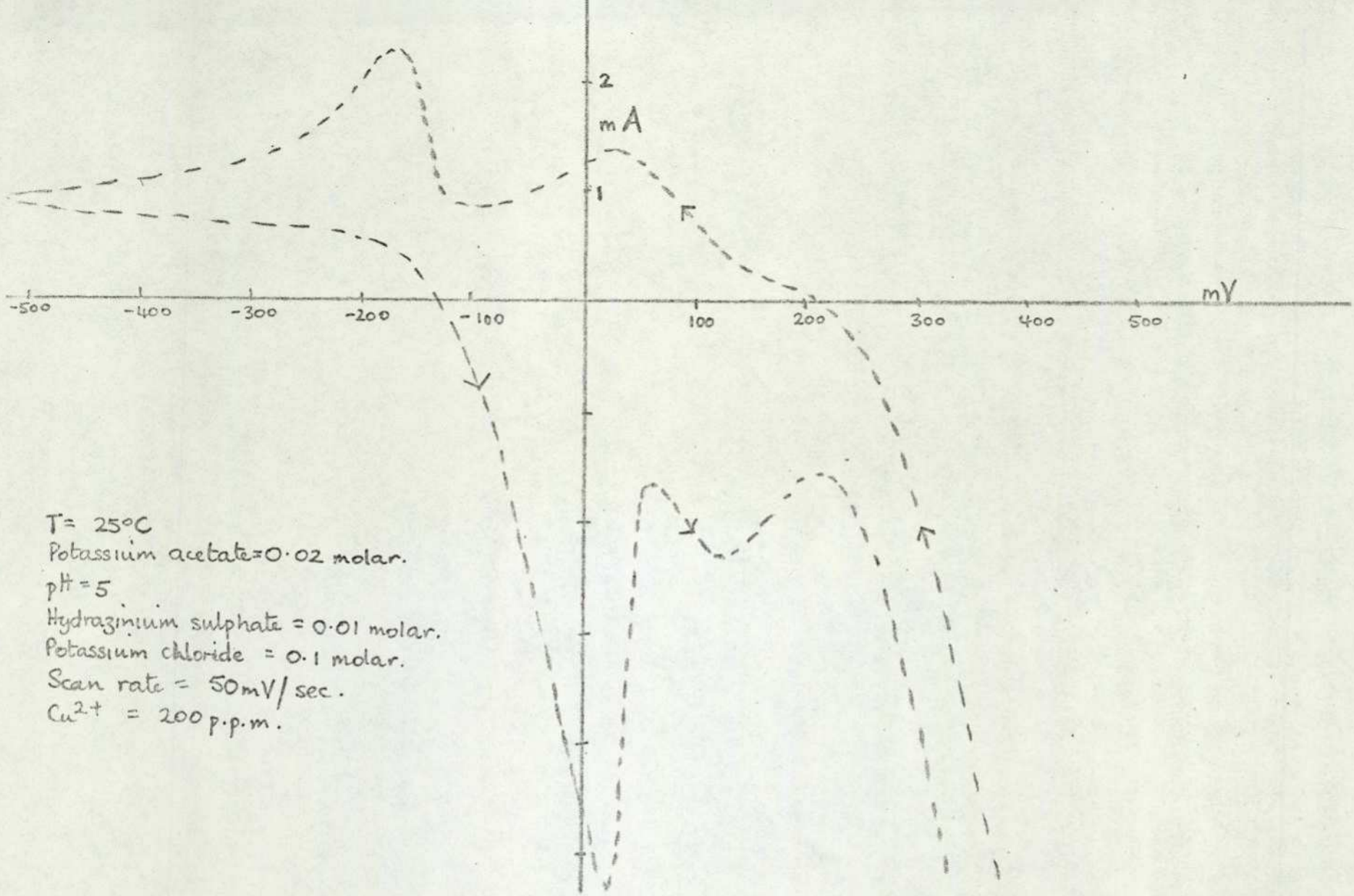


Fig 4.26. Current-potential curve of $CuSO_4$ (unstirred solution) using platinum electrode ($3.2 cm^2$)

REFERENCES

CHAPTER 4

1. Latimer, Oxidation Potential, Prentice-Hall, New York, 1952.
2. J.J. Lingane, Electroanalytical Chemistry, Interscience, New York, 1958
3. Reference (2) page 378
4. S. Karp and L. Meites, J. Am. Chem. Soc., 1962, 84, 906
5. S. Szpak, S. Stonehart and T. Katan, Electrochim. Acta, 1965 10, 563
6. J.W. Cahn and R. Powell, J. Am. Chem. Soc., 1954, 76, 2568
7. W.C.E. Higginson, D. Sutton and P. Wright, J. Chem. Soc., 1953, 1380
8. W.C.E. Higginson and D. Sutton, J. Chem. Soc., 1953, 1402
9. W.C.E. Higginson and P. Wright, J. Chem. Soc., 1955, 1551
10. D.R. Rosseinsky, J. Chem. Soc., 1957, 4685
11. R.G. Bates, Determination of pH, John Wiley, 1964
12. J.J. Lingane and S.L. Jones, Anal. Chem., 1951, 23, 1798
13. D.G. Peters and S.A. Cruser, J. Electroanal. Chem., 1965, 9, 27
14. J. Bjerrum, G. Schwarzenbach and L.G. Sillen, Stability Constants, Special Publication No. 17, The Chemical Society, London, 1964.
15. K. Korinex, J. Koryta and M. Musilova, J. Electroanal. Chem., 1969, 21, 319
16. J.A. Harrison, and Z.A. Khan, J. Electroanal. Chem., 1970, 26, 1.
17. J.A. Harrison and Z.A. Khan, J. Electroanal. Chem., 1970, 28, 131

APPENDIX ONE

a. Predominant Ion of Hydrazine in the pH range 2 to 6

Hydrazine can form two acidic species according to the following reactions (1)

$$N_2H_4 + H^+ \rightleftharpoons N_2H_5^{1+} \quad (1a)$$

$$K_1 = \frac{\left[N_2H_5^+\right]}{\left[N_2H_4\right]\left[H^+\right]} = 10^{7.94} \quad (1)$$

$$K_2 = \frac{\left[N_2H_6^{2+}\right]}{\left[N_2H_4\right]\left[H^+\right]^2} = 10^{8.2} \quad (2)$$

$$N_2H_4 + 2H^+ \rightleftharpoons N_2H_6^{2+} \quad (2a)$$

where [ ] represents concentration.

Hence hydrazine can exist in solution as N_2H_4, $N_2H_5^+$ and $N_2H_6^{2+}$ depending on the pH of the solution investigated.

Let,

C_T = Total concentration of hydrazine salt added to the solution, then

$$C_T = \left[N_2H_4\right] + \left[N_2H_5^+\right] + \left[N_2H_6^{2+}\right] \quad (3)$$

But

$$\left[N_2H_5^+\right] = \left[N_2H_4\right]\left[H^+\right] K_1 \quad (4)$$

and

$$\left[N_2H_6^{2+}\right] = \left[N_2H_4\right]\left[H^+\right]^2 K_2 \quad (5)$$

Therefore, substituting equations (4) and (5) into equation (3), equation (3) is reduced to

$$C_T = \left[N_2H_4\right]\left\{1 + \left[H^+\right]K_1 + \left[H^+\right]^2 K_2\right\} \quad (6)$$

Now let

$$\alpha_o = \frac{[N_2H_4]}{C_T} \quad (7)$$

$$\alpha_1 = \frac{[N_2H_5^{1+}]}{C_T} \quad (8)$$

$$\alpha_2 = \frac{[N_2H_6^{2+}]}{C_T} \quad (9)$$

where α_o, α_1 and α_2 represent the fraction of N_2H_4, $N_2H_5^{1+}$ and $N_2H_6^{2+}$ present in the solution under investigation. Therefore by substituting equations (4), (5) and (6) in equations (7), (8) and (9) one can calculate the fraction of each species present.

Table I shows the fraction of $N_2H_5^+$ in the pH range 2 to 6.

Table I

% of $N_2H_5^{1+}$ at different pH values.

pH	% of $N_2H_5^{1+} = 100\alpha_1$
2	98.0
3	99.8
4	99.9
5	99.8
6	89.7

As can be seen from Table I, the $N_2H_5^+$ ion is the predominant ion in the pH range two to six.

b. Electrode Potential (in mV)

The electrode potential for the reaction

$$N_2 + 4H_2O + 4e \rightleftharpoons N_2H_4 + 4OH^- \quad (10a)$$

is given by (2)

$$E = -1160 - 15 \log \left[N_2H_4\right] + 60pOH \qquad (10)$$

Since,

$$pOH = 14 - pH \qquad (11)$$

∴ Substituting (11) in (10)

$$E = -1160 + 60(14 - pH) - 15 \log \left[N_2H_4\right]$$

$$= -320 - 60\ pH - 15 \log \left[N_2H_4\right] \qquad (12)$$

In section (a) it was shown that the predominant ion is the $N_2H_5^{1+}$ ion in the pH range two to six, therefore, using equation (4)

$$\left[N_2H_4\right] = \frac{\left[N_2H_5^+\right]}{\left[H^+\right] K_1} \qquad (4b)$$

Hence substituting equation (4b) into equation (12)

$$E = -320 - 60\ pH - 15 \left\{\log \left[N_2H_5^+\right] - \log \left[H^+\right] - \log K_1\right\}$$

$$E = -200 - 75\ pH - 15 \log \left[N_2H_5^+\right] \qquad (13)$$

Therefore the main electrochemical reaction which is represented by equation (13) is

$$N_2 + 5H^+ + 4e \rightleftharpoons N_2H_5^+ \qquad (13a)$$

The standard electrode potential of reaction 13a is given by

$$E^o = -200 - 75\ pH \quad \text{(against S.H.E.)}$$

Table II shows the variation of E^o with pH.

Table II

(All potentials are referred to S.C.E.)

Variation of E^{o} values of reaction (13a) with pH

pH	E^{o} mV (referred to S.C.E.)
2	-590
3	-665
4	-740
5	-815
6	-890

References

1. Stability Constants, Compiled by L.G. Sillen, G. Schwarzenbach and J. Bjerrum, The Chemical Society Special Publication No. 17, London, 1964.

2. J.A. Harrison and Z.A. Khan, J. Electroanal. Chem., 1970, 26, 1.

APPENDIX TWO

PREDOMINANT COPPER (II) COMPLEXES IN TARTRATE SOLUTION

Tartaric acid is a di-basic acid. Its acid formation constants are shown in equations 1a and 2a (Ref. 1)

$$H + L \rightleftharpoons HL \tag{1}$$

$$K_1 = \frac{[HL]}{[H]\,[L]} = 10^{3.94} \tag{1a}$$

$$2H + L \rightleftharpoons H_2L \tag{2}$$

$$K_2 = \frac{[H_2L]}{[H]^2\,[L]} = 10^{6.82} \tag{2a}$$

where L = tartrate ion

[ ] = concentration

Let, (signs are omitted for convenience)

$$C_T = [L] + [HL] + [H_2L] \tag{3}$$

But

$$[HL] = [L][H]\,K_1 \tag{4}$$

$$[H_2L] = [L][H]^2\,K_2 \tag{5}$$

$$\therefore\ C_T = [L]\{1 + [H]\,K_1 + [H]^2\,K_2\} \tag{6}$$

Let

$$\alpha_o = \frac{[L]}{C_T} \tag{7}$$

$$\alpha_1 = \frac{[HL]}{C_T} \tag{8}$$

$$\alpha_2 = \frac{[H_2L]}{C_T} \tag{9}$$

where α_o, α_1 and α_2 represent the fraction of L, HL and H_2L present in solution. The values of α_o, α_1

and α_2 can be calculated by substituting equations (4), (5) and (6) into equations (7), (8) and (9). Table I shows the result of such calculation.

Table I

% of L, HL and H_2L present in Solution

pH	$100\,\alpha_0$	$100\,\alpha_1$	$100\,\alpha_2$
1	0.0015	1.30	98.7
2	0.11	11.6	88.2
3	6.13	53.4	40.9
4	51.6	44.9	3.4
5	92	8	-
6	99.1	0.90	-

Therefore if C_T = 0.02 molar, then the concentration of free tartrate ion in the solution at different pH is given in Table II below.

Table II

Concentration of free Tartrate ion at different pH in a solution containing 0.02 molar Potassium Tartrate

pH	$[L] = \alpha_0 \times C_T$
1	negligible
2	negligible
3	0.00123 molar
4	0.0102 molar
5	0.0184 molar
6	0.0198 molar

Copper-Tartrate Complexes

The cupric ion forms the following complexes with Tartrate ion (signs are omitted for convenience)

Cu L, Cu L_2, Cu L_3 and Cu L_4 as shown in the equations below. (Ref. 1)

$$Cu + L \rightleftharpoons CuL \quad (10)$$

$$Cu + 2L \rightleftharpoons CuL_2 \quad (11)$$

$$Cu + 3L \rightleftharpoons CuL_3 \quad (12)$$

$$Cu + 4L \rightleftharpoons CuL_4 \quad (13)$$

$$\beta_1 = \frac{[ML]}{[M][L]} = 10^{3.2} \quad (10a)$$

$$\beta_2 = \frac{[ML_2]}{[M][L]^2} = 10^{5.11} \quad (11a)$$

$$\beta_3 = \frac{[ML_3]}{[M][L]^3} = 10^{4.67} \quad (12a)$$

$$\beta_4 = \frac{[ML_4]}{[M][L]^4} = 10^{6.4} \quad (13a)$$

The metal and Ligand mass balance equations are (14) and (15)

$$C_M = [M] + [ML] + [ML_2] + [ML_3] + [ML_4] \quad (14)$$

$$C_L = [L] + [ML] + 2[ML_2] + 3[ML_3] + 4[ML_4] \quad (15)$$

where

C_M = concentration of copper sulphate

C_L = concentration of free tartrate ion as calculated in table II.

Assuming (as a first approximation) that $[L] = C_L$, one can calculate

$$\sigma_o = \frac{[M]}{C_M} \quad (16)$$

$$\sigma_1 = \frac{[ML]}{C_M} \quad (17)$$

$$\sigma_2 = \frac{[ML_2]}{C_M} \quad (18)$$

$$\sigma_3 = \frac{[ML_3]}{C_M} \quad (19)$$

$$\sigma_4 = \frac{[ML_4]}{C_M} \quad (20)$$

These calculations show that σ_3 and σ_4 are very small at pH 3 - 5, i.e. the species ML_3 and ML_4 are practically absent. At pH 3 σ_2, σ_3, σ_4 are very small which indicates the corresponding absence for all practical purposes. Hence the mass balance equations (14) and (15) are reduced to

$$C_M = [M] + [ML] + [ML_2] \quad (21) \text{ for pH 4 - 5}$$

$$C_L = [L] + [ML] + 2[ML_2] \quad (22) \text{ for pH 4 - 5}$$

and

$$C_M = [M] + [ML] \quad (23) \text{ pH 3}$$

$$C_L = [L] + [ML] \quad (24) \text{ pH3}$$

$$\therefore \sigma_o = \frac{1}{1 + \beta_1 [L] + \beta_2 [L]^2} \quad (25)$$

$$\sigma_1 = \frac{\beta_1 [L]}{1 + \beta_1 [L] + \beta_2 [L]^2} \quad (26)$$

$$\sigma_2 = \frac{\beta_2 [L]^2}{1 + \beta_1 [L] + \beta_2 [L]^2} \qquad (27)$$

By substituting as a first approximation $C_L = [L]$ one can calculate the new values of σ_o, σ_2 and σ_1 from which the value of $[M]$, $[ML]$ and $[ML_2]$ can be calculated. The calculated values of $[ML]$ and $[ML_2]$ are substituted in equations (22) or (24) and corrected values of $[L]$ are calculated. Then the new calculated value of $[L]$ is substituted in equations (25), (26) and (27) and so on until a constant value of $[L]$, $[ML]$, $[ML_2]$ and $[M]$ are obtained.

Table III shows the result of such calculations.

Table III

% of different copper ions present in solution.

pH	% $[M]$ = 100 σ_o	% $[ML]$ = 100 σ_1	% $[ML_2]$ = 100 σ_2
1	100		
2	100		
3	70	30	-
4	6.3	62.2	31.5
5	1.83	43.8	54.3

References

1. J. Bjerrum, G. Schwarzenbach and L.G. Sillen, Stability Constants, Special Publication No. 17, The Chemical Society, London, 1964.